ANL/PHY-97/1
Conf-9607156

Proceedings of the Conference on Nuclear Structure at the Limits

July 22 - 26, 1996
Argonne National Laboratory
Argonne, Illinois

DISTRIBUTION OF THIS DOCUMENT IS UNLIMITED

International Advisory Committee:

C. Baktash (Oak Ridge)
J.A. Cizewski (Rutgers)
G.D. Dracoulis (Canberra)
B. Hass (Strasbourg)
I. Hamamoto (Lund)
B. Herskind (Copenhagen)
S. Lunardi (Padova)
W. Nazarewicz (Oak Ridge)
D.C. Radford (Chalk River)
L.L. Riedinger (Knoxville)
M.A. Riley (Tallahassee)
P. Ring (Munich)
D. Schwalm (Heidelberg)
F.S. Stephens (Berkeley)
P.J. Twin (Liverpool)

Local Organizing Committee:

I. Ahmad (Argonne)
M.P. Carpenter (Argonne)
R.R. Chasman (Argonne)
U. Garg (Notre Dame)
J. Glover (Secretary)
R.V.F. Janssens (Argonne)
T.L. Khoo (Argonne)
T. Lauritsen (Argonne)
C.J. Lister (Argonne)

MASTER

DISCLAIMER

Portions of this document may be illegible in electronic image products. Images are produced from the best available original document.

FOREWORD

These Proceedings constitute a written record of the Conference on Nuclear Structure at the Limits held at Argonne on July 22-26, 1996. The Conference was attended by 197 scientists including 90 from abroad. The program sessions were characterized by very lively and spirited discussions. There was a general feeling among the participants that the nuclear structure field is in a healthy state right now. From the comments received from the attendees we feel that the conference achieved its aim of reviewing the status of nuclear structure physics while stimulating new ideas.

We express our thanks to the members of the advisory committee for their suggestions concerning the program. We also thank the participants for making the conference successful. The assistance of Jeannie Glover and Colleen Tobolic in handling the many secretarial duties before and during the conference is greatly appreciated.

The Organizing Committee

Acknowledgments

The Organizing Committee greatfully acknowledges financial support from the following companies and organizations:

Bicron/Crismatec BGO Detectors

EG&G/Ortec

LeCroy

Sun Microsystems

The University of Chicago

Argonne National Laboratory

TABLE OF CONTENTS

SESSION I-A (Monday Morning)
Chairperson: R. M. Diamond

Spectroscopy In and Decay Out of the Second Well in Actinide Nuclei
D. Schwalm ..... *

Discrete-Line Transitions from Superdeformed to Yrast States in ^{194}Hg and ^{192}Hg
G. Hackman, T. L. Khoo, D. Ackermann, A. Lopez-Martens, M. P. Carpenter, T. Lauritsen, S. Agarwala, I. Ahmad, H. Amro, D. J. Blumenthal, I. Calderin, T. Dössing, S. M. Fischer, F. Hannachi, R. V. F. Janssens, A. Korichi, I. Y. Lee, A. O. Macchiavelli, E. F. Moore, D. Nisius, and J. Young 1

Observation of the Single Step Links of the Yrast Superdeformed Band in ^{194}Pb
F. Hannachi, A. Lopez-Martens, A. Korichi, S. Leoni. C. Schück, E. Gueorguieva, Ch. Vieu, B. Haas, R. Lucas, A. Astier, G. Baldsiefen, M. Carpenter, G. de France, R. Duffait, L. Ducroux, Y. Le Coz, Ch. Finck, A. Gorgen, H. Hübel, T. L. Khoo, T. Lauritsen, M. Meyer, D. Prévost, N. Redon, C. Rigollet, H. Savajols, J. F. Sharpey-Schafer, O. Stezowski, Ch. Theisen, U. Van Severen, J. P. Vivien, and A. N. Wilson 6

Primary Transitions Between the Yrast Superdeformed Band and Low-Lying Normal Deformed States in ^{194}Pb
K. Hauschild, L. A. Bernstein, J. A. Becker, D. E. Archer, R. W. Bauer, D. P. McNabb, J. A. Cizewski, K.-Y. Ding, W. Younes, R. Krücken, G. J. Schmid, R. M. Clark, P. Fallon, I.-Y. Lee, A. O. Macchiavelli, R. MacLeod, R. M. Diamond, M. A. Deleplanque, F. S. Stephens, and W. H. Kelly 11

SESSION I-B (Monday Morning)
Chairperson: B. Hass

Decay Out of the Yrast and Excited Highly-Deformed Bands in the Even-Even Nucleus ^{134}Nd
C. M. Petrache, D. Bazzacco, S. Lunardi, C. Rossi Alvarez, R. Venturelli, P. Pavan, N. H. Medina, M. N. Rao, R. Burch, G. de Angelis, A. Gadea, G. Maron, D. R. Napoli, L. H. Zhu, and R. Wyss 17

Search for Linking Transitions in ^{143}Eu
F. Lerma, D. R. LaFosse, M. Devlin, D. G. Sarantites, S. Asztalos, R. M. Clark, P. Fallon, I. Y. Lee, A. O. Macchiavelli, R. W. Macleod, C. Baktash, M. J. Brinkman, and D. Rudolph 23

Single-Step Linking Transition from Superdeformed to Spherical States in ^{143}Eu
A. Ataç, A. Axelsson, I. Bearden, M. Bergström, *B. Herskind*, J. Nyberg, M. Palacz, J. Persson, M. Piiparinen, C. Fahlander, G. Hagemann, S. Leoni, M. Lipoglavšek, P. Nolan, E. Paul, N. Redon, L. Roos, G. Sletten, and K.Tuček 29

**No Submission*

The Quasi-Continuum of Gamma Rays Following the Decay of Superdeformed Bands in the Hg Region
T. Lauritsen, A. Lopez-Martens, T. L. Khoo, R. V. F. Janssens, M. P. Carpenter, G. Hackman, D. Ackermann, I. Ahmad, H. Amro, D. J. Blumenthal, S. M. Fischer, F. Hannachi, A. Korichi, E. F. Moore, and D. T. Nisius 35

First Measurement of the Degree of Fragmentation of the Decay Out Cascade from the Superdeformed Yrast Band in ^{192}Hg
A. Lopez-Martens, F. Hannachi, C. Schück, R. Collatz, E. Gueorguieva, Ch. Vieu, T. Dossing, S. Leoni, B. Herskind, I. Ahmad, D. Blumenthal, M. Carpenter, D. Gassmann, R. V. F. Janssens, T. L. Khoo, T. Lauritsen, D. Nisius, A. Korichi, C. Bourgeois, A. Astier, L. Ducroux, Y. Le Coz, M. Meyer, N. Redon, J. F. Sharpey-Schafer, A. N. Wilson, W. Korten, A. Bracco, and R. Lucas 41

SESSION II-A (Monday Afternoon)
Chairperson: B. Herskind

Superdeformation
F. S. Stephens 47

Microscopic Description of Nuclear Shapes
J. L. Egido, L. M. Robledo, A. Valor, and A. Villafranca 54

Around the Back-Bend in an Excited ^{150}Gd Superdeformed Band
P. J. Twin, S. Ertürk, C. W. Beausang, P. Fallon, D. Appelbe, S. Asztalos, A. Macchiavelli, T. Lauritsen, I. Y. Lee, F. S. Stephens, and M. A. Deleplanque-Stevens 60

SESSION II-B (Monday Afternoon)
Chairperson: M. A. Deleplanque-Stephens

Microscopic Study of Superdeformation in the A = 150 Mass Region
C. Rigollet, P. Bonche, H. Flocard, P.-H. Heenen, and B. Gall 66

Lifetime Measurements and Identical SD Bands in the A = 190 and A = 150 Regions
E. F. Moore, D. Nisius, R. V. F. Janssens, T. L. Khoo, T. Lauritsen, D. Ackermann, I. Ahmad, H. Amro, D. Blumenthal, M. P. Carpenter, S. Fischer, G. Hackman, P. Fallon, S. J. Asztalos, R. M. Clark, M. A. Deleplanque, R. M. Diamond, R. Krucken, I-Y. Lee, A. O. Macchiavelli, F. S. Stephens, F. Hannachi, A. Lopez-Martens, J. A. Becker, L. Bernstein, L. P. Farris, E. A. Henry, A. Korichi, P. Chowdhury, R. H. Mayer, A. V. Afanasjev, and I. Ragnarsson 72

RDDS Lifetime Measurements of Low-Lying Superdeformed States in ^{194}Hg
R. Kühn, A. Dewald, R. Krücken, C. Meier, R. Peusquens, H. Tiesler, O. Vogel, S. Kasemann, P. von Brentano, *D. Bazzacco*, C. Rossi-Alvarez, G. De Angelis, and J. de Boer 78

**No Submission*

Change of Deformation at the Backbending in the Yrast Superdeformed Band of ^{144}Gd
C. A. Ur, G. P. Bolzonella, *L. H. Zhu*, D. Bazzacco, S. Lunardi, N. H. Medina C. M. Petrache, M. N. Rao, C. Rossi Alvarez, G. de Angelis, D. De Acuna, D. R. Napoli, W. Gast, R. M. Lieder, T. Rzaca-Urban, S. Utzelmann, and R. Wyss 84

SESSION III-A (Tuesday Morning)
Chairperson: S. Lunardi

Superdeformation in the Mass A ~ 80 Region
Cyrus Baktash 90

Systematic Description of Superdeformed Bands in the Mass-190 Region
Yang Sun, Jing-ye Zhang, and Mike Guidry 99

New Results on the Superdeformed ^{196}Pb Nucleus: The Decay of the Excited Bands to the Yrast Band
S. Bouneau, *F. Azaiez*, J. Duprat, I. Deloncle, M-G. Porquet, U. J. van Severen, T. Nakatsukasa, M. M. Aleonard, A. Astier, S. Baldsiefen, C. W. Beausang, F. A. Beck, C. Bourgeois, D. Curien, N. Dozie, L. Ducroux, B. Gall, H. Hubel, M. Kaci, W. Korten, M. Meyer, N. Redon, H. Sergolle, and J. F. Sharpey-Schafer 105

Microscopic Structure of High-Spin Vibrational States in Superdeformed A = 190 Nuclei
Takashi Nakatsukasa, Kenichi Matsuyanagi, Shoujirou Mizutori, and Yoshifumi R. Shimizu 111

SESSION III-B (Tuesday Morning)
Chairperson: L. L. Riedinger

Selfconsistent Calculations for Hyperdeformed Nuclei
H. Molique, J. Dobaczewski, *J. Dudek*, and W. D. Luo 117

How Close are Hyperdeformed States to the Scission Point?
L. M. Robledo, R. R. Chasman, and J. L. Egido 124

Test of $\Delta I = 2$ Staggering in the Superdeformed Bands of ^{194}Hg
R. Krücken, G. Hackman, M. A. Deleplanque, R. V. F. Janssens, I. Y. Lee, D. Ackermann, I. Ahmad, H. Amro, S. Asztalos, D. J. Blumenthal, M. P. Carpenter, R. M. Clark, R. M. Diamond, P. Fallon, S. M. Fischer, B. Herskind, T. L. Khoo, T. Lauritsen, A. O. Macchiavelli, R. W. MacLeod, D. Nisius, G. J. Schmid, F. S. Stephens, and K. Vetter 130

$\Delta I = 2$ Energy Staggering in Normal Deformed Dysprosium Nuclei
M. A. Riley, J. Simpson, T. B. Brown, D. E. Archer, J. Döring, P. Fallon, C. Kalfas, J. F. Sharpey-Schafer, and S. L. Tabor 136

**No Submission*

SESSION IV-A (Tuesday Afternoon)
Chairperson: N. Benczer-Koller

Evidence for "Magnetic-Rotation" in Nuclei: New Results on the M1-Bands of $^{198,199}Pb$
R. M. Clark 142

Multi-Quasiparticle Isomers Near Stability and Reduced Pairing
G. D. Dracoulis 148

Return of *K* Selection at High Spin: Decay of Bandheads in ^{178}W
P. M. Walker, C. S. Purry, G. D. Dracoulis, T. Kibédi, F. Kondev, S. Bayer, A. M. Bruce, A. P. Byrne, M. Dasgupta, W. Gelletly, P. H. Regan, and C. Thwaites 154

Direct Transitions from High-*K* Isomers to Low-*K* Bands — γ Softness or Coriolis Coupling
Yoshifumi R. Shimizu, Kanako Narimatsu, Shin-Ichi Ohtsubo, and Toshiyuki Shizuma 159

SESSION IV-B (Tuesday Afternoon)
Chairperson: D. Cline

Tilted Axis Rotation in Odd-Odd ^{164}Tm
W. Reviol, L. L. Riedinger, X. Z. Wang, J.-Y. Zhang, H. J. Jensen, G. B. Hagemann, R. A. Bark, P. O. Tjøm, S. Leoni, T. Lönnroth, H. Schnack-Petersen, T. Shizuma, and J. Wrzesinski 165

Properties of Rotational Bands at the Spin Limit in A ~ 50, A ~ 65 and A ~ 110 Nuclei
V. P. Janzen, A. V. Afanasjev, H. R. Andrews, G. C. Ball, J. A. Cameron, M. Cromaz, J. DeGraaf, T. E. Drake, S. Flibotte, A. Galindo-Uribarri, G. Hackman, D. M. Headly, J. Jonkman, S. Mullins, D. C. Radford, I. Ragnarsson, J. L. Rodriguez, C. E. Svensson, J. C. Waddington, D. Ward, and G. Zwartz 171

First Excited States in Doubly-Odd ^{110}Sb: Smooth Band Termination in the A ≈ 110 Region
G. J. Lane, D. B. Fossan, I. Thorslund, P. Vaska, R. G. Allat, E. S. Paul, L. Käubler, H. Schnare, I. M. Hibbert, N. O'Brien, R. Wadsworth, W. Andrejtscheff, J. de Graaf, J. Simpson, I. Y. Lee, A. O. Macchiavelli, D. J. Blumenthal, C. N. Davids, C. J. Lister, D. Seweryniak, A. V. Afanasjev, and I. Ragnarsson 178

Rotational Bands Terminating at Maximal Spin in the Valence Space
I. Ragnarsson and A. V. Afanasjev 184

SESSION V-A (Wednesday Morning)
Chairperson: D. G. Sarantites

Status of Development of the Gamma Ray Energy Tracking Array (GRETA)
I. Y. Lee, G. J. Schmid, K. Vetter, M. A. Deleplanque, R. M. Diamond, P. Fallon, A. O. Macchiavelli, R. W. Macleod, F. S. Stephens, R. M. Clark, and R. Krücken 191

**No Submission*

EUROBALL: Present Status and New Possibilities for Nuclear Structure Studies
F. A. Beck ..... *

The Holifield Radioactive Ion Beam Facility at Oak Ridge National Laboratory
J. D. Garrett 197

SESSION V-B (Wednesday Morning)
Chairperson: U. Garg

High Spin Isomer Beam Line at RIKEN
T. Kishida, Y. Gono, E. Ideguchi, T. Morikawa, M. Kidera, M. Shibata, H. Tsuchida, K. Miyazaki, H. Watanabe, H. Y. Wu, A. Tarokura, S. S. Yamamoto, A. Yoshida, S. Mitarai, A. Odahara, T. Murakami, M. Oshima, H. Kusakari, M. Sugawara, M. Kubo, T. Murata, M. Shimura, H. Kumagai, and M. Ishihara 204

High Spin Spectroscopy Near the N = Z Line: Channel Selection and Excitation Energy Systematics
C. E. Svensson, J. A. Cameron, S. Flibotte, G. Gervais, D. S. Haslip, J. M. Nieminen, J. C. Waddington, J. N. Wilson, G. C. Ball, A. Galindo-Uribarri, V. P. Janzen, D. C. Radford, D. Ward, M. Cromaz, and T. E. Drake 209

Alpha Particle Spectra in Coincidence with Normal and Superdeformed States in ^{150}Tb
G. Viesti, M. Lunardon, D. Bazzacco, R. Burch, G. de Angelis, M. Cinausero, D. Fabris, E. Farnea, E. Fioretto, S. Lunardi, N. H. Medina, G. Nebbia, G. Prete, C. Rossi Alvarez, and G. Vedovato 215

The Microball and Gammasphere: Research Highlights and Future Directions
M. Devlin, D. G. Sarantites, D. R. LaFosse, and F. Lerma 220

SESSION VI-A (Thursday Morning)
Chairperson: W. Nazarewicz

Structure and Reactions of Drip-Line Nuclei
P. G. Hansen 226

Proton-Radioactivity - A Look at Nuclear Structure Beyond the Proton Drip Line
C. N. Davids ..... *

Shell-Model Monte Carlo Calculations Near N = Z
D. J. Dean 232

SESSION VI-B (Thursday Morning)
Chairperson: M. Thoennessen

A Number-Projected Model with Generalized Pairing Interaction in Application to Rotating Nuclei
W. Satuła and R. Wyss 237

**No Submission*

In-Beam Studies of ^{98}Cd and ^{102}Sn
M. Lipoglavšek, M. Górska, J. Nyberg, A. Ataç, A. Axelsson, R. Bark, J. Blomqvist, J. Cederkäll, B. Cederwall, G. de Angelis, C. Fahlander, H. Grawe, A. Johnson, S. Leoni, A. Likar, M. Matiuzzi, S. Mitarai, L.-O. Norlin, M. Palacz, J. Persson, H. A. Roth, R. Schubart, D. Seweryniak, T. Shizuma, D. Sohler, G. Sletten, W. B. Walters, and M. Weiszflog 243

First In-Beam Observation of Excited States in $^{156}_{72}Hf_{84}$ Using the Recoil-Decay Tagging Method
D. Seweryniak, I. Ahmad, H. Amro, D. J. Blumenthal, L. T. Brown, M. P. Carpenter, C. N. Davids, S. Fischer, D. J. Henderson, R. V. F. Janssens, T. L. Khoo, C. J. Lister, D. Nisius, T. Davinson, R. J. Irvine, P. J. Woods, W. B. Walters, I. Hibbert, C. Parry, and R. Wadsworth 247

Collective Properties of Drip-Line Nuclei
I. Hamamoto and H. Sagawa 253

SESSION VII-A (Thursday Afternoon)
Chairperson: A. M. Baxter

Discovery of Element 112
S. Hofmann 259

Synthesis of Superheavy Elements and Dinuclear-System Concept of Compound-Nucleus Formation
N. V. Antonenko, G. G. Adamian, E. A. Cherepanov, A. K. Nasirov, and V. V. Volkov 265

High Spin States in Neutron-Rich Nuclei
S. Mizutori ..... *

SESSION VII-B (Thursday Afternoon)
Chairperson: D. Ward

Relativistic Hartree-Bogoliubov Description of the Halo Nuclei
J. Meng and P. Ring 271

New High Spin States and Isomers in the ^{208}Pb and ^{207}Pb Nuclei
R. Broda, J. Wrzesinski, T. Pawlat, B. Fornal, Z. Grabowski, D. Bazzacco, S. Lunardi, C. Rossi Alvarez, G. de Angelis, A. Gadea, and K.-H. Maier 276

Yrast Excitations Around ^{132}Sn: The Two and Three Valence-Proton N = 82 Isotones ^{134}Te and ^{135}I
P. J. Daly, C. T. Zhang, P. Bhattacharyya, R. Broda, Z. W. Grabowski, D. Nisius, I. Ahmad, T. Ishii, M. P. Carpenter, L. R. Morss, W. R. Phillips, J. L. Durell, M. J. Leddy, A. G. Smith, W. Urban, B. J. Varley, N. Schulz, E. Lubkiewicz, M. Bentaleb, and J. Blomqvist 282

**No Submission*

Role of Nuclear Couplings in the Inelastic Excitation of Weakly-Bound Neutron-Rich Nuclei
C. H. Dasso, S. M. Lenzi, and *A. Vitturi* 288

SESSION VIII-A (Friday Morning)
Chairperson: J. A. Cizewski

The Nuclear Structure of Neutron-Rich Isotopes with Z from 38-42
J. L. Durell, M. A. Jones, W. R. Phillips, A. G. Smith, W. Urban, B. J. Varley, I. Ahmad, C. J. Lister, L. R. Morss, K. L. Nash, C. W. Williams, N. Schulz, A. Guessous, E. Lubkiewicz, and M. Bentaleb 294

Spectroscopy of Reflection-Asymmetric Nuclei Using Multinucleon Transfer Reactions
J. F. C. Cocks, P. A. Butler, K. J. Cann, P. T. Greenlees, G. D. Jones, R. Broda, B. Fornal, P. M. Jones, R. Julin, S. Juutinen, D. Müller, M. Piiparinen, A. Savelius, J. F. Smith, I. Ahmad, S. Aszalos, P. Bhattacharyya, D. J. Blumenthal, M. P. Carpenter, R. M. Clark, B. Crowell, M. A. Delaplanque, R. M. Diamond, P. Fallon, R. V. F. Janssens, T. L, Khoo, T. Lauritsen, I. Y. Lee, A. O. Macchiavelli, R. W. MacLeod, D. Nisius, F. S. Stephens, and C. T. Zhang 300

Deformation in the Neutron Rich Sulfur Isotopes ^{40}S and ^{42}S
T. Glasmacher, H. Scheit, B. A. Brown, P. D. Cottle, M. Hellström, R. Ibbotson, J. K. Jewell, K. W. Kemper, D. J. Morrissey, M. Steiner, P. Thirolf, and M. Thoennessen 306

SESSION VIII-B (Friday Morning)
Chairperson: D. B. Fossan

Identical Gamma-Vibrational Bands in ^{165}Ho
D. C. Radford, A. Galindo-Uribarri, V. P. Janzen, D. Ward, S. Flibotte, S. M. Mullins, J. C. Waddington, M. Cromaz, J. DeGraaf, and T. E. Drake 311

Fragmentation of Two-Phonon γ-Vibrational Strength in Deformed Nuclei
C. Y. Wu and D. Cline 317

Onset of Deformation in Polonium Nuclei
W. Younes and J. A. Cizewski 323

Recent Studies of Heavy Nuclei Far From Stability at JYFL
R. Julin, T. Enqvist, K. Helariutta, P. Jones, S. Juutinen, P. Jämsen, H. Kankaanpää, P. Kuusiniemi, M. Leino, M. Muikku, M. Piiparinen, A. Savelius, W. H. Trzaska, S. Törmänen, J. Uusitalo, R. G. Allatt, P. A Butler, K. J. Cann, J. F. C. Cocks, P. T. J. Greenlees, and R. D. Page 329

**No Submission*

SESSION IX (Friday Afternoon)
Chairperson: J. C. Waddington

A Multitude of Rotational Bands in ^{163}Er and Their Mutual Interaction
P. Bosetti, A. Brockstedt, *G. B. Hagemann*, H. Ryde, H. Carlsson, L. P. Ekström, A. Nordlund, R. A. Bark, B. Herskind, S. Leoni, A. Bracco, F. Camera, S. Frattini, M. Mattiuzzi, B. Million, C. Rossi-Alvarez, G. de Angelis, D. Bazzacco, S. Lunardi, and M. de Poli 335

Shell Model for Warm Rotating Nuclei
M. Matsuo, K. Yoshida, T. Dössing, E. Vigezzi, and R. A. Broglia 341

Possible Conservation of K-Quantum Number in Excited Rotating Nuclei
A. Bracco, P. Bosetti, S. Leoni, S. Frattini, T. Dössing, B. Herskind, G. B. Hagemann, M. Matsuo, and E. Vigezzi 347

Nuclear Structure at the Limits of Resolution: Looking Through Individual Wave Functions
V. G. Zelevinsky 353

List of Participants 359

Author Index 375

*No Submission

Discrete–Line Transitions from Superdeformed to Yrast States in ^{194}Hg and ^{192}Hg

G. Hackman,[a] T.L. Khoo,[a] D. Ackermann,[a] A. Lopez–Martens,[b] M.P. Carpenter,[a] T. Lauritsen,[a] S. Agarwala,[a] I. Ahmad,[a] H. Amro,[a] D.J. Blumenthal,[a] I. Calderin,[a] T. Døssing,[c] S.M. Fischer,[a] F. Hannachi,[b] R.V.F. Janssens,[a] A. Korichi,[d] I.Y. Lee,[e] A.O. Macchiavelli,[e] E.F. Moore,[f] D. Nisius,[a] and J. Young[a]

[a] *Argonne National Laboratory, 9700 S. Cass Ave., Argonne, IL 60439, U.S.A.*
[b] *C.S.N.S.M., IN2P3–CNRS, bat 104–108, 91405 Orsay, France*
[c] *Niels Bohr Institute, DK-2100 Copenhagen 0, Denmark*
[d] *I.P.N., bat 104, 91405 Orsay, France*
[e] *Lawrence Berkeley National Laboratory, Berkeley, CA 94720, U.S.A.*
[f] *North Carolina State University, Raleigh, NC 27965, U.S.A.*

Discrete–line γ-ray decay from superdeformed (SD) to yrast states in ^{194,192}Hg has been studied with the Gammasphere spectrometer. The previously established decay for the yrast SD band of ^{194}Hg has been characterized further. In addition, one–step decays have been observed for ^{194}Hg SD band 3, which fixes the excitation energy and spin of the last observed level of this band at $E^* = 7.455$ MeV, $J = 11\hbar$. So far no direct decays from superdeformed to yrast states have been observed in ^{192}Hg or in ^{194}Hg band 2, a result which is consistent with fluctuations of the transition strengths.

High–spin superdeformed (SD) bands have been known for some time now [1] , and a considerable effort has been devoted to understanding their many fascinating properties, *e.g.* the exact nature of excited bands and the physical origin of the identical bands phenomenon. Progress on these fronts has in the past been impeded by the fact that the spins and excitation energies of these SD bands could not be measured by traditional discrete–line γ spectroscopy, *i.e.* by the straightforward application of coincidence relationships and energy differences (the Ritz principle) to deduce with confidence a level scheme. At the point of decay–out, the lowest members of the SD bands are located at very high excitation energies relative to the yrast line. The coupling to excited "normal–deformed" (ND) states is very weak, but once the wave function picks up a small component of the hot ND states, the decay can proceed via a multitude of paths which are difficult to resolve. The branching ratio for a primary γ decay directly from a SD state to a ND yrast or near–yrast level is very small, and until recently, the ever–evolving γ-ray spectroscopy arrays simply did not have the sensitivity to detect these primary decays. Early attempts to measure the spins and excitation energies of SD bands [2-4] did not or could not use coincidence and Ritz principle information, and therefore were not fully satisfactory.

Recently, a network of primary decays from ^{194}Hg SD band 1 to yrast states [5] was observed. Shortly thereafter, experiments on ^{194}Pb [6] revealed a network comprising both "one–step" primary decays from SD to yrast levels and "two–step" decays, that is, primary decays to non–yrast ND states where the deexcitations from these previously unknown ND states to the yrast line were also observed.

Clearly, the third–generation γ-ray detector arrays have reached one of their most important milestones; they have the sensitivity to measure the spin and excitation energies of SD states directly through traditional discrete–line spectroscopy methods. Two new Gammasphere experiments have been undertaken to search for the one–step decays from SD bands 2 and 3 of ^{194}Hg, and band 1 of ^{192}Hg. The main motivation behind these experiments lies in the fascinating, and always controversial, problem of identical bands: one of the excited bands of ^{194}Hg (band 3) is isospectral with ^{192}Hg band 1, that is, the in-band γ rays have the same energy. Determining the spins and parities

of these two bands would constrain the possible explanations for identical bands, for example, by ascertaining whether or not states emitting γ rays of the same energy also have the same spin and parity. Furthermore, measuring the excitation energies of bands 2 and 3 in ^{194}Hg would lend further insight into the nature of these excitations, namely whether they are two-quasiparticle excitations or whether they pertain to octupole vibrations or some other collective excitation mode. Finally, by better characterising the one-step decay network for band 1 (including measurements of the transition probabilities), it was hoped to gain insight about the nature of the fluctuations in transition intensity.

At the time of the experiments, Gammasphere comprised 85 high-purity germanium detectors. The reactions employed were ^{150}Nd(^{48}Ca,4n)^{194}Hg at E_{beam}=202 MeV and ^{160}Gd(^{36}S,4n)^{192}Hg at E_{beam}=160 MeV. In both cases, the targets were backed with a $\sim$ 15 mg/cm^2 Au layer. The first, highest-spin transitions in the SD cascade were emitted while the recoiling Hg nucleus was in flight. In contrast, the lowest transitions in the band were emitted from a fully stopped nucleus, as were all of the normal deformed lines following the decay-out. This provided a *distinctive signature* for primary decay γ rays; they also had to be *fully stopped* and their peaks had to be *sharp*.

The sum of double-gated γ-γ-γ coincidence spectra of band 1 of ^{194}Hg and ^{192}Hg are shown in Figure 1, which demonstrates the quality of the data. Most of the analyses have been done with triple-coincidence events. For the high-energy primary transitions, this yields the best tradeoff between statistics and background, and therefore the best sensitivity.

In the new data on ^{194}Hg, the previously-reported [5]4485, 4195 and 3489 keV lines associated with the primary decay of SD states, as well as their coincidence relationships with intraband SD and yrast transitions, are spectacularly reproduced. In addition, two more primary transitions have been added to the decay scheme; a 3942 keV "one-step" decay from the 12$^+$ SD state to the 13$^-$ ND state, and a 3565 keV transition which de-excites the 10$^+$ SD state. The level fed by the latter transition should be highly non-yrast, and there is evidence in the coincidence spectrum for a 919 keV decay to the 9$^-$ yrast state which completes this "two-step" path.

For three primary transitions, angular distributions have been measured and A_2/A_0 coefficients extracted. (See Figure 2.) The new data show with much greater confidence that the A_2/A_0 coefficient

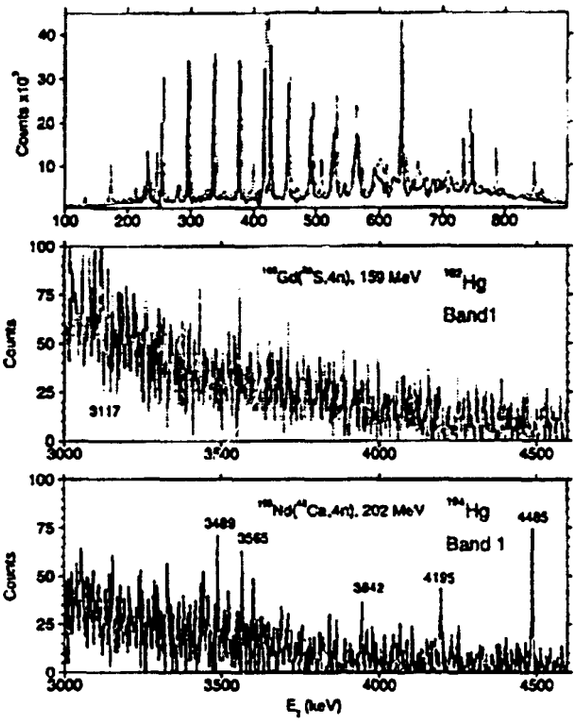

Figure 1: Sums of double-gated coincidence spectra on ^{192}Hg band 1 (gray) and ^{194}Hg band 1 (black). Top panel: low-energy portion of both spectra, overlaid, showing the SD band members. Note that the higher-energy transitions of the SD band become broadened due to Doppler shift. Middle and bottom panels: High-energy portion of these spectra in the range where one-step decays would be expected.

of the 4485 keV line is negative and consistent with stretched or anti-stretched dipole radiation. The measured A_2/A_0 values for the 3489 and 4195 keV transitions also favour the same multipole character. Furthermore, the coefficients all rule out the possibility of stretched quadrupole transitions or dipole transitions with a spin change of 0. All of these results are fully consistent with the spin assigments given previously. Dipole transitions are more likely E1 in nature than M1, since neutron capture data [7] show that the transition rate for the former should be five times that of the latter.

For ^{194}Hg band 3, which is isospectral to ^{192}Hg band 1, two γ rays with energies of 4980 and 5032 keV have been assigned as one-step primary transitions de-exciting the SD band. Figure 3 shows how these transitions have been placed. In the top-left coincidence spectrum, which is the sum

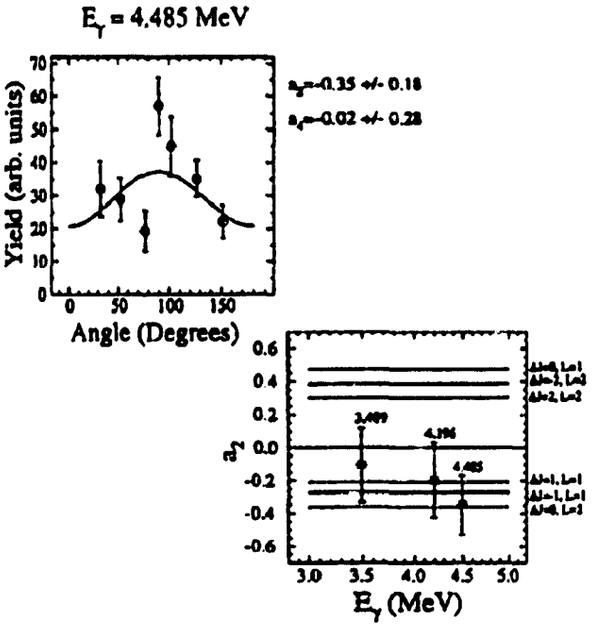

Figure 2: Top left panel: angular distribution and best polynomial fit for the 4485 keV primary transition. Bottom right panel: extracted A_2/A_0 coefficients for the three strongest primary transitions associated with ^{194}Hg SD band 1, compared with expected values for indicated multipolarities and spin-changes.

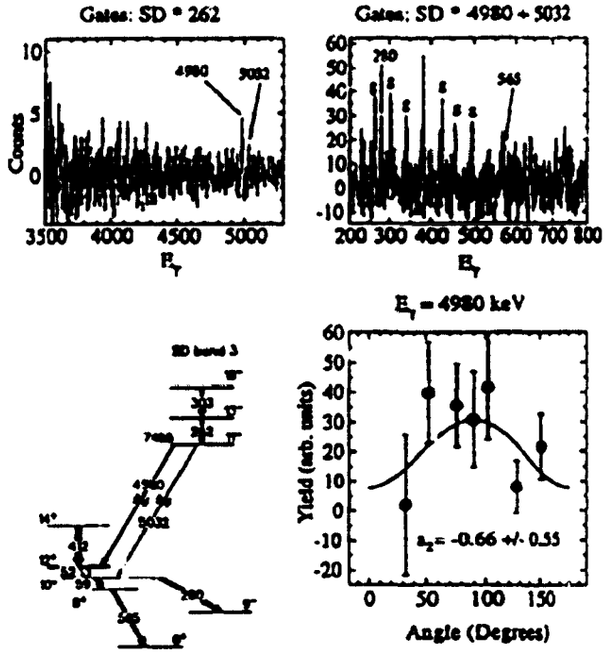

Figure 3: Details of the primary transitions of band 3. Top left: spectrum gated once on the 262 keV SD transition and once on the remaining members of the SD band. Top right: spectrum gated once on all SD transitions and once on the primary transitions. Bottom left: proposed level scheme. Bottom right: angular distribution and best polynomial fit for the 4980 keV γ ray.

of double-gates where one of the gating transitions was always the last transition observed in the band, both primary lines are present, indicating they must both be emitted from the bottom of the band. In the coincidence spectrum where one gate is part of the SD band and the second gate is either of the primary lines, there is clear evidence for the γ rays associated with the positive-parity ground state band. Finally, the difference in measured γ-ray energies between these two primary lines, 52±2 keV, corresponds to the energy difference betwen the 12^+ and 10^+ levels. Based on this evidence the level scheme shown in Figure 3 is proposed, and the last observed state of band 3 is assigned as $J^\pi = 11^-$ at an excitation energy of 7.455 MeV. Here again, the parity is expected on the basis of relative E1/M1 strengths seen in neutron capture. The measured angular distribution of the 4980 keV primary line yields a negative A_2 coefficient, consistent with an anti-stretched dipole character.

Knowing the spins and excitation energies of both ^{194}Hg SD bands 1 and 3, we can calculate the experimental routhians e' in the prescription of Bengston and Frauendorf [8] . The Harris parameters have been adjusted to match the dynamic moment $\mathcal{J}^{(2)}$ of band 1, and the results are shown in Figure 4. If the routhians are extrapolated to zero rotational frequency, their difference is about $\Delta e'_0 = 0.8$ MeV. Any model of the band 3 excitation, whether collective (*e.g.* octupole phonon) or quasiparticle, must account for this energy. For example, it has been proposed [9] that the lowest excitations in the even-Hg SD well are octupole vibrations, and the calculated routhians for the $K = 2$ octupole component yield slopes which compare favourably to the experimental data, although the excitation energy $\Delta e'_0 = 1.1$ MeV is a bit too high. By contrast, if band 3 is interpreted as a two-quasiparticle excitation [10] , then in a simple BCS picture, this places an upper limit of 0.4 MeV on the pairing gap at zero rotational frequency, compared to neutron pairing gaps of typically ~ 0.8 MeV adopted for such calculations [11] . (It should be noted that a self-consistent solution to a two-quasiparticle system could yield $\Delta e'_0 < 2\Delta_{BCS}$.) Clearly there is a need for more

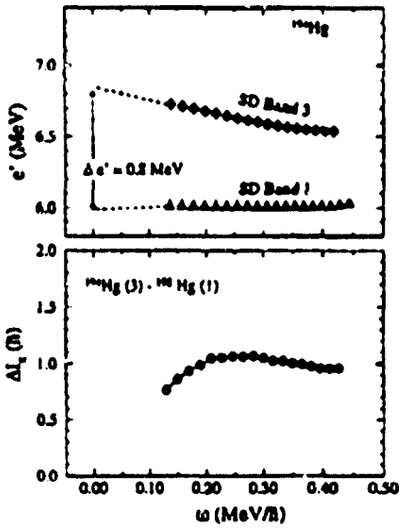

Figure 4: Upper panel, routhians for ^{194}Hg bands 1 and 3. Lower panel, difference in spin projection I_x between ^{194}Hg band 3 and its isospectral partner ^{192}Hg band 1.

detailed theoretical predictions (*e.g.* crossover M1 strengths for bands 2 and 3 and intraband E1 strength to band 1) before the exact nature of the excitation leading to band 3 can be determined.

As presented above, band 3 has odd spin and negative parity. Since band 1 of ^{192}Hg is believed to be the vacuum SD band and, hence, should have even spin and positive parity, one may conclude that states emitting γ rays of the same energy do not necessarily have the same spin and parity. Another way of looking at this feature is to project the spins onto the rotation axis and look at the difference between ^{194}Hg band 3 and ^{192}Hg band 1. This is presented in Figure 4; it is clear that at high ω, states with the same rotational frequency, and hence emitting γ rays with the same energies, have one extra unit of projected spin in ^{194}Hg band 3 than ^{192}Hg band 1.

Itis believed that the states in ^{192}Hg SD band 1 *almost certainly* have even spin and positive parity. Nevertheless, it is essential to confirm this expectation through the detection of the primary decays. Figure 1 shows that data of comparable quality were accumulated for bands 1 in both ^{192}Hg and ^{194}Hg. Assuming that the SD bands in these nuclei have roughly the same excitation energy, then all other things being equal, it would seem reasonable to expect to see primary decays from the ^{192}Hg SD to normal states with the same quality as was seen in ^{194}Hg. Yet, the high-energy portion of the spectrum, where the ^{192}Hg one-step transitions are expected, is remarkably free of any salient candidates. In fact, out of all of the peak-like fluctuations in the spectrum, only a line at 3117 keV near the low end of the spectrum has been very tentitatively placed as the first component of a two-step cascade to the yrast line, where one possible candidate for a second step is a 696 keV transition to the 10^+ ND state. With this information it is not possible to make any statements regarding the spin or parity of this band, but the analysis is on-going. It should be noted that for ^{194}Hg band 2, which is likely to be a signature partner to band 3 (based on the transition energies of one being midway between those of the other), no respectable candidates for a network of primary decays could be observed, even though the expected energies are known.

Reduced transition probabilities for the observed primary transitions were calculated and tabulated (see Table 1). It was assumed that the transition quadrupole moment of the low-spin members of the SD band is the same as that measured recently by Moore *et al.* [12] at higher spin. These primary transitions are extremely retarded, for example the two transitions from the 12^+ state of band 1, have values of about 10^{-8} of a Weisskopf unit.

There are fluctuations in the strengths of the primary γ rays from the SD levels, which can be understood in the following manner. A SD state exists in a sea of highly excited normal states (ND*). These ND* states are complex, much like the compound states populated in neutron capture. The SD band mixes with one or two of the nearest-lying ND* states, *i.e.* its wave function acquires a small admixture of this ND state,

$$|\Psi\rangle = |\mathrm{SD}\rangle + \alpha|\mathrm{ND}^*\rangle.$$

The decay then occurs due to this admixed component, *i.e.*

$$\langle \mathrm{ND}|\mathcal{M}|\Psi\rangle \simeq \alpha\langle \mathrm{ND}|\mathcal{M}|\mathrm{ND}^*\rangle.$$

If the ND* states are indeed compound states, then they should not be charactarized by any quantum numbers apart from spin and parity, and the transition strengths $|\langle\mathcal{M}\rangle|^2$ of primary decays should exhibit the same Porter-Thomas fluctuations as seen in neutron capture. At the current sensitivity levels, this would be manifest in observing the one-step decays only when one is fortunate enough to select a case which samples the high-strength portion of the distribution.

Band, Q_0 (eb)	E_γ (keV)	$J_i^\pi \to J_f^\pi$	I_γ/I_{SD} (%)	B(E1) (W.u.)	B(M1) (W.u.)
^{194}Hg	3489	$12^+ \to 13^-$	1.2(1)	$2.8(3)\times10^{-8}$	
Band 1,	3565	$10^+ \to$?	0.5(1)	$< 8\times10^{-7}$	$< 9\times10^{-5}$
18.4 ± 1.1	3942	$10^+ \to 11^-$	0.3(1)	$< 8\times10^{-7}$	
	4195	$12^+ \to 11^-$	0.8(1)	$1.1(3)\times10^{-8}$	
	4485	$10^+ \to 9^-$	1.0(1)	$< 4\times10^{-7}$	
	(3710)	$12^+ \to 12^-$		$< 4\times10^{-9}$	
	(4076)	$10^+ \to 10^-$	< 0.2		
	(4205)	$10^+ \to 10^+$			
	(4408)	$12^+ \to 12^+$			$< 3\times10^{-7}$
^{194}Hg	4980	$11^{(-)} \to 12^+$	3.7(8)	$< 2\times10^{-7}$	$< 2\times10^{-5}$
Band 3	5032	$11^{(-)} \to 10^+$	2.0(6)	$< 1\times10^{-7}$	$< 1\times10^{-5}$
17.7 ± 1.4					

Table 1: Reduced transition rates for ^{194}Hg SD decay-out primary transitions.

In ^{192}Hg, only one primary transition can be tentatively placed as part of a two-step decay. ^{194}Hg band 1 exhibits a robust network of strong one-step transitions to the yrast line. In ^{194}Hg band 2, there are no reputable candidates for primary decays, and band 3 has two one-step decays directly to the yrast line. Clearly the primary decays are governed by some form of transition strength fluctuation, although whether it has a Porter-Thomas distribution is an open question which we hope to answer in the near future.

One interesting observation is that in the decay of ^{194}Hg band 1, four dipole transitions with $\Delta J = \pm 1\hbar$ are observed. However, there was no evidence for $\Delta J = 0$ transitions to yrast states, with or without a parity change. The non-observation of the $\Delta J = 0$ transitions may hint at the persistence of some quantum number (beyond spin and parity) in the ND* states at excitations of ~ 4.3 MeV above yrast. It is interesting to note that the Clebsch-Gordon coefficient $\langle J, 0; 1, 0 | J, 0\rangle$ is identically 0 for all J. One might expect this to be relevant, for example, to $K = 0$ components in the intrinsic frame. SD band 1 is very likely a $K = 0$ band, and one might speculate that if it coupled only to the $K = 0$ components of the hot ND* states, and if in turn the near-yrast states are mostly $K = 0$, then dipole transitions with no spin change might be suppressed.

In conclusion, a new study of the primary decays of the SD states of ^{194}Hg has shown that the level fed by the 262 keV transition of band 3 is a $J^\pi = 11^-$ state at an excitation energy of 7.455 MeV. This gives band 3 an excitation energy of ~ 0.8 MeV relative to band 1 at zero rotational frequency. The spins of the states in band 3 are likely $1\hbar$ higher than those in ^{192}Hg band 1 that emit γ rays of the same energy. The transition rates for the primary transitions are very retarded, typically 10^{-8} Weisskopf units.

1. P.J. Twin *et al.*, Phys. Rev. Lett. 57, 811 (1986).
2. A. Ataç *et al.*, Phys. Rev. Lett. 70, 205 (1993).
3. R.G. Henry *et al.*, Phys. Rev. Lett. 73, 777 (1994).
4. M.J. Brinkman *et al.*, Phys. Rev. C 53, R1461 (1996).
5. T.L. Khoo *et al.*, Phys. Rev. Lett. 76, 1583 (1996).
6. A. Lopez-Martens *et al.*, Phys. Lett. B380, 18 (1996); K. Hauschild *et al.*, these proceedings.
7. L.M. Bollinger, Phys. Rev. C 2, 1951 (1970).
8. R. Bengtsson and S. Frauendorf, Nucl. Phys. A327, 139 (1979).
9. T. Nakatsukasa *et al.*, Phys. Rev. C 53, 2213 (1996), and these proceedings.
10. M.A. Riley *et al.*, Nucl. Phys. A512, 178 (1990).
11. R. Wyss, W. Satula, W. Nazarewicz and A. Johnson, Nucl. Phys. A511, 324 (1990).
12. E.F. Moore *et al.*, private communication.

Observation of the Single Step Links of the Yrast Superdeformed Band in ^{194}Pb

F. Hannachi[1], A. Lopez-Martens[1], A. Korichi[2], S Leoni[3], C. Schück[1], E. Gueorguieva[1], Ch. Vieu[1], B. Haas[4], R. Lucas[5], A. Astier[6], G. Baldsiefen[7], M. Carpenter[8], G. de France[4], R. Duffait[6], L. Ducroux[6], Y. Le Coz[5], Ch. Finck[4], A. Gorgen[7], H. Hübel[7], T.L. Khoo[8], T. Lauritsen[8], M. Meyer[6], D. Prévost[4], N. Redon[6], C. Rigollet[4], H. Savajols[4], J.F. Sharpey-Schafer[9], O. Stezowski[4], Ch. Theisen[5], U. Van Severen[7], J.P. Vivien[4], A.N. Wilson[10]

[1] *CSNSM, IN2P3-CNRS, bat 104-108, F-91405 Orsay, France*
[2] *IPN, F-91406, Orsay Cedex, France*
[3] *Niels Bohr Institute, 4000 Roskilde, Denmark*
[4] *CRN, IN2P3-CNRS, F-67037 Strasbourg, France*
[5] *DAPNIA SPhN, CEA Saclay, 91191 Gif sur Yvette, France*
[6] *IPN, IN2P3-CNRS and Univ. Lyon-1, F-69622 Villeurbanne Cedex, France*
[7] *ISKP, Universitat Bonn, D-53115 Bonn, Germany*
[8] *ANL, Argonne, Illinois 60439, USA*
[9] *NAC, PO Box 72, Faure, ZA-7131 South Africa*
[10] *Oliver Lodge Laboratory, University of Liverpool, PO Box 147, L69 3BX UK*

Abstract

The EUROGAM array has been used to investigate the decay out of the yrast superdeformed (SD) band in ^{194}Pb. Eigth single step decays from the lowest observed SD states to low-lying states at normal deformation (ND) have been identified. From this observation, the excitation energy (4877 ± 1.5 keV) and the spin (6^+) of the lowest observed SD state in ^{194}Pb are established.

Superdeformation in lead nuclei was first discovered in 1990 in two independent experiments, using respectively the Osiris array in Berlin and the Hera array at LBL [1, 2]. The yrast SD band in ^{194}Pb was found as a sequence of 12 transitions with energies ranging between 169 keV and 602 keV and an intensity of 1 % relative to the the 2^+ - 0^+ 965 keV transition. The survival of the SD band down to very low rotational frequency (and therefore low spin) and the substantial intensity of the band together with the fact that the level density in the first well of this nucleus is reduced due to the close proton shell Z=82 already indicated that this nucleus should be a good candidate to investigate the decay out of the SD band. Several attempts have been made in order to find the linking transitions between the superdeformed (SD) and the normally deformed (ND) states in this nucleus [3, 4, 5]. On figure 1 are shown the results of a comparative study of the decay-out spectra of the ^{192}Hg and ^{194}Pb yrast SD bands, using the fluctuation analysis method [6, 7]. The data were obtained with the Eurogam1 array which consisted of 45 compton suppressed Ge detectors [9, 10]. Excited states in ^{192}Hg and ^{194}Pb were populated in the ^{160}Gd(^{36}S,4n) and ^{184}W (^{16}O,6n) reactions at beam energies of 159 MeV and 113 MeV respectively. The beam was provided by the 20 MV tandem Van de Graaff accelerator of the Nuclear Structure Facility at Daresbury Laboratory. The targets consisted of 1 mg/cm^2 of ^{160}Gd (enriched to 98.7%) deposited on a 10 mg/cm^2 gold backing

in the ^{192}Hg experiment and of two stacked 325 μg/cm^2 enriched ^{184}W deposited on 10 μg/cm^2 Carbon backing in the ^{194}Pb experiment. Two data sets consisting of 660 $\times$ 10^6 (^{192}Hg) and 860 $\times$ 10^6 events (^{194}Pb) were recorded on tape with the requirement that at least 5 unsuppressed Ge detectors fired in prompt coincidence. The μ_2/μ_1 fluctuation spectra obtained for ^{192}Hg and ^{194}Pb in the 1 to 3 MeV transition energy region are shown in the bottom of figure 1, in comparison to the intensities of the discrete peaks which we proposed as possible decay out transitions (top part of figure 1). As one can see, strong fluctuations were observed in the case of ^{194}Pb which were correlated with the measured discrete peak intensities, while in the ^{192}Hg, not only was the fluctuation spectrum more smooth and closer to the statistical limit, but also the measured peak intensities were weaker, which indicates a higher degree of fragmentation in the statistical decay. This provided strong indications that a search for discrete linking transitions would be more promising in ^{194}Pb than in ^{192}Hg.

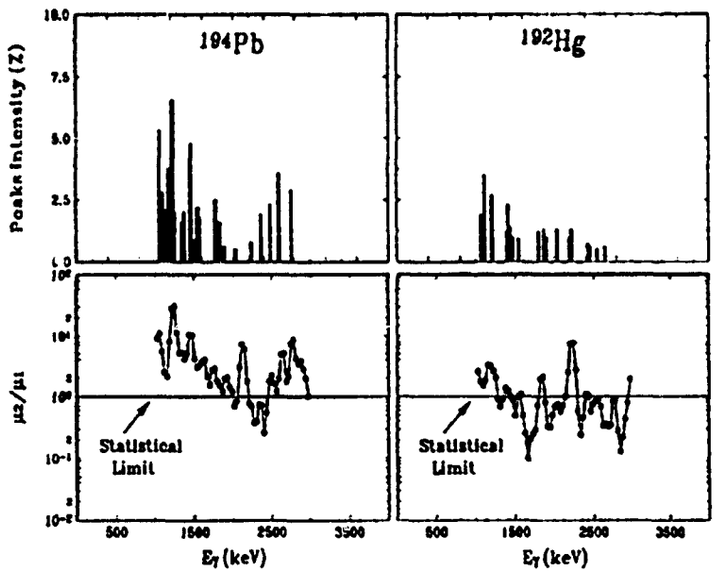

Figure 1: The top part of the figure shows the intensities of the lines proposed as decay out transitions in the 1 to 3 MeV region, normalized to 100% in the SD band plateau region, for both ^{194}Pb (left part) and ^{192}Hg (right part). The bottom of the figure shows the μ_2/μ_1 fluctuation spectra calculated on basis of triple SD gated spectra.

We have recently investigated again the deexcitation of the SD band in ^{194}Pb using the Eurogam2 array in similar experimental conditions (same target, beam and beam energy). Eurogam2 consists of 54 Compton-suppressed Ge detectors. Thirty of these are 73 % efficiency coaxial Ge detectors located in the forward and backward hemispheres, and 24 are clover detectors located in two rings near 90 degrees relative to the beam direction [11, 12]. The higher statistics collected in this experiment (10^9 triple and higher-fold events) has allowed the identification of some high energy transitions connecting the SD

states to the ND states of the first well in ^{194}Pb. These are visible around E_γ = 2.5 MeV in figure 2.

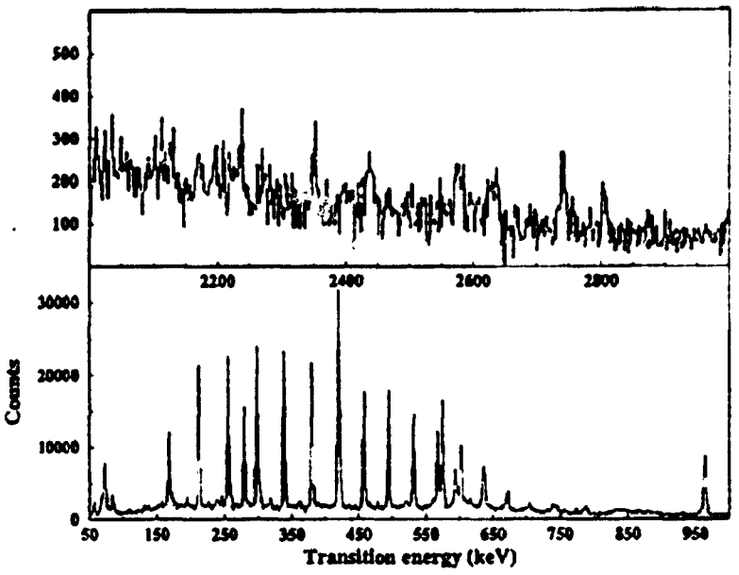

Figure 2: Background subtracted triple SD gated spectrum of the yrast SD band of ^{194}Pb showing the high energy transitions directly connecting the SD and the ND levels. The background is a fraction of the corresponding double SD gated spectrum.

Their concidence relationships establish the level scheme presented in figure 3 for the deexcitation of the yrast SD band [13].
The excitation energy of the last observed SD state is measured for the first time as 4877 keV ± 1.5 keV and its spin is uniquely determined to be $6\hbar$. This is in very good agreement with the theoretical predictions [14, 15]. The SD band decay is mainly of a statistical nature [6, 16, 17, 18], that is, it proceeds via a quasi-continuum of transitions and resolved lines (for less than 15% of the SD band intensity) and both positive and negative parity states are populated. The transition strengths have been obtained for the decay transitions under the reasonable assumption of a dipole nature (it was not possible with the available statistics to measure their angular distributions). Assuming a constant quadrupole moment of 20 eb for the SD band [19], the lifetimes of the 8^+ and 6^+ SD levels can be obtained. From the branching ratios of the primary transitions, transition strengths ranging from 10^{-8} to $5\text{x}10^{-8}$ W.u. and from $1.5\text{x}10^{-6}$ to $5.3\text{x}10^{-6}$ W.u. have been obtained assuming E1 and M1 transitions respectively. These represent highly retarded transitions and indicate very small mixing between ND states and SD states at the point of decay. From the in-band / out-of-band intensity ratios, again assuming a constant quadrupole moment in the SD band and using a standard level density formula together with the GDR strength function of Bartholomew et al [20], it has been possible to deduce the mixing of the decaying SD states with the ND states. The α^2 values obtained are respectively 0.0016 and 0.005 for the 8^+ and 6^+ SD states.

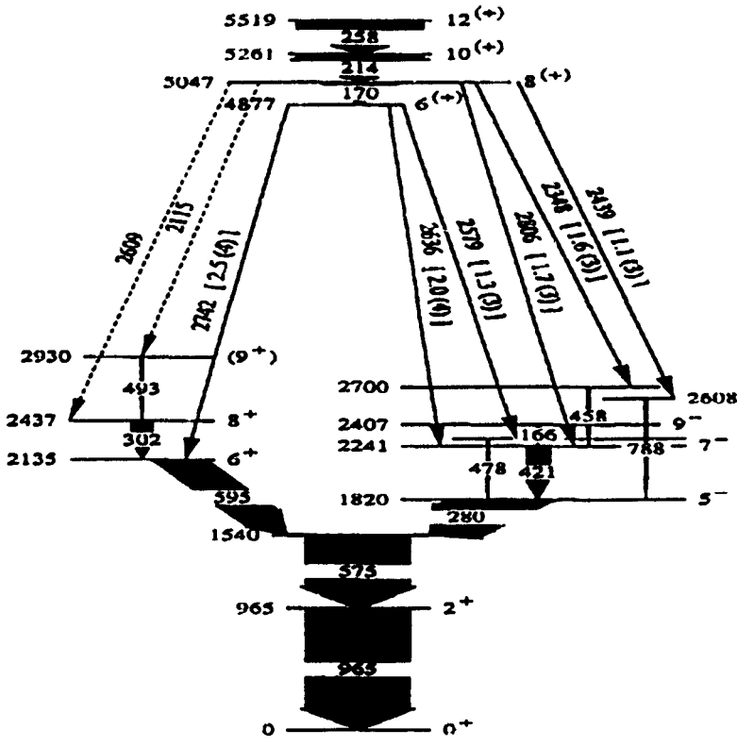

Figure 3: Partial decay scheme of the yrast SD band in ^{194}Pb. The precision on the new transitions and on the SD states energies is of the order of 1.5 keV. The intensities of the linking transitions are indicated in brackets (in % of the SD band intensity). The dashed arrows indicate tentative emplacements for the transitions.

The factor 3.2 increase of α^2 over one transition explains the sudden disappearance of the SD band at low rotational frequency.
In conclusion, by discovering eight high energy γ-rays directly connecting the SD states to the ND states in ^{194}Pb, the excitation energy and spins of the SD yrast states have been measured for the first time using the Eurogam2 array. This method, which was successfully used for the first time in the case of ^{194}Hg [21], allows, 10 years after the discovery of superdeformation at high spin, the precise measurement of some of the most fundamental properties of the SD nuclei.

Acknowledgements
The EUROGAM project is funded jointly by the EPSRC (UK) and the IN2P3 (France). We would like to thank all the staff members of the Vivitron, all the EUROGAM collaborators involved in the setting up of the array and R. Darlington from the Daresbury Laboratory for making the targets. One of us (ANW) acknowledges the receipt of an EPSRC postgraduate studentship. Work at Bonn was supported by the BMBF (Germany), under contract 06BN664-I, and at Argonne by the U.S. DOE, Nuclear Physics Division, under contract W-31-109-ENG-38.

References

[1] K. Theine et al., Z. Phys. A336(1990)113

[2] M. Brinkman et al., Z. Phys. A336(1990)115

[3] F. Hannachi et al., Proc of Int. Conf. on Nucl. Struct. at high angular momentum, Ottawa May 18-21 1992 and Nucl. Phys. A557 (1993)75c-82c

[4] W. Korten et al., Z. Phys. A344 (1993)475

[5] M. Brinkman et al, Phys Rev C53 (1996)R1461

[6] A. Lopez-Martens et al., Phys. Rev. Letts 26(1996)1707, and contribution to this conference

[7] T. Dossing *et al.*, to be published in Physics Reports

[8] B. Herskind and S. Leoni, Nucl. Phys. A520 , (1990) 539c-554c

[9] P.J. Nolan, Nucl. Phys. A520 (1990) 657

[10] F. A. Beck, Prog. Part. Nucl. Phys. 28 (1992) 443

[11] G. Duchêne et al., Proc of Int. Conf. on Nucl. Struct. at high angular momentum, Ottawa May 18-21 1992 and Nucl. Phys. A557 (1993)359-375

[12] P.M. Jones et al., NIM A362 (1995) 556

[13] A. Lopez-Martens et al., Phys. Lett. B380(1996)18

[14] S.J. Krieger et al., Nucl. Phys. A542(1992)43

[15] M. Girod et al., cont. to the Int. conference on nuclear structure around the turn of the century, Crete, Greece, July 1996

[16] E. Vigezzi et al., Phys. Lett. B249(1990)163

[17] R.G. Henry et al., Phys. Rev. Lett. 73 (1994) 777

[18] T. Lauritsen et al., contribution to this conference

[19] P. Willsau et al., Z. Phys. A344(1992)351 and R. Krucken et al., Phys. Rev. Letts 73(1994)3359

[20] Bartholomew et al., Adv. Nucl. Phys. 7(1973)229

[21] T. L. Khoo et al., Phys. Rev. Lett. 76(1996)1583

Primary transitions between the Yrast Superdeformed Band and Low-lying Normal deformed states in ^{194}Pb

K. Hauschild, L.A. Bernstein, J.A. Becker, D.E. Archer, R.W. Bauer
Lawrence Livermore National Laboratory, Livermore, California 94550

D.P. McNabb, J.A. Cizewski, K.-Y. Ding, W. Younes
Rutgers University, New Brunswick, New Jersey 08903

R. Krücken, G.J. Schmid, R.M. Clark, P. Fallon, I.-Y. Lee, A.O. Macchiavelli, R. MacLeod, R.M. Diamond, M.A. Deleplanque, F.S. Stephens
Nuclear Science Division, Lawrence Berkeley Laboratory Berkeley, California 94720

W.H. Kelly
Iowa State University, Ames, Iowa 50011

The observation of one-step "primary" gamma-ray transitions directly linking the superdeformed (SD) states to the normal deformed (ND) low-lying states of known excitation energies (E_x), spins and parities (J^π) is crucial to determining the E_x and J^π of the SD states. With this knowledge one can begin to address some of the outstanding problems associated with SD nuclei, such as the identical band issue, and one can also place more stringent restrictions on theoretical calculations which predict SD states and their properties. This information may also lead to a more detailed understanding of the SD de-excitation process itself.

The resolving power of the new generation of 4π γ-ray spectrometers allows the prospect realizing this goal. Brinkman, *et al.*, used the early implementation of the GAMMASPHERE spectrometer array (32 detectors) and proposed a single, candidate γ ray linking the ^{194}Pb yrast SD band to the low-lying ND states in ^{194}Pb [1]. Using 55 detectors in the GAMMASPHERE array Khoo, *et al.*, observed multiple links between the yrast SD band in ^{194}Hg and the low-lying level scheme and conclusively determined E_x and J of the yrast SD states [2]. Here we report on an experiment in which Gammasphere with 88 detectors were used and the E_x and J^π values of the yrast SD states in ^{194}Pb were uniquely determined. Twelve one-step linking transitions between the yrast SD band and low-lying states in ^{194}Pb have been identified, including the transition proposed by Brinkman. These transitions have been placed in the level scheme of ^{194}Pb using coincidence relationships and agreements between the energies of the primary transitions and the energy differences in level spacings. Furthermore, measurements of angular asymmetries have yielded the multipolarities of the primaries which have allowed J^π assignments of the ^{194}Pb SD states to be unambiguously determined for the first time without *a priori* assumptions about the character of SD bands. A study performed in parallel to our work using the EUROGAM-II array reports similar, but somewhat less extensive, results [3].

The experiment was performed at the Lawrence Berkeley Laboratory 88-Inch Cyclotron facility. High-spin states in ^{194}Pb were populated following the ^{174}Yb(^{25}Mg,5n) reaction at E(^{25}Mg) = 130 MeV. Coincident γ rays emitted during the decay of these high-spin states were detected using the GAMMASPHERE array [4]. The isotopically enriched (>98%) ^{174}Yb target was 1.21-mg/cm^2 thick, and was evaporated directly onto a 6.13-mg/cm^2 Au backing. The signal-to-noise ratio of the SD primary γ rays is enhanced when a thick backing is used. (The lower-lying SD states have lifetimes that are longer than the characteristic stopping times of the evaporation residuals in the Au foil. Therefore, the linking transitions do not exhibit angle-dependent Doppler shifts, or broadening, and the intrinsic detector lineshape is expected.) Approximately 7×10^9 events were recorded with suppressed Ge fold ≥ 4.

The search for linking transitions was performed using a RadWare cube [5], gated by at least one γ ray with an energy that corresponded to a ^{194}Pb yrast SD transition energy [7-11]. The SD-gate list excluded the 419.9-keV γ ray of the SD cascade due to its proximity to the 421.1-keV $7^- \rightarrow 5^-$ low-lying transition. In addition, the γ rays were required to be in prompt coincidence with respect to the beam pulse. Events were sorted with the Beausang correction, which ensured that the increments to the cube were not weighted by fold or gating conditions [6]. Energy and efficiency calibrations over the range 0.100 – 3.548 MeV were obtained from the standard ^{56}Co, ^{152}Eu and ^{182}Ta sources. Figure 1 illustrates two energy regions of a triple-gated, background subtracted spectrum for the yrast SD band in ^{194}Pb projected from this cube. All possible combinations of double gates on the SD lines between 170 – 532 keV, inclusive, were summed to produce this spectrum. Relative in-band intensities are given in Table 1; 56(4), 34(6) and 10(7)% of the SD band decay out occurs from the three lowest observed SD states, respectively. Figure 1(a) illustrates that a

number of γ-ray transitions from the low-lying ND states in ^{194}Pb [12], labeled by the corresponding $J_i^\pi \rightarrow J_f^\pi$, are in coincidence with the SD cascade. Twelve candidates for the discrete single-step transitions feeding into these low-lying ND states can be seen in the higher energy portion of the triple SD-gated spectrum, Figure 1(b). These transitions have energies in the range corresponding to those expected for the primary linking γ rays [13].

Coincidence relationships between these candidate primaries, the low-lying γ rays, and the yrast SD transitions in ^{194}Pb were used to verify which, indeed, are linking transitions, and to place them in the ^{194}Pb level scheme. We give two examples: (1) coincidence relationships for the 2743-keV primary transition were deduced from the background-subtracted spectra shown in Figure 2. Figure 2(a) was obtained by summing all double-gate combinations between the 2743-keV transition and the yrast SD band in ^{194}Pb. From this spectrum we determined that the 2743-keV γ ray depopulates the band below the 170-keV intra-band SD transition since the 170-keV line is observed. Another important feature is the enhancement of the 595-keV $6^+ \rightarrow 4^+$ low-lying yrast transition in comparison with Figure 1(a). Therefore, the 2743-keV transition decays into, or above, the state from which the 595-keV line depopulates. (2) Figures 2(b) and 2(c) present partial spectra obtained by a summation of double gates on the 595-keV and in-band SD transitions. It is apparent from these Figures that the 595-keV γ ray is in coincidence with the SD band, the 303-keV $8^+ \rightarrow 6^+$ transition and the 2116-, 2610- and 2743-keV primary transitions.

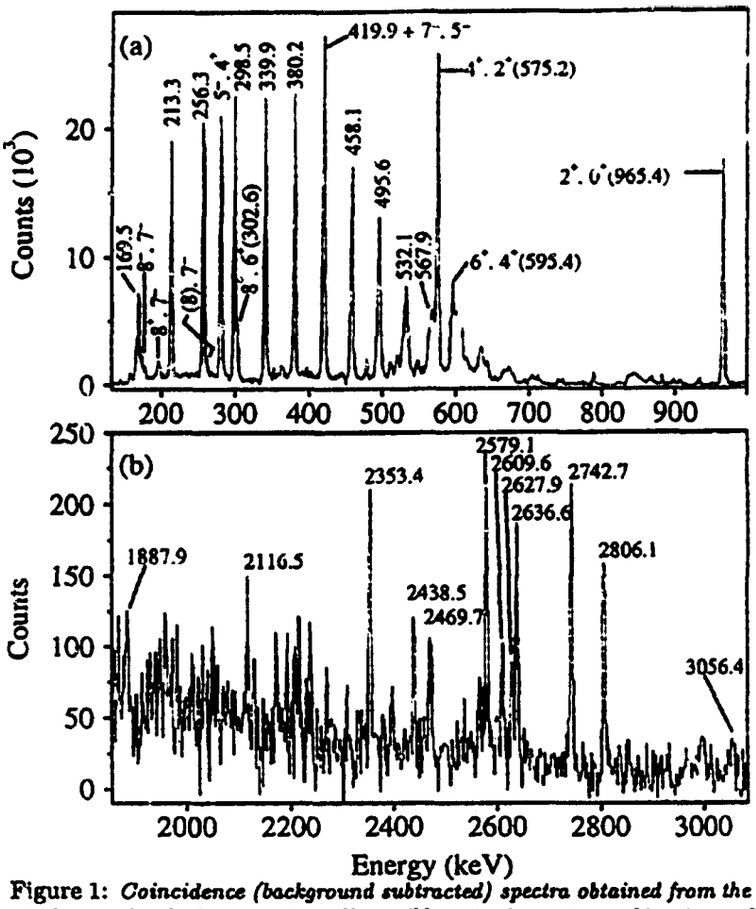

Figure 1: *Coincidence (background subtracted) spectra obtained from the singly-gated cube by summing all possible pairwise gate combinations of the 170 - 532 keV ^{194}Pb yrast SD transitions. (Exclusion of the 419.9-keV SD-line in the gate list used to create the cube results in it's apparent increased intensity.) The low-energy portion, panel (a), displays the yrast SD band and transitions arising from de-excitation of the low-lying ND states, while (b) presents the one-step transitions (primaries) directly linking the SD and ND states. Transition energies are labeled in keV. Yrast transitions in (a) are labeled by $J_i^\pi \rightarrow J_f^\pi$.*

Table 1: *The in-band SD transitions: γ-ray energies E_γ, relative intensities I_γ[a], intensity decaying out of the band I_{out}, asymmetry ratio R_{asym}, spin and parity information J^π, and multipolarities σL.*

E_γ (keV)	I_γ (%)	I_{out} (%)	R_{asym}	σL	favored σL	$J_i^\pi \rightarrow J_f^\pi$
380.20(5)	91(4)	-	1.42(5)	$\Delta L=1, \Delta J=0$ or $\Delta L=2, \Delta J=2$	E2	$18^+ \rightarrow 16^+$
339.90(5)	92(4)	-	1.40(5)	$\Delta L=1, \Delta J=0$ or $\Delta L=2, \Delta J=2$	E2	$16^+ \rightarrow 14^+$
298.49(3)	94(4)	-	1.47(5)	$\Delta L=1, \Delta J=0$ or $\Delta L=2, \Delta J=2$	E2	$14^+ \rightarrow 12^+$
256.32(3)	100(5)	-	1.40(5)	$\Delta L=1, \Delta J=0$ or $\Delta L=2, \Delta J=2$	E2	$12^+ \rightarrow 10^+$
213.26(3)	90(5)	10(7)	1.45(4)	$\Delta L=1, \Delta J=0$ or $\Delta L=2, \Delta J=2$	E2	$10^+ \rightarrow 8^+$
169.52(4)	56(4)	34(6)	1.48(8)	$\Delta L=1, \Delta J=0$ or $\Delta L=2, \Delta J=2$	E2	$8^+ \rightarrow 6^+$
-	-	56(4)	-	-	-	-

[a]Corrected for detector efficiency and electron internal conversion, and normalized to the intensity of the 256.3 keV transition.

Only 7 of the 12 candidate linking transitions could be placed with the adopted level scheme of ^{194}Pb compiled by Browne and Singh [12]. A 0.67 keV/channel RadWare cube was therefore sorted to build a more complete low-lying level scheme. The resulting decay scheme (see Figure 3) is essentially that of Refs. [14] and [15] with the addition of the 664- and 672-keV transitions observed in Ref. [16]. These two transitions depopulate states with $E_x = 2800$ and 2914 keV, respectively. Also, the 283-, 479-, 722- and 788-keV transitions observed in Ref. [16] were placed at $E_x = 2525$, 2299, 2609 and 3522 keV, respectively. Additional states were added at 3471 and 3374 keV. Eleven of the twelve candidate primaries were placed with the aid of the new decay scheme of ^{194}Pb; the placement of the 2470-keV line is tentative.

Multipolarities of the SD lines and the linking transitions were deduced from an empirical asymmetry ratio R_{asym}. Matrices were constructed which contained $\gamma-\gamma$ coincidences between any detector with: (1) detectors located at the three most "forward" (for) and "backward" (back) angles (Θ=17.3°, 31.7°, 37.4°, and 142.6°, 148.3° and 162.7° with respect to the beam line) and, (2) detectors at $\overline{90}°$ (Θ=69.8°, 79.2°, 80.7°, 90.0°, 99.3°, 100.3° and 110.2° with respect to the beam line). The asymmetry ratio $R_{asym} = I_\gamma(\text{for + back})/I_\gamma(\overline{90}°)$, multiplied for convenience by the ratio of the number of detectors at $\overline{90}°$ to the number at forward and backward angles, was deduced for relevant γ rays in these matrices. Mean R_{asym} values of known low-lying stretched $L=2$ and $L=1$ transitions are 1.35(3) and 0.71(2), respectively. R_{asym} values obtained for the SD and linking transitions are given in Tables 1 and 2, respectively. One should note that with these R_{asym} ratios it is not possible to distinguish between (1) $\Delta L=1, \Delta J=1$ and $\Delta L=2, \Delta J=0$ and (2) $\Delta L=1, \Delta J=0$ and $\Delta L=2, \Delta J=2$ transitions. Nevertheless, these measurements can be used to place *restrictions* on the primary multipolarities and, since J_f^π is known, limits on J_i^π (see Table 2: cols. 3-6). On comparing the possible J_i^π values deduced for each SD level from the measured linking transition anisotropies (see Table 2: col. 6), one finds that the two lowest SD can only be assigned $J^\pi = 6^+$ and $J^\pi = 8^+$, respectively. These assignments have been made without any assumptions about the SD band spin parity values. In addition, a mean value of $R_{asym} = 1.43(2)$ was measured for the intra-band SD transitions, consistent with the above J^π assignments, confirming their $E2$ character (see Table 1).

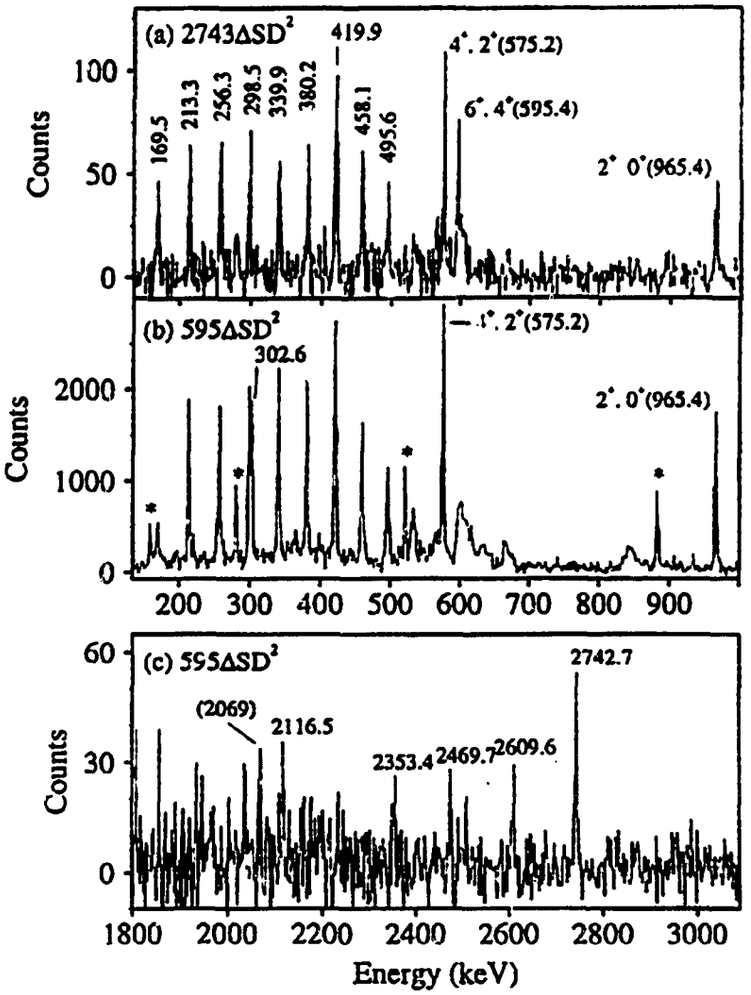

Figure 2: *Coincidence spectra projected from an SD-gated cube obtained from the summation of pairwise gates between the yrast SD band and (a) the 2743-keV transition and, (b,c) the 595-keV yrast $6^+ \rightarrow 4^+$ transition. An asterisk denotes a contaminant from ^{193}Pb brought in by the 213⊗595 keV gate. Transition energies are labeled in keV. Yrast transitions in (a) and (b) are labeled by $J_i^\pi \rightarrow J_f^\pi$.*

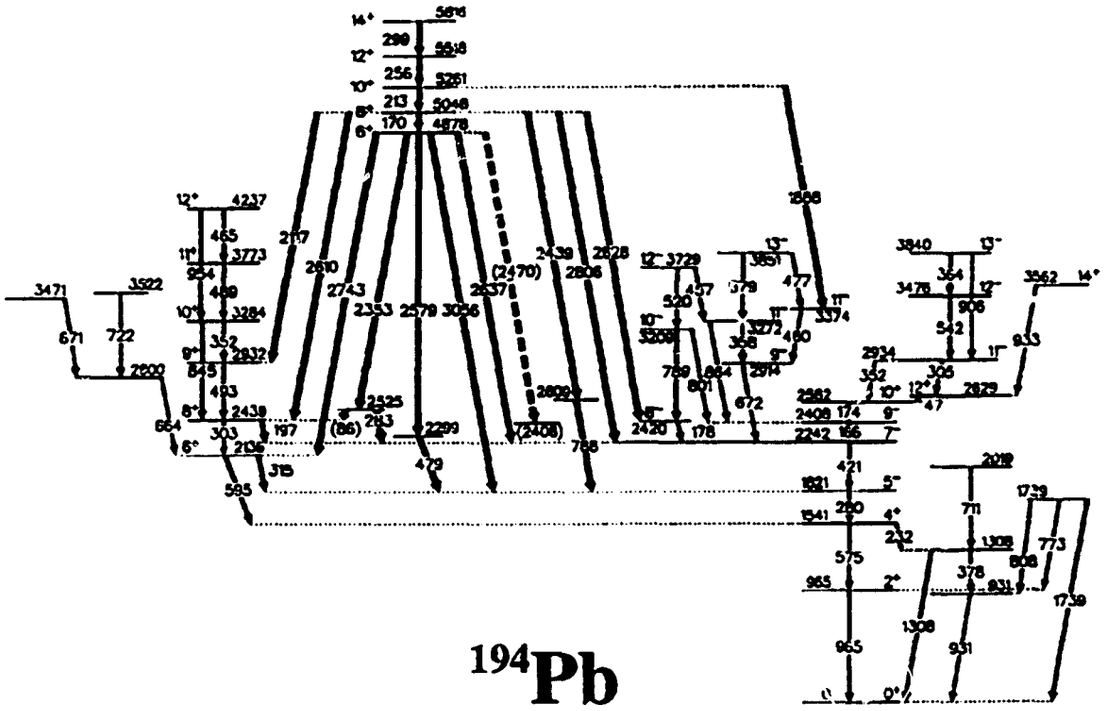

Figure 3: *Decay paths out of the ^{194}Pb yrast SD band. Levels are labeled by E_x in keV and J^π. Transition energies are labeled in keV. For clarity, only states in the immediate E_x and J^π region of the lowest observed SD levels are shown.*

Table 2: *The primary decay data: E_γ, I_γ, data R_{asym}, J^π, σL and reduced transition probabilities $B(\sigma L)$. I_γ is given as a percentage of the SD band population*[a].

E_γ (keV)	I_γ (%)	R_{asym}	σL	J_f^π	J_i^π	favored σL	$B(\sigma L)$ (W.U)
			Decays out of the third lowest SD level ($J_i^\pi = 10^+$)				
1887.9(3)	1.0(4)	0.9(1)	$\Delta L=1, \Delta J=1$ or $\Delta L=2, \Delta J=0$	11^-	$10^+, 11^-, 12^+$	(E1)	$5(2).10^{-8}$
			Decays out of the second lowest SD level: $J_i^\pi = 8^+$				
2116.5(4)	0.9(5)	0.3(1)	mixed M1/E2	9^+	$8^+, 9^+, 10^+$	M1/E2	-
2438.5(4)	0.9(4)	1.0(2)	mixed M1/E2	-	-	-	-
2609.6(4)	1.7(6)	1.4(3)	$\Delta L=1, \Delta J=0$ or $\Delta L=2, \Delta J=2$	8^+	$6^+, 8^\pm, 10^+$	M1	$2.3(9).10^{-6}$
2627.9(4)	1.3(6)	1.4(3)	$\Delta L=1, \Delta J=0$ or $\Delta L=2, \Delta J=2$	8^-	$6^-, 8^\pm, 10^-$	E1	$1.6(7).10^{-8}$
2806.1(3)	1.7(5)	0.7(1)	$\Delta L=1, \Delta J=1$ or $\Delta L=2, \Delta J=0$	7^-	$6^\pm, 7^-, 8^\pm$	E1	$1.7(6).10^{-8}$
			Decays out of the lowest SD level: $J_i^\pi = 6^+$				
2353.4(3)	2.8(6)	0.8(1)	$\Delta L=1, \Delta J=1$ or $\Delta L=2, \Delta J=0$	-	-	-	-
2469.7(4)	1.5(6)	1.4(3)	$\Delta L=1, \Delta J=0$ or $\Delta L=2, \Delta J=2$	-	-	-	-
2579.1(2)	3.0(6)	0.7(1)	$\Delta L=1, \Delta J=1$ or $\Delta L=2, \Delta J=0$	-	-	-	-
2636.6(2)	1.8(6)	0.8(2)	$\Delta L=1, \Delta J=1$ or $\Delta L=2, \Delta J=0$	7^-	$6^\pm, 7^-, 8^\pm$	E1	$\geq 12(4).10^{-8}$
2742.5(2)	3.3(6)	1.1(2)	mixed M1/E2	6^+	$5^+, 6^+, 7^+$	M1	$\geq 2.2(5).10^{-5}$
3056(1)	0.8(5)	-	-	5^-	-	E1	$\geq 4(2).10^{-8}$
TOTAL $I_\gamma = 21(2)\%$ of SD band intensity accounted for by primaries							

[a]Corrected for detector efficiency and normalized to the intensity of the 256.3 keV SD line.

These results have allowed the excitation energy of the yrast 6^+ SD state in ^{194}Pb to be unambiguously determined; we find $E_x(6^+)_{SD} = 4878.4(3)$ keV, in agreement with [3]. Assuming a smooth extrapolation to $J = 0$ [17], the bandhead of the SD band is estimated to have $E_x \simeq 4640.7(4)$ keV. This is in very good agreement with the Hartree–Fock–Bogoliubov calculations of Krieger, *et al.* [13], which predict $E_x(0^+_{SD}) =$ 4.86 MeV. For comparison, $E_x(0^+_{SD})$ is estimated to be 6.017 MeV in ^{194}Hg [2]. (The only other example in the $A \sim 190$ region of an SD cascade to have been unambiguously linked into the low-lying level scheme via primary transitions.) In this case, the same calculations predict the bandhead to lie at 5.00 MeV, approximately one MeV too low. Although the calculations are expected to predict the bulk properties of these nuclei very well it is not clear whether this is a significant discrepancy.

Reduced transition probabilities $B(\sigma L)$ for the primary decays have been calculated by relating the branching ratio of each primary to the in-band $B(E2)$ value assuming a constant in-band transition quadrupole moment $Q_t = 20.6(13)$ eb, derived from both Doppler Shift Attenuation [18] and Recoil Distance measurements [19]. $B(\sigma L)$ values are given in Table 2. Obtaining $B(\sigma L)$'s for the primaries depopulating the 6^+ SD state required the following additional assumptions about the unobserved $6^+ \rightarrow 4^+$ intra-band transition. Firstly, the energy (124.6 keV) was calculated from a smooth extrapolation of known transition energies. Secondly, the intensity of this transition is estimated to be *leq*1%. The resulting transition strengths indicate that the decay out of the SD states is highly retarded – typical values were found to be $B(E1) \sim 10^{-8}$ W.u. and $B(M1) \sim 10^{-6} - 10^{-5}$W.u. Similar results were obtained for the primary decays from SD states in ^{194}Hg as summarized in Table 3.

However, there are a number of striking differences between the character of the linking transitions observed in these two cases. From a comparison of Tables 2 and 3 it is apparent that many more primaries are observed in ^{194}Pb – 12 compared to 4 in ^{194}Hg. Also, in contrast to ^{194}Hg in which only E1's have been observed, the linking transitions in ^{194}Pb are of E1, M1 and mixed M1/E2 multipolarities. A surprisingly large proportion of the ^{194}Pb band intensity, 21(2)%, is accounted for by the direct one-step decays. Current calculations treating the decay from SD states as a statistical process estimate the branching ratio of single-step primaries to be ~5% compared to the unresolved statistical decays [20]. Indeed, recent results in ^{194}Hg indicate that only ~ 5% of the yrast SD band intensity is attributed to the primary decays [2]. The root cause of these differences reflects the greater phase space for decay available in ^{194}Hg compared to ^{194}Pb. The factors that contribute to this are: (1) The excitation energies of the SD bandheads in ^{194}Pb and ^{194}Hg are estimated to be 4.640 and 6.017 MeV, respectively. (2) The spin of the SD states at de-excitation is higher in ^{194}Hg. (3) The E_x of the ND states into which the primaries decay is ~2.4 and ~ 2.8 MeV for ^{194}Pb and ^{194}Hg , respectively. (4) ND ^{194}Pb is singly magic, and coexisting oblate and prolate minima at low excitation energy further increases the density of ND states in ^{194}Hg compared to ^{194}Pb. Therefore, the greater number of final states in ^{194}Hg leads to a more highly fragmented decay. One should also note that the decays of the shape isomers in ^{236}U [21] and ^{238}U [22] are also very different; the predominant γ-branches are $E1$ and $E2$, respectively. Evidently each case is different and any generalizations about the nature of the primary decays based on a singly case must be viewed cautiously.

In summary, eleven discrete one-step "primary" γ-ray transitions have been observed linking three members of the ^{194}Pb yrast SD band to low-lying ND levels. Anisotropy measurements have determined that the primary decays include both E1 and mixed M1/E2 transitions. $J^\pi = 6^+$ $E_x = 4878.4(3)$ keV and $J^\pi = 8^+$ $E_x = 5047.8(3)$ keV have been unambiguously assigned to the two lowest lying observed superdeformed states without making assumptions about the properties of SD bands. These results represent the first self-consistent J^π assignments to an SD band. Unique determination of the J^π and E_x values of SD bands

Table 3: *The primary decay data for* ^{194}*Hg.* E_γ, I_γ, *and* σL *taken from* [2].

E_γ (keV)	I_γ (%)	σL	$B(\sigma L)$ W.U.[a]
3489.3	1.4	E1	$2.6(6)\times10^{-8}$
3709.6	0.7	E1	$1.1(3)\times10^{-8}$
4195.2	1.2	E1	$1.3(3)\times10^{-8}$
4485.3	1.5	E1	$1.1(3)\times10^{-7}$[b]

[a] Assumes constant in-band $Q_t = 17.2(20)$ eb [23].
[b] Assumes $E_\gamma^{SD}(10^+ \rightarrow 8^+) = 211.7$ keV and $I_\gamma^{SD}(10^+ \rightarrow 8^+) = 3\%$ [24].

are needed to place more stringent restrictions upon theoretical calculations which predict the SD states and their properties, and in particular, to address the phenomena of "identical" bands. The yrast SD bands in ^{194}Pb and ^{192}Hg, and ^{194}Hg SD(3) are examples of "identical" bands. Although unambiguous assignments to the ^{194}Pb yrast SD band have been possible, this has unfortunately not been the case for ^{194}Hg SD(3) [25] and ^{192}Hg [26]. However, with the resolving power of the "complete" GAMMASPHERE and EUROBALL arrays, greater understanding of these properties is anticipated.

We would like to thank Torben Lauritsen for help with data acquisition and David Radford for RADWARE. Joanne Heagney of MicroMatter fabricated the targets. The 88–Inch Cyclotron crew is thanked for faultless operation. This work has been funded in part by the U.S. Department of Energy, under Contracts No. W-7405-ENG-48 (LLNL) and AC03-76SF00098 (LBNL), and the National Science Foundation (Rutgers and Iowa State).

References

[1] M. J. Brinkman, *Proceedings of the Conference on Physics from Large γ-Ray Detector Arrays*, Berkeley, California, p. 242, August 1994; Phys. Rev. C **53**, R1461 (1996).

[2] T. L. Khoo *et al.*, *Phys. Rev. Letts.* **76**, 1583 (1996).

[3] A. Lopez-Martens *et al.*, *Phys. Lett. B* **380**, 18 (1996); *Proceedings of the Conference on Nuclear Structure at the Limits, Argonne National Laboratory, 1996 (unpublished).*

[4] I. Y. Lee, *Nucl. Phys.* **A520**, 641c (1990).

[5] D. C. Radford, *Nucl. Instr. and Methods* **A361**, 306 (1995).

[6] C. W. Beausang, D. Prevost, M. H. Bergstrom, G. deFrance, B. Haas, J. C. Lisle, Ch. Theisen, J. Timàr, P. J. Twin, and J. N. Wilson, *Nucl. Instr. and Meth.* **A364**, 560 (1995).

[7] K. Theine *et al.*, *Z. Phys.* **A336**, 113 (1990).

[8] M. J. Brinkman *et al.*, *Z. Phys.* **A336**, 115 (1990).

[9] H. Hübel *et al.*, *Nucl. Phys.* **A520**, 125c (1990).

[10] W. Korten *et al.*, *Z. Phys.* **A334**, 475 (1993).

[11] B. J. P. Gall *et al.*, *Phys. Lett.* **B345**, 124 (1995).

[12] E. Browne and B. Singh, *submitted to Nucl. Data Sheets* (1996).

[13] S. J. Krieger, P. Bonche, M. S. Weiss, J. Meyer, H. Flocard, and P. H. Heenen, *Nucl. Phys.* **A542**, 43 (1992).

[14] D. Metha *et al.*, *Z. Phys.* **A345**, 169 (1993).

[15] M. G. Porquet *et al.*, *J. Phys.* **G20**, 765 (1994).

[16] P. Van Duppen, E. Coenen, K. Deneffe, M. Huyse and J. L. Wood, *Phys. Rev.* **C35**, 1861 (1987).

[17] J. A. Becker *et al.*, *Nucl. Phys.* **A520**, 187 (1990).

[18] P. Willsau *et al.*, *Z. Phys.* **A344** 351 (1993).

[19] R. Krücken *et al.*, *Phys. Rev. Lett.* **73**, 3359 (1994).

[20] T. Døssing *et al.*, *Phys. Rev. Letts.* **75**, 1276 (1995).

[21] J. Schirmer, J. Gerl, D. Habs, and D. Schwalm, *Phys. Rev. Letts.* **63**, 2196 (1989).

[22] J. Kantele, W. Stöffl, L. E. Ussery, D. J. Decman, E. A. Henry, R. J. Estep, R. W. Hoff, and L. G. Mann, *Phys. Rev.* **C29**, 1693 (1984).

[23] J. R. Hughes *et al.*, *Phys. Rev. Lett.* **72**, 3150 (1994).

[24] M. P. Carpenter *et al.*, *Proceedings of the Workshop on* GAMMASPHERE *Physics, Berkeley, California, 1995.*

[25] G. Hackman *et al.*, *Proceedings of the Conference on Nuclear Structure at the Limits, Argonne National Laboratory, 1996 (unpublished).*

[26] D. Ackermann *et al.*, *Proceedings of the Conference on Nuclear Structure at the Limits, Argonne National Laboratory, 1996 (unpublished).*

Decay Out of the Yrast and Excited Highly-Deformed Bands in the Even-Even Nucleus ^{134}Nd

C.M. Petrache[1], D. Bazzacco[1], S. Lunardi[1], C. Rossi Alvarez[1], R. Venturelli[1], P. Pavan[1], N.H. Medina[1], M.N. Rao[1], R. Burch[2], G. de Angelis[2], A. Gadea[2], G. Maron[2], D.R. Napoli[2], L.H. Zhu[2], R. Wyss[3]

[1] *Dipartimento di Fisica and INFN, Sezione di Padova, Padova, Italy*
[2] *INFN, Laboratori Nazionali di Legnaro, Legnaro, Italy*
[3] *Royal Institute of Technology, Physics Department Frescati, Stockholm, Sweden*

The resolving power achieved by the new generation of γ-ray detector arrays allows now to observe transitions with intensities of the order of $\sim 10^{-3}$ of the population of the final residual nucleus, making therefore feasible the study of the very weakly populated excited bands built on the superdeformed (SD) minimum or of the decay out of the SD bands. As a matter of fact, numerous excited SD bands have been observed in the different regions of superdeformation, which led to a deeper understanding of the single-particle excitation in the second minimum [1]. However, the lack of experimentally determined excitation energies, spins and parities for the SD bands prohibited to infer definitive conclusions. The first experimental breakthrough in the study of the decay out process has been achieved in the odd-even ^{133,135}Nd nuclei of the A=130 mass region [2,3,4]. There, the observation of the discrete linking transitions has been favored by the relatively higher intensity of the highly-deformed bands ($\sim$10%), as well as by the small excitation energy with respect to the yrast line in the decay-out region ($\sim$ 1 MeV). We call highly deformed (HD) the bands built on the second well in the A=130 mass region; they have elipsoidal shapes with major to minor axis ratios of 3:2 and a smaller deformation ($\beta \sim 0.3 - 0.4$) than that of the SD bands of the A=80, 150, 190 regions ($\beta \sim 0.5 - 0.6$). Unlike the A=150, 190 nuclei, which have nearly spherical shapes in the first minimum, the A=130 nuclei are prolate ($\beta \sim 0.2$) at normal deformation (ND). The transition from low to high deformation in these nuclei requires only one or two level crossings, and therefore induces much less fragmentation of the decay-out flux than in the other regions of superdeformation [5]. Very recently, Khoo et al. [6] discovered a few linking transitions in ^{194}Hg, which account for $\sim$ 5% of the decay-out strength. Following this first result in the A=190 region, other one step linking transitions have been observed in nuclei of the same region, which are reported in this conference. No discrete linking transitions have been so far observed in the A=80, 150 mass regions.

The HD bands in the even-even Nd nuclei are much weaker than in the odd-even ones, being of the order of 1% of the total population of the nucleus. The task to identify the discrete linking transitions is as difficult as that in the other regions of superdeformation. As a matter of fact, no linking transition have been so far observed in the even-even ^{134,136}Nd nuclei, where HD bands have been identified [7,8,9]. The configuration assigned to these bands are based on the behavior of the dynamical moments of inertia and therefore are only tentative. The identification of discrete linking transitions, which would establish the excitation energies, spins and eventually parity of the band levels, was highly requested, in order

to discriminate between the different theoretical scenarios proposed for the configurations of the HD bands. On the other hand, the study of the decay out mechanism in an even-even Nd nucleus was expected to help, through the comparison with the odd-even ones, the understanding of the interplay between the pairing correlations and mixing between the ND and SD states in the decay-out process [10,11].

With the goal of answering to the above questions, we have undertaken a study of the decay out in the even-even nucleus ^{134}Nd. The reaction used for populating the high spin states in ^{134}Nd was ^{28}Si+^{110}Pd at 130 MeV. The target consisted of two self-supporting foils of ^{110}Pd with a total thickness of 1.36 mg/cm^2. The GASP array with 40 Compton-suppressed Ge detectors and the 80-element BGO ball has been used for a coincidence measurement. Events were accepted when at least three suppressed Ge detectors and three detectors of the BGO ball fired in coincidence. A total of 1.9×10^9 events have been collected.

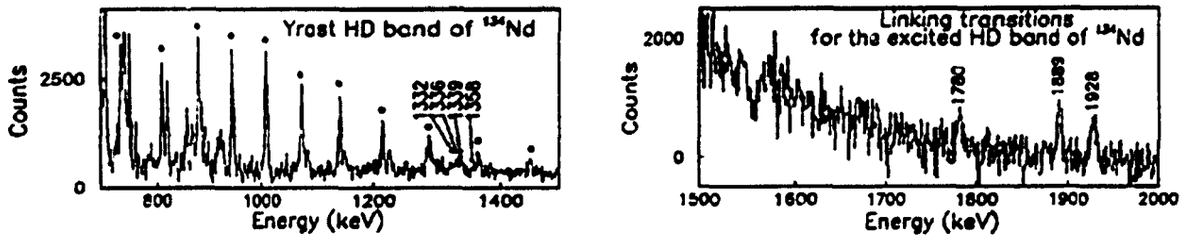

Figure 1: Left panel: doubly-gated spectrum of the yrast HD band in which the γ-rays of the HD band are indicated by asterisks. Right panel: high-energy part of the single-gated spectrum of the excited HD band.

The excited HD band has been extended at lower spins by two transitions (765.1 and 726.4 keV) and the two lowest γ-rays in the yrast HD band have been determined with higher precision (733.3 and 667.9 keV). Furthermore, transitions linking both HD bands to the ND states have been identified. Examples of spectra proving the coincidence relationships of the identified linking transitions with transitions in the HD bands and in the low-spin part of the level scheme are given in Figs. 1 and 2. A partial level scheme of ^{134}Nd relevant for the decay-out process is given in Fig. 3.

The spectra obtained by double-gating on decay-out transitions and on transitions in the HD yrast band, shown in the left panel of Fig. 2, clearly indicate the position of the linking transitions in the decay scheme. The gate on the 1332 keV γ-ray proves that it is in coincidence with the HD band and with the 740 keV γ-ray, whereas the gates on the 1336 keV and 1339 keV γ-rays prove that they are in coincidence with the 736 keV and 733 keV γ-rays, respectively. The sum of all these three couples of transitions gives 2072 keV, firmly establishing the energy difference between the third low-lying state of the HD band and the 18^+ state of band 3. Spectra obtained by double-gating on the decay-out transitions or on transitions of the excited HD band are shown in the right panel of Fig. 2. The gate on 726 keV γ-ray shows in coincidence only the 1889 keV high-energy transition, whereas the 765 keV γ-ray is in coincidence with all three high-energy linking transitions. The gate on the 1889 keV linking transition shows both the HD and the ND transitions. The spins of the HD states have been determined from the analysis of the DCO ratios using the procedure described e.g. in Ref. [12].

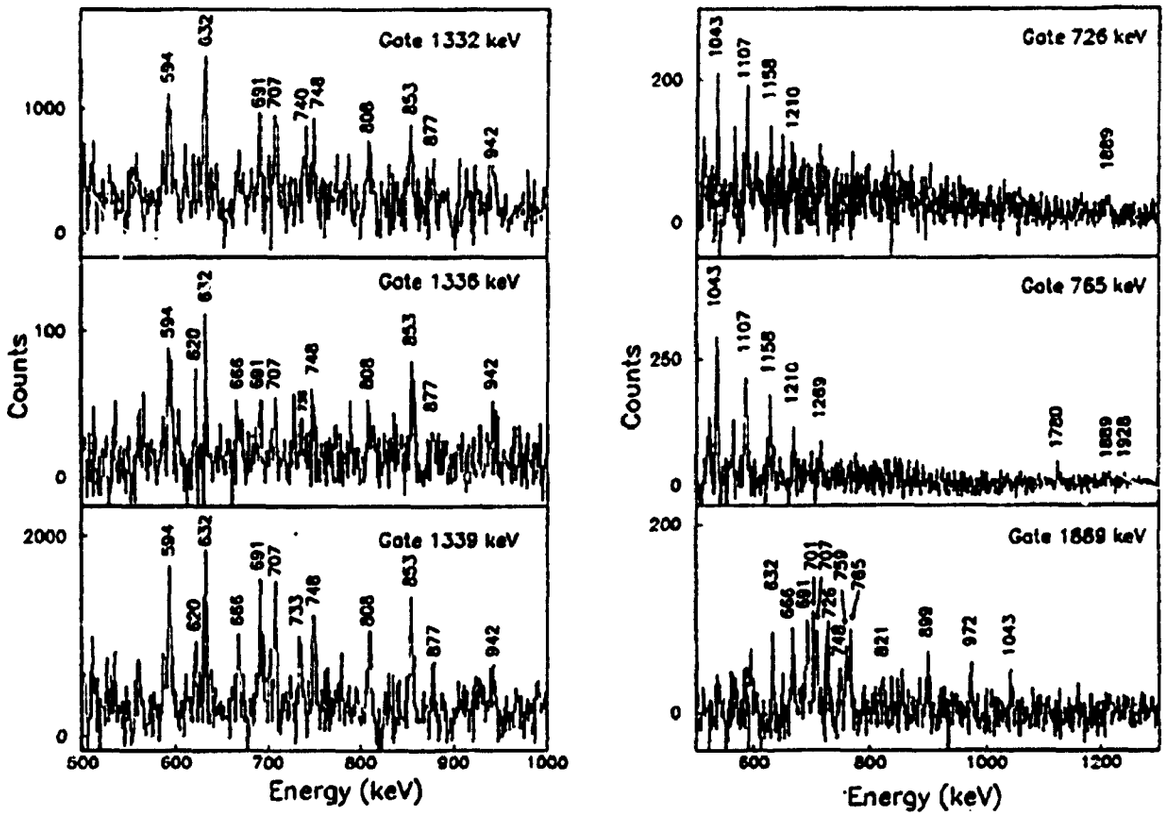

Figure 2: Left panel: doubly-gated spectra with gates on the transitions of the yrast HD band and on the 1332, 1336 and 1339 keV linking transitions. Right panel: doubly-gated spectra with gates on the transitions of the excited HD band and on the 726 and 765 keV in-band transitions and on the 1889 linking transition.

Because of the very weak intensity of the high-energy linking transitions, definite values of their DCO ratio could not be obtained. However, the linking transitions of the yrast HD band show strong 90°-34° anisotropy when gating on all in-band E2 transitions and therefore their dipole character is established. For the 736 and 740 keV γ-rays which are strongly contaminated, no DCO ratios could be obtained. They are assumed to have $\Delta I=2$, E2 character. The negative parity indicated in parenthesis for the yrast HD band accounts for the theoretically assigned configuration (see discussion below). The linking transitions of the excited HD band do not show significant anisotropy between 90° and 34°; this is consistent with a $\Delta I=2$, E2 character and leads to even spins and positive parity. The present measured energies and spins of the HD band-head levels determine their excitation energy relative to the yrast ND line in the decay-out region, which is ~1100 keV for the yrast HD band and ~1200 keV for the excited HD band.

Two different types of decay-out pathways are observed experimentally: that of the excited HD band, which most likely consists of stretched E2 transitions, and that of the yrast HD band, where the decay out proceeds via E2 and E1 transitions. For the 1780 and 1928 keV linking transitions of the excited HD band we estimated the B(E2)-strengths from the ratio between the decay-out and the in-band (726 keV) transition intensities by a simple energy scaling of the transition operators. Assuming an in-band B(E2)-strength of 400 W.u., similar to that measured for the HD band in the neighboring ^{133}Nd nucleus [13], B(E2)-strengths

of the order of 1 W.u. are obtained for the linking transitions. Such sizable out-of-band strengths clearly indicate a spread of the ND states into the HD minimum, which leads to a significant mixing between the HD and ND states. The final 1889 keV decay-out transition de-exciting the lowest observed HD state has somewhat stronger intensity than the other linking transitions. Since the energy of the in-band transitions is decreasing in contrast to that of the out-of-band ones, the enhanced decay-out strength is indeed expected. Examining the decay out of the yrast HD band one observes that the 21^- state decays into three 19^- levels, that are within 6 keV of excitation energy. It is difficult to give an exact assignment for the additional two states. However, knowing the limited number of HD configurations and the high level density at that excitation energy, we can rather firmly conclude that their origin involves states with ND shapes. The presence of even a very small interaction will lead to a sizable mixing of the corresponding wavefunctions, a fact which is indicated by the similar de-excitation pattern of the three $19^{(-)}$ states. The analysis of the out-of-band strengths of both HD bands in ^{134}Nd, together with the ~50% intensity of the observed discrete transitions, suggests that the decay-out mechanism in ^{134}Nd is only partially due to the stochastic mixing between the ND and HD states as proposed by Vigezzi et al. for the A=150, 190 regions [10]. In other words, it indicates that the quantum structure of the ND bands in the region where the HD bands decay is still of importance.

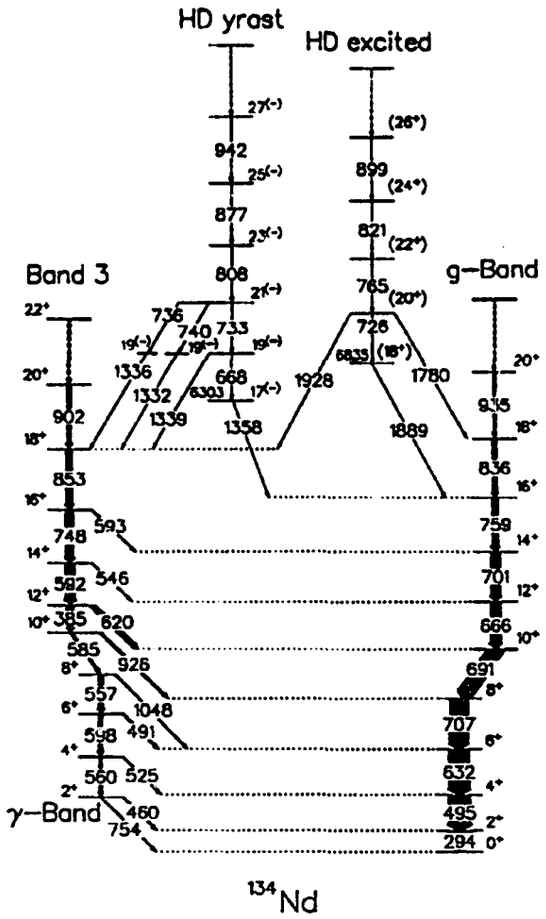

Figure 3: The level scheme of ^{134}Nd relevant for the decay out process.

The identification of one more state in the yrast HD band below the 19^- level, allows to extract a value of 0.11×10^{-6} (fm^{-2}) for the B(E1)/B(E2) ratio between the 668 keV (E2) and 1339 (E1) transitions. Assuming again a B(E2) value of 400 W.u., we get a B(E1)-strength of $\sim10^{-3}$ W.u., comparable to those observed in the heavy Ba-Sm region, for which stable octupole deformations have been predicted. Since the neutron Fermi-surface at high deformation is almost between the $f_{7/2}$ and $i_{13/2}$ orbitals and the HD yrast band of ^{134}Nd is assumed to involve the $\nu i_{13/2}-h_{9/2}/f_{7/2}$ configuration [7], one can indeed expect octupole couplings to be present. Apparently, the enhanced deformation has a similar effect as an increase of the neutron number.

Possible configurations of the HD bands of ^{134}Nd were already discussed in Ref. [7] in terms of occupation of the available Nilsson orbitals at high deformation. In order to interpret the present more detailed informations, we have performed new calculations for ^{134}Nd within the cranked Strutinsky approach based on a Woods-

Saxon potential including pairing interaction [14,15]. Each configuration is treated diabatically, thus avoiding unphysical level crossings between different structures.

As established previously [7], a proton gap is present at Z=60 for deformations ranging from $\beta_2 \approx 0.20$ to 0.37, which cover the quadrupole deformations of the ND and HD states. The occupied proton orbitals do not encounter therefore any level crossing in the collective path from high to low deformation. The situation is different for neutrons, in that a pair of particles is moved from the up-sloping $[404]7/2^+$ Nilsson orbit into the down-sloping $[541]1/2^-$ one when the deformation is changing from ND to HD (see also the Fig. 3 in Ref. [7]). In addition, at least one neutron is moved from the $[402]5/2^+$ Nilsson state into the $[660]1/2^+$ ($i_{13/2}$) one. In our assignment, the excited HD band involves the $\nu i_{13/2} - [402]5/2^+$ configuration that is crossed at higher frequencies by the $\nu(i_{13/2})^2$ one, whereas the yrast HD band involves the $\nu i_{13/2} - \nu h_{9/2}/f_{7/2}$ configuration. The spins and parities indicated for the HD bands in Fig. 2 are in accord with these assignments. A more detailed discussion about the configurations of the different bands involving the neutron $i_{13/2}$ orbital can be found in Ref. [16].

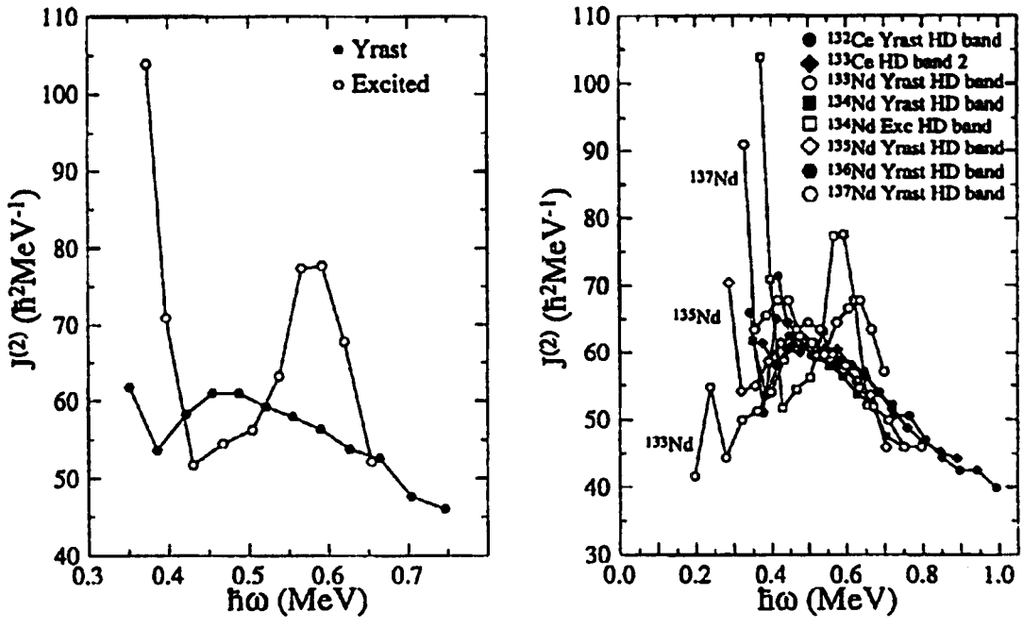

Figure 3: Left panel: dynamical moments of inertia of the yrast and excited HD bands of ^{134}Nd. Right panel: dynamical moments of inertia of HD bands in several nuclei of the A=130 mass region.

In the decay-out region, the dynamical moments of inertia of both HD bands show an irregularity which is also observed in all HD bands of the other Nd nuclei [2,3,4,9,12] and appears at rotational frequencies which decrease with decreasing neutron number. From the present calculations, but also from an inspection of the single-particle diagram (see e.g. Fig. 3 of Ref. [7]), one can easily see that the $\nu i_{13/2}$ intruder crosses the $\nu[402]5/2^+$ ($d_{5/2}$) Nilsson orbital in the frequency region where the increase in $\mathcal{J}^{(2)}$ is observed in the HD bands of Nd nuclei. As the variation of $\mathcal{J}^{(2)}$ is always associated with a change in structure of the corresponding rotational band, we associate the observed irregularity to the crossing between the $\nu i_{13/2}$ and $\nu d_{5/2}$ orbitals. The rise in $\mathcal{J}^{(2)}$ thus corresponds to a partial de-occupation

of the strongly deformation driving $\nu i_{13/2}$ intruder orbital. When no pairing is present, the transition between the states at different deformations (which form orthogonal sets) are severely hindered, since the related operators act only on a single particle. The presence of pairing correlations, on the other hand, helps the nucleus to tunnel between the minima.

A further insight into the role played by the pairing correlations in the decay-out process can be obtained from a comparison of the decay-out pattern in the even-even nucleus ^{134}Nd with the known decay out in the odd isotope ^{133}Nd. There, the crossing between the N=4 and N=6 ($i_{13/2}$) neutron orbitals is actually observed, but the HD band is traced to lower spin values. The reason for this difference can be related to the lower excitation energy of the $\nu i_{13/2}$ band in ^{133}Nd: in fact, the crossing here occurs when the HD band is rather cold and this explains why it continues at lower spins. In the case of ^{134}Nd the HD structures involve two-quasiparticle (qp) excitations that lie higher in energy with respect to the ground state, because of the pair gap. Moreover, the pairing correlations are smaller in the two-qp HD bands of ^{134}Nd than in the one-qp HD band of ^{133}Nd. As the decay out occurs at similar excitation energies above yrast in both HD nuclei, we can conclude that the mixing with the ND states plays a more important role than the slicing via the pairing interaction. In all cases however, static pair gaps are calculated to exist and pairing is believed to be essential for the decay towards the ND states.

In conclusion, the present results suggest that the decay out of the HD bands in ^{134}Nd is triggered by the crossing with the N=4 [402]5/2$^+$ Nilsson orbital, that has a smaller deformation than the corresponding N=6 intruder configuration. The crossing favours the mixing with the ND rotational bands strongly enhancing the decay-out process and weakening the in-band transition strength. The HD band becomes fragmented and looses part of its character. The intensity of the decay-out transitions increases when the spin of the HD state decreases, indicating enhanced ND amplitude in the wavefunction when going down the band. Lifetime measurements of the HD bands are crucial to further elucidate the decay-out process.

References

1) W. Nazarewicz, R. Wyss and A. Johnsson, Nucl. Phys. **A503**, 285 (1989).
2) E.M. Beck et al., Phys. Rev. Lett. **58**, 2182 (1987).
3) M.A. Deleplanque et al., Phys. Rev. **C52**, R2302 (1995).
4) D. Bazzacco et al., Phys. Lett. **B309**, 235 (1993).
5) J. Dudek et al., Phys. Rev. **C38**, 940 (1988).
6) T.L. Khoo et al., Phys. Rev. Lett. **76**, 1583 (1996).
7) C.M. Petrache et al., Phys. Lett. **B335**, 307 (1994).
8) R.M. Clark et al., Phys. Lett. **B343**, 59 (1995).
9) C.M. Petrache et al., Phys. Lett. **B373**, 275 (1996).
10) E. Vigezzi, R.A. Broglia and T. Døssing, Phys. Lett. **B249**, 163 (1990).
11) T. Døssing et al., Phys. Rev. Lett. **75**, 1276 (1995).
12) S. Lunardi et al., Phys. Rev. **C52**, R6 (1995).
13) S.A. Forbes et al., Z. Phys. **A352**, 15 (1995).
14) R. Wyss et al., Phys. Lett. **B215**, 211 (1988).
15) W. Satula and R. Wyss, Phys. Scr. **T56**, 159 (1995).
16) C.M. Petrache et al., Phys. Lett. **B**, in press.

Search for Linking Transitions in ^{143}Eu

F. Lerma, D.R. LaFosse, M. Devlin, D.G. Sarantites
Chemistry Department, Washington University, Saint Louis, MO 63130

S. Asztalos, R.M. Clark, P. Fallon, I.Y. Lee, A.O. Macchiavelli, R.W. Macleod
Lawrence Berkeley National Laboratory, Berkeley, CA 94720

C. Baktash, M.J. Brinkman, D. Rudolph
Oak Ridge National Laboratory, Oak Ridge, TN 37831

August 23, 1996

Abstract

Six SD bands were populated in ^{143}Eu and ^{144}Eu, two of which had not been previously observed. Sum spectra were generated to search for two step links from the yrast SD band in ^{143}Eu. However, no two step links were found. A single link from the SD band in ^{143}Eu was found at 3364 keV. The level where it feeds into has not been identified. Alpha-particle energy (E_α) spectra leading to the SD band and to normal states in ^{143}Eu were measured and a correlation was found between E_α and the level spin of the residual nucleus.

1 Experimental

An experiment was performed at the 88-inch Cyclotron at Lawrence Berkeley National Laboratory. A 230-MeV beam of ^{51}V and a ^{100}Mo 328μg/cm^2 self-supporting target were used to induce the ^{100}Mo(^{51}V,αxn) reaction, populating high-spin states in ^{143}Eu and ^{144}Eu. The Gammasphere array, which consisted of 57 Compton-suppressed high purity Ge detectors, was used to detect the gamma-rays emitted by the residual nuclei. The charged particles emitted by the compound nuclei were detected by the Microball, a 4π array consisting of 95 CsI(Tl) scintillators. The Microball allowed for good identification of the α particles as well as determination of α−particle energies. A total of 4.3×10^8 α−gated events were selected, 67% of which were 4-fold Ge-coincidences, the remaining events being 5-fold and higher Ge-coincidences. Partial recoil momentum correction was applied using the measured α−particle energies. This led to a more accurate Doppler shift correction which improved the γ−ray energy resolution.

2 Six SD Bands Identified

Six superdeformed (SD) bands were identified in the data. Three of them have been previously identified and assigned to ^{144}Eu [1]. Another SD band in the data is the known yrast SD band in ^{143}Eu [2]. The other two SD bands had not been observed before; one of these was assigned to ^{143}Eu, the other to ^{144}Eu. The new SD band in ^{144}Eu has identical transitions to those in the known SD band [2] in ^{143}Eu above 1 MeV γ−ray energies (see Fig. 1).

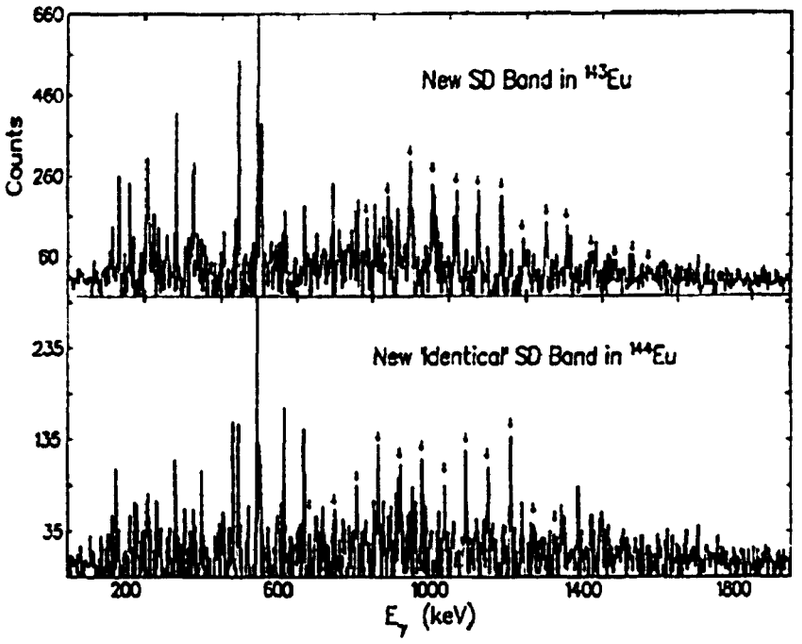

Figure 1: Double gated coincidence spectra of the two new SD bands in ^{143}Eu and ^{144}Eu. The arrows point to the transitions in the SD bands.

3 Linking Transitions

An attempt was made to link the yrast SD band in ^{143}Eu to the normal deformed (ND) states in the ^{143}Eu decay scheme by one-transition and two-transition links (see Ref. [2] for level scheme). A nucleus which decays out from an SD state to an ND state by a cascade of two discrete transitions may have many intermediate levels due to the high level density available, but the sums of the energies involved in a two step link must be sharply defined. The sums of pairs of γ−ray energies in coincidence with the SD band were generated in order to identify such links, and confirm previously reported [2] two step links in ^{143}Eu.

The sum spectra were created using two different methods. First, the events were gated from a list of SD transition energies; when a γ ray was found to be inside one of the gates, the remaining γ rays in the event were added pair-wise, and the sums incremented into a sum spectrum. This analysis was performed in a spike-free manner, as described in Ref. [3]. Not all of the available pairs of E_γ were incremented into sum spectra. E_γ pairs were incremented if the difference in E_γ was less than 1 MeV, and if both E_γ were greater than 300 keV. These criteria were employed in single, double, and triple gating of the data. The spectra produced in this first method were not background subtracted. Background subtracted n-fold-gated sum spectra were obtained by subtracting a portion of the (n-1)-fold-gated sum spectrum from the n-fold-gated sum spectrum. A portion of a sum spectrum of the ungated data became the zero-fold-gated sum spectrum subtracted from the singly-gated sum spectrum.

In the second approach, the data were single, double, and triple gated with a list of SD transitions into spike-free [3] E_γ−E_γ matrices. The matrices were background subtracted via the Palameta-Waddington method [4]. Individual (E_i, E_j) pairs were extracted from the background subtracted matrices and their sums were incremented into sum spectra, yielding single, double,

and triple gated background subtracted sum spectra. This method of background subtraction was successful in the 2-fold, and 3-fold gating, however, the single gated sum spectrum displayed an under-subtracted background. The background in the single gated matrix was therefore subtracted

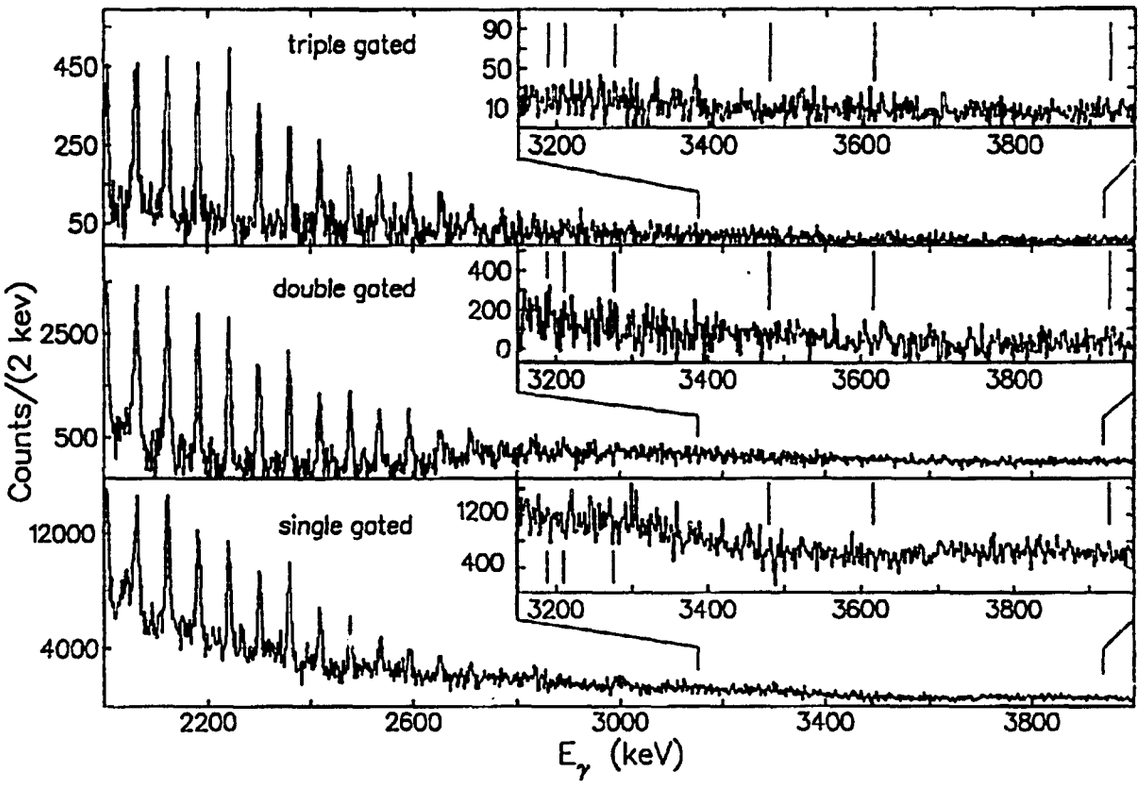

Figure 2: Spectra of the sums of individual (E_i,E_j) pairs from the backgound subtracted single, double, and triple gated matrices. The gates used were transitions in the yrast SD band in ^{143}Eu. Vertical lines in the expanded inserts show the energies of previously reported sum peaks.

by another method [5]. A background E_γ–E_γ matrix was sorted by single gating the data on E_γ which did not include SD band transition energies or any strong ^{143}Eu transitions. This background E_γ–E_γ matrix was subtracted from an SD single gated matrix. The resultant matrix was further background subtracted according to Ref. [4]. The single gated sum spectrum was extracted from this final matrix.

All sum spectra displayed large peaks corresponding to the sums of transitions in the SD band (see Fig. 2). A description of the pairing and summing details explains why these large peaks arise. If an event has met the gating conditions, it is more likely that the remaining γ rays in the event will also correspond to members of the SD band. The transitions in the SD band are evenly spaced at intervals of 59 keV to 61 keV, so that several combinations of pairs of transitions in the SD band will sum to the same peak in the sum spectrum, enhancing the intensity of the sums of transitions in the SD band.

The sum spectra generated by either method do not display the previously reported peaks [2]. There are some peak-like features in other regions of the spectra above 3 MeV which are not sums of transitions in the SD band, nor sums of transitions in the ND level scheme, and do not correspond to the previously reported sum links. The origin of these features in the sum spectra is not clear.

These features may be statistical fluctuations in the spectra. If these features were real sum links then they should appear at the same energies in all the fold spectra, yet most of them do not appear in more than one of the sum spectra, and no sum spectrum contained all of these peaks. As a result, the sum spectra do not seem to contain well-defined sum links. This does not imply that a significant fraction of the SD band does not decay out in two step links. The evidence suggests, however, that there are not strong two step links in ^{143}Eu, and if a significant fraction of the SD band does feed out by two step links then it may feed out through many weak, two step links which are unobservable in a sum spectrum at the available level of sensitivity.

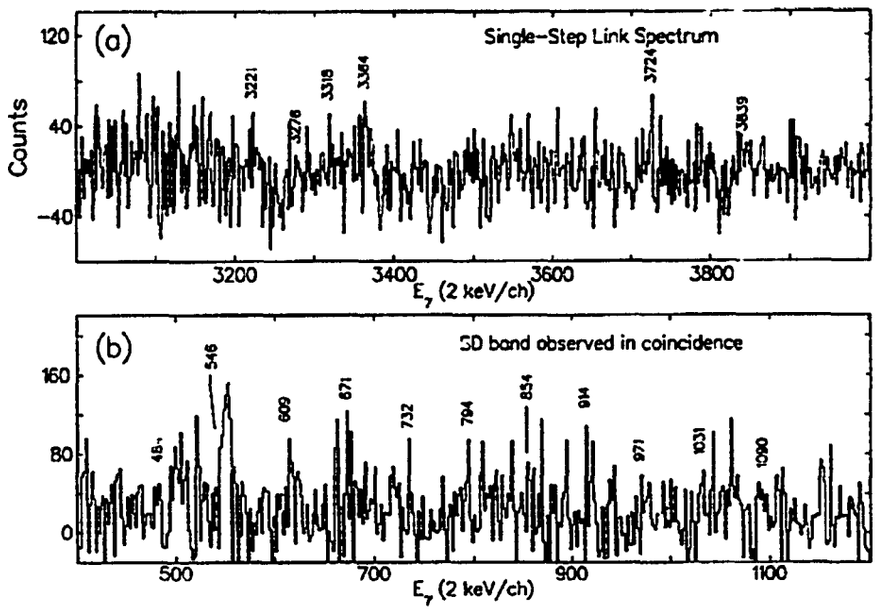

Figure 3: A sum of double gates on transitions in the yrast SD band produces the single-step transition link in panel (a). Transitions in the SD band are observed in the spectrum in panel (b) when the single gated matrix is gated on the 3364 keV single-step link. .

The same $E_\gamma - E_\gamma$ matrices, and $E_\gamma - E_\gamma - E_\gamma$ cubes were employed to investigate the transitions in the decay schemes of ^{143}Eu and ^{144}Eu. Several SD bands were identified, and the feeding-out of the yrast SD band in ^{143}Eu was studied. One single step linking transition was conclusively identified in ^{143}Eu. The linking transition was observed when a single gated matrix was gated on members of the SD band [see Fig. 3(a)]. The energy of the linking transition was found to be 3364±2 keV. This same transition could be observed in spectra generated by gating on the double and triple gated matrices, and double gating the cube. There were three other potential links around 3.5 MeV which could be in coincidence with the SD band. The coincidence of the 3364 keV peak with the SD band was confirmed when a gate at 3364 keV was paired with a list of SD transition gates into double gates, and the double gates were added, producing a spectrum which contained transitions in the SD band [see Fig. 3(b)]. Similar spectra were generated using the other three transitions in place of the 3364 keV gate, but the SD band did not appear in the spectra. So far, double gating directly on the 3364 keV transition in combination with the SD band has produced spectra with too few counts to help in determining the level into which the 3364 keV transition feeds.

4 Alpha-Particle Energy Spectra

In order to shed some light on the entry state regions responsible for the population of the SD states one can use α–particle spectra as a probe. If the SD states preferentially originate from high (E^*,I) entry states, then downward shifts in the E_α spectra are expected due to reduced available phase space.

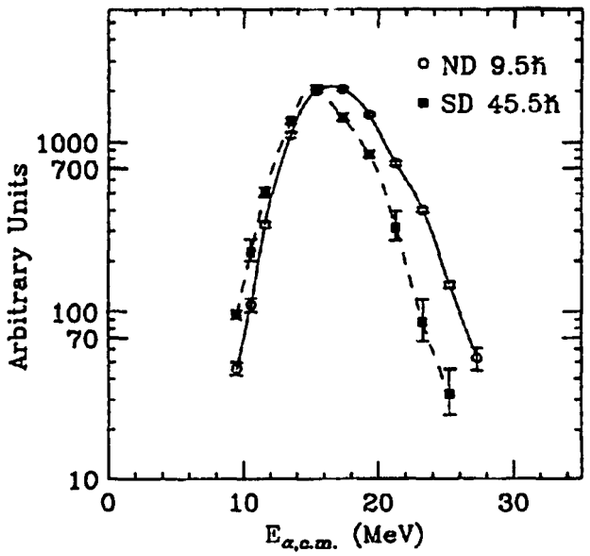

Figure 4: Alpha-particle energy spectra by doubly gating on transitions in the decay of ^{143}Eu. The spins corresponding to the depopulated levels by the measured γ transitions are indicated.

Alpha-particle energy spectra in coincidence with several ND transitions and SD transitions of ^{143}Eu were produced. The data were gated on E_α, in 2 MeV bins. A separate E_γ–E_γ–E_γ cube was then sorted from each E_α bin. Each cube was doubly gated on a list of transitions in the yrast SD band in ^{143}Eu to produce an E_α–E_γ–E_γ–gated γ spectrum. Additional spectra in coincidence with ND transitions were also produced by gating on ND transitions in ^{143}Eu. Background was subtracted from these spectra using standard methods [6]. The intensities of non-gated SD transitions were measured in the spectra gated on the SD band. Similarly, the intensities of non-gated ND transitions were measured in the spectra gated on ND transitions. This procedure was performed for all of the E_α–gated cubes, resulting in spectra representing the intensity of the transitions as a function of E_α. In all cases the second gating transitions were lower in the level scheme than the measured transition. Two such spectra coincident with the 443-keV (19/2 level) and 1266-keV (91/2 level) transitions from the ND and SD cascades, respectively, are shown in Fig. 4. A large downward shift in the α spectrum is indeed observed when the SD band is fed. A similar shift was seen in the α spectra for the SD band in ^{150}Tb [7].

In addition, the average α–particle energy showed a clear decrease in $< E_\alpha >$ with increasing spin of the populated level. This trend includes both ND ans SD levels and it is shown in Fig. 5.

Furthermore, the present data allowed a measurement of the relative population of the SD band as a function of E_α. It was found that the relative intensity of the SD band at E_α = 9.5 MeV was approximately 10 times higher than the relative population at E_α =25.5 MeV. The top 3 transitions in the SD band were identifiable only in the lower E_α–gated γ spectra, and were not observed in coincidence with higher energy α particles.

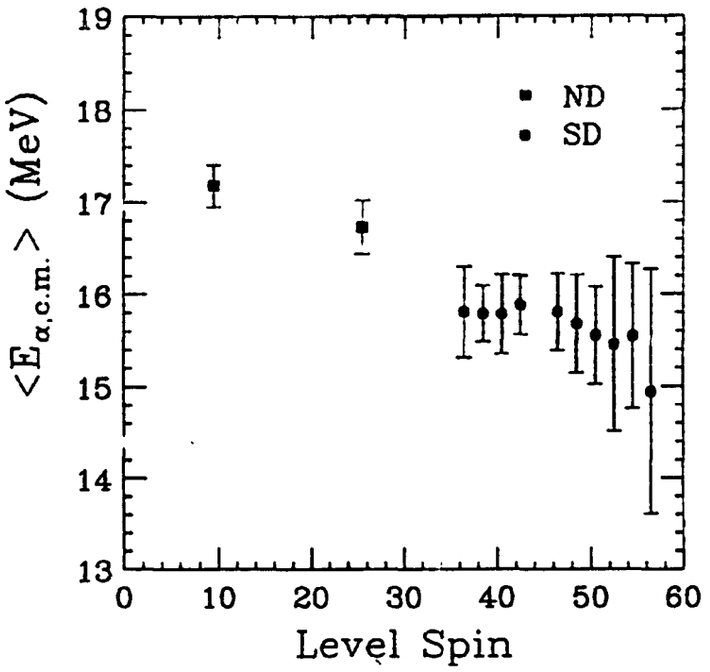

Figure 5: Average α−particle energy as a function of spin of the level (ND shown by full squares and SD by full circles) populated in ^{143}Eu.

5 Conclusion

An experiment was performed to study high-spin states in ^{143,144}Eu. Six SD bands were identified in the data, two of which had not been previously observed. A search for linking transitions revealed that there is a single link from the yrast SD band in ^{143}Eu to the ND states. However, this transition could not be placed definitively in the level scheme. In addition an analysis of sum spectra was performed. Previously reported sum-links were not observed in our data. There was also no evidence for other sum-links. A correlation has been observed between evaporated particle energies and the population of high spin states of ^{143}Eu in the ^{100}Mo(^{51}V, α4n) reaction. It was also found that the SD band was populated at the highest relative intensity and highest spin when the data were gated on the lower α−particle energies.

Work supported in part by the U.S. Department of Energy under grant number DE FG05-88ER40406.

References

[1] S.M.Mullins *et al.*, to be published.
[2] A. Ataç *et al.*, Phys. Rev. Lett., **70**, 1069, (1993).
[3] C.W. Beausang *et al.*, Nucl. Instrum. Meth. Phys. Res., A **364**, 560 (1995).
[4] G. Palameta and J.C.Waddington, Nucl. Instrum. Meth. Phys. Res.A **234**, 476 (1985).
[5] J.C.Waddington, private communication (1996).
[6] D.C.Radford, Nucl. Instrum. Meth. Phys. Res., A **361**, 297 (1995).
[7] G.Viesti *et al.*, Phys. Lett. B **382**, 24 (1996).

Single-Step Linking Transition from Superdeformed to Spherical States in ^{143}Eu

A. Ataç[1], A. Axelsson[1], I. Bearden[2], M. Bergström[2], B. Herskind[2], J. Nyberg[3], M. Palacz[4,5], J. Persson[1], M. Piiparinen[6], C. Fahlander[3], G. Hagemann[2], S. Leoni[2], M. Lipoglavšek[1,7], P. Nolan[8], E. Paul[8], N. Redon[9], L. Roos[1], G. Sletten[2], K. Tuček[3]

[1] Department of Radiation Sciences, Uppsala University, Uppsala, Sweden
[2] The Niels Bohr Institute, University of Copenhagen, Copenhagen, Denmark
[3] The Svedberg Laboratory, Uppsala University, Uppsala, Sweden
[4] Soltan Institute for Nuclear Studies, Swierk, Poland
[5] Physics Department, Royal Institute of Technology, Stockholm, Sweden
[6] Department of Physics, University of Jyväskylä, Jyväskylä, Finland
[7] J. Stefan Institute, Ljubljana, Slovenia
[8] Oliver Lodge Laboratory, University of Liverpool, Liverpool, U K.
[9] Institut de Physique Nucléaire, IN2P3-CNRS and Université Lyon-1, France

Abstract: A discrete γ-ray transition which connects the second lowest SD state with a normally deformed one in ^{143}Eu has been discovered. It has an energy of 3360.6 keV and carries 3.2 % of the full intensity of the SD band. It feeds into a nearly spherical state which is above the I = $35/2^+$, E_x=4947 keV level. The exact placement of the single-step link could, however, not be established due to the especially complicated level scheme in the region of interest. The angular correlation study favours a stretched dipole character for the 3360.6 keV transition. The single-step link agrees well with the previously determined two-step links, both with respect to energy and spin.

The linking transitions between the SD bands and the normally deformed (ND) states have been one of the greatest challenges in the study of superdeformation. Identification of the linking transitions not only gives the spins, excitation energies and parities of the SD bands but also provides valuable information on the decay mechanism itself and the structure of the nucleus in the transition region. From a theoretical point of view [1], the deexcitation of an SD band occurs due to small admixtures with the ND states. The SD state is embedded in a sea of hot ND states and it decays statistically by γ-ray emission. In the mass 150 and 190 regions the SD bands lie at high energies and the deexcitation pattern is expected to be governed by multi-step transitions, although it has now been proven in the mass 190 region [2,3,4] and in ^{143}Eu [5] that single-step transitions do occur.

Recently, with modern Ge arrays it has been possible to identify single-step linking transitions and to localize the SD bands in a few nuclei in the mass 130 [6] and 190 regions. The situation is, however, more complicated for the ^{143}Eu nucleus. The lowest SD states in this nucleus lie higher in energy above the yrast line as compared to the mass 130 region and they have a higher spin as compared to the mass 190 region.

One possible way of studying the linking transitions is to assume that a significant fraction of the decay goes via cascades of two γ-ray transitions (two-step link) and to search for the corresponding discrete sums of the two γ-ray energies. In an earlier paper [7] several discrete sum energies were identified in ^{143}Eu and the lowest SD state was proposed to be at I=35/2, E_x=8582 keV.

The present experiment was carried out in Strasbourg using the EUROGAM II array [8]. Excited

states in ^{143}Eu were populated in the reaction ^{110}Pd(^{37}Cl,4n)^{143}Eu with a beam energy of 160 MeV. The ^{110}Pd target was enriched to 98.9% and consisted of three thin foils with a total thickness of 1.1 mg/cm^2. With a trigger requirement of seven or more γ rays in prompt coincidence (before Compton suppression) a total of 1.8×10^9 Compton-suppressed events with an average fold of 4.4 were collected. A much compressed version of the data set was stored on magnetic hard disks for fast access and sorting. A short experiment by using a 1.1 mg/cm^2 layer of ^{110}Pd sputtered onto a 10 mg/cm^2 Au backing was also carried out at the end of the main experiment. With a trigger requirement of six or more γ rays in prompt coincidence a total of 2.2×10^8 Compton-suppressed events were collected. The aim of the backed target experiment was to improve the ND level scheme.

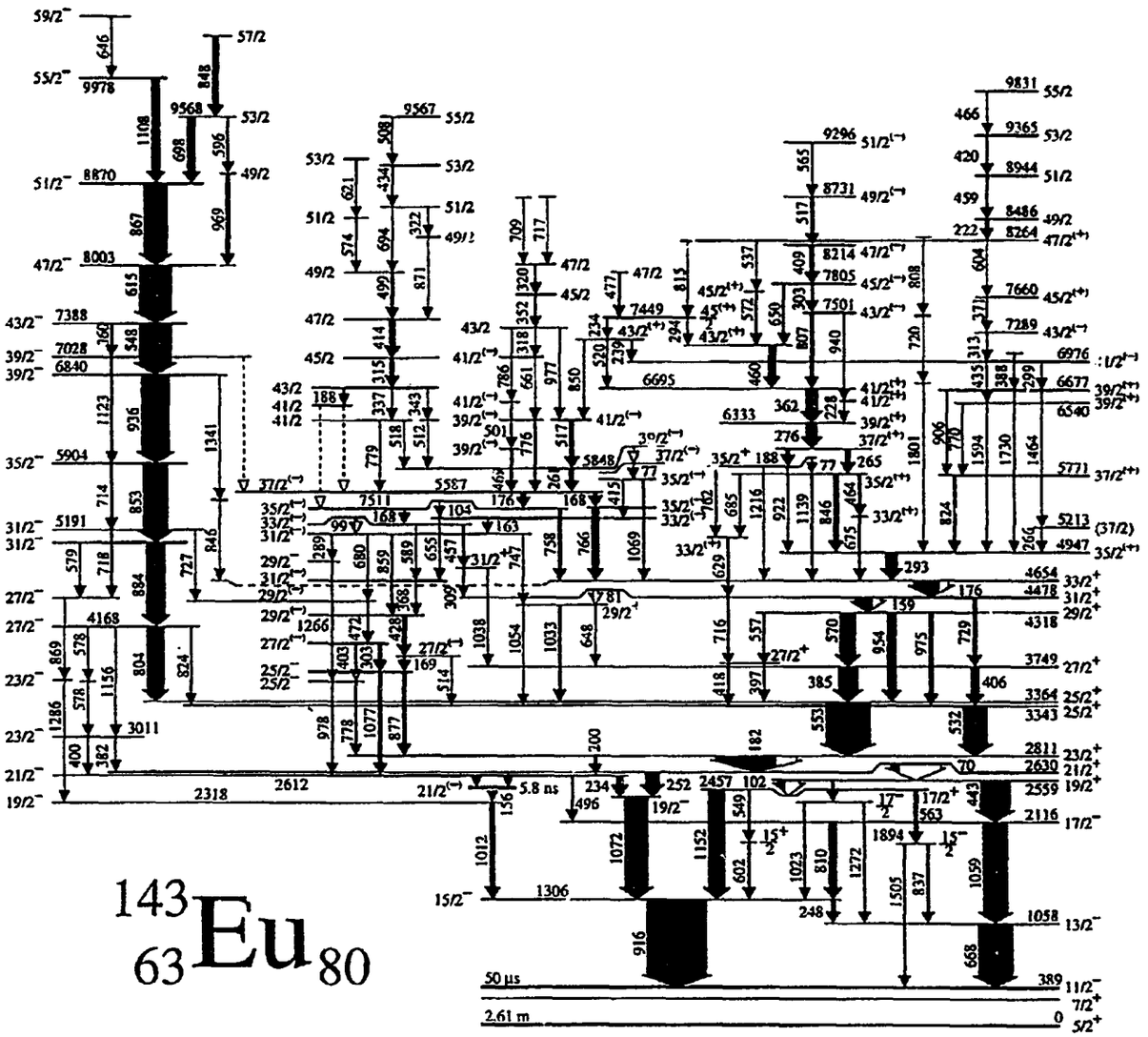

Fig. 1 : Level scheme of ^{143}Eu basically taken from ref. [9] and slightly modified. The widths of the arrows are proportional to the intensities observed in the ^{110}Pd(^{37}Cl,4n)^{143}Eu reaction at 160 MeV.

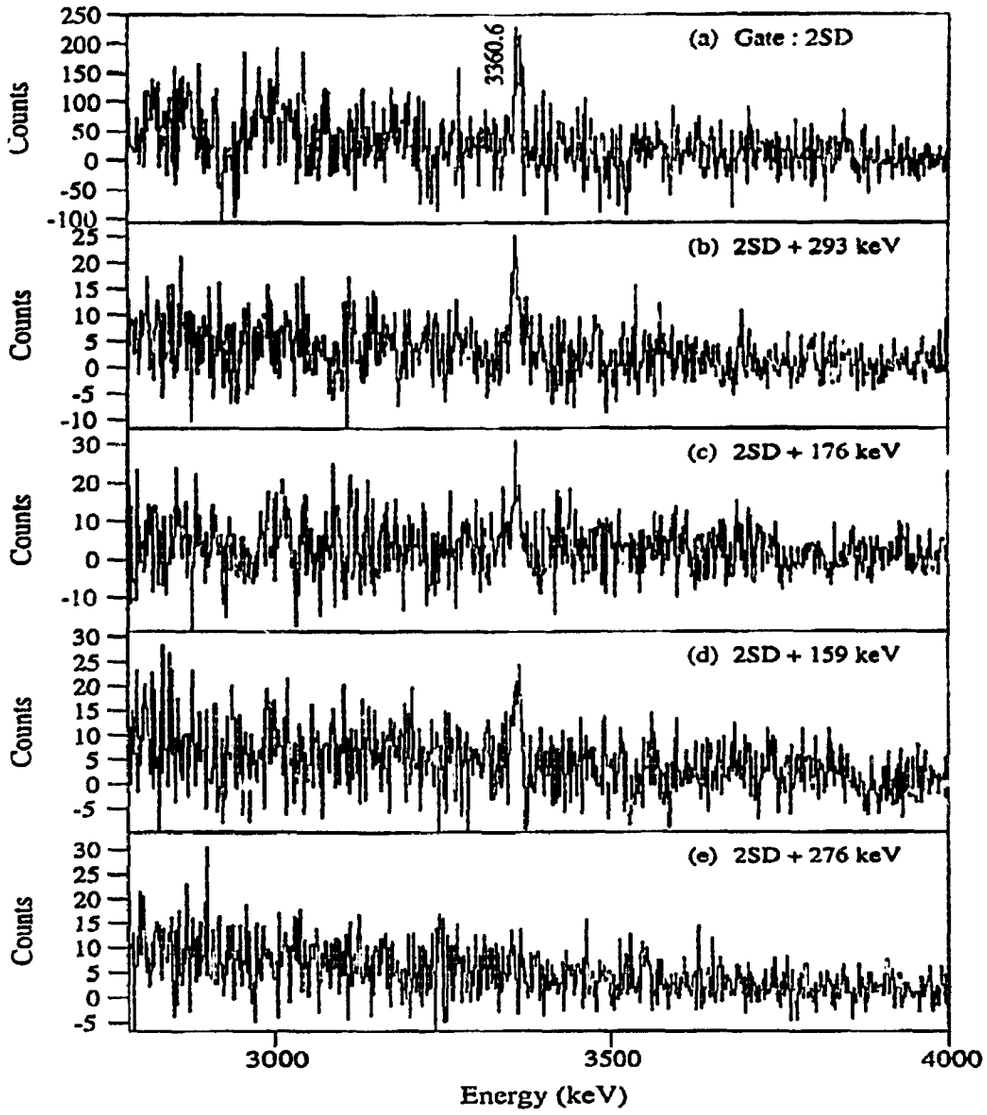

Fig. 2 : The high energy part of a γ-ray spectrum (a) coincident with three SD band members. All 22 SD transitions were used to gate on in order to increase the statistics and a portion of the total projection was subtracted as the background. The transition observed at 3360.6 $\pm$ 0.7 keV with a FWHM of 10.1 keV is proposed to be a single-step linking transition. The lower spectra have two gates on the cleanest SD transitions and a gate on the 159 keV (b), 176 keV (c), 293 keV (d) and 276 keV (e) lines in the ND level scheme.

Fig. 1 shows the level scheme of ^{143}Eu. It is basically taken from ref. [9] and modified using the current data set. The irregular and very complex structure of the level scheme at low spins is typical of a nearly spherical, slightly oblate nucleus. A sequence of collective states starting from I = 27/2, E_x = 4.2 MeV and forming a triaxially deformed band is also observed coexisting with the spherical states. A study of the triple or quadruple gated spectra shows that the SD yrast band feeds into the spherical near-yrast states bypassing the triaxial states which lie about 1 MeV above the yrast states in the feeding region. This result is also confirmed by a recent study [10] of the

quasicontinuum of the SD transitions in this nucleus.

Fig. 2a shows the high energy part of a γ-ray spectrum. It is double gated on the 22 transitions [7] of the SD band in ^{143}Eu. The peak at 3360.6(7) keV is observed at a 5.5 σ level and is identified as a one-step link to a ND state since it is in coincidence with the SD band and some of the ND states. The 3360.6 keV line represents 3.2 % of the total intensity in the SD band.

Once a single-step linking transition is observed, it is a big challenge to localize it by determining the SD state it comes from and the ND level it feeds into. The SD state from which the 3360.6 keV transition deexcites was investigated in double gated spectra where one gate was set on one of the three lowest transitions in the SD band, namely the 483, 547 or 609 keV transitions and the second gate was set on one of the few clean, higher lying transitions in the band (fig.3). The two spectra with gates at 483 and 609 keV are relatively clean. There is, however, a strong 548 keV transition lower in the ND level scheme (triaxial band) making the 547 gate specially difficult. Therefore it is important to select carefully the cleanest gate combinations especially for this case. The result is that the 3360.6 keV transition is seen in the spectra gated by the 609 and 547 keV transitions whereas it disappears in the spectrum gated by the 483 keV transition. Therefore we propose that the 3360.6 keV linking transition depopulates the SD state just below the 547 keV transition, i.e. the second lowest state of the SD band.

Fig. 4 shows the low energy part of a triple gated spectrum. It has two gates on the cleanest transitions in the SD band and a gate on the 3360.6 keV high energy line. The 159, 176 and 293 keV transitions are in a cascade in the ND level scheme and the 293 keV transition lies highest in excitation energy. The 3360.6 keV line is also clearly seen in the spectra gated on these lines (see fig. 2 b, c, d). The 182 keV transition deexcites a $23/2^+$, 2813 keV state and it collects nearly all the intensity coming from above. The intensities of the strongest peaks of fig. 4 were determined and corrected for internal conversion. Normalizing to the strength of the 182 keV transition, the 159 and 176 keV transitions carry 93 % and 92 % of the intensity, respectively, while the intensity of the 293 keV transition is only 38 %. Thus, we conclude that the 3360.6 keV transition does not directly populate the $35/2^{(+)}$, 4947 keV state from which the 293 keV transition decays. It rather populates a higher energy level which partially decays into the 4947 keV level and partially down to the $33/2^+$, 4654 keV level from which the 176 keV transition decays.

Fig. 2e shows that the 3360.6 keV transition is not in coincidence with the 276 keV transition indicating that it either feeds into a level which has a lower energy than the $39/2^+$, 6333 keV state or it selects a parallel branch feeding into the $35/2^{(+)}$, 4947 keV level. Above E_x=4947 keV, the level scheme of ^{143}Eu is particularly complicated and the decay paths feeding into this state are fragmented making it difficult to locate the linking transition. An identification of a few other single-step links would be of great help for reaching more conclusive results.

An angular correlation study of the 3360.6 keV line gives a value of R = 1.0(2) where R is the ratio between γ rays detected by the tapered and clover detectors located at an average angle of 38.4° and 75.5° respectively, relative to the beam axis. This ratio is 0.85(2) for the known E1 transition at 252 keV [9] and 1.59(7) for the 1443 keV E2 transition in the SD band. Thus, the 3360.6 keV transition is either a stretched dipole transition or it can be a mixed E2/M1 transition with ΔI = 0 or 1. A pure statistical decay would, however, favour an E1 transition.

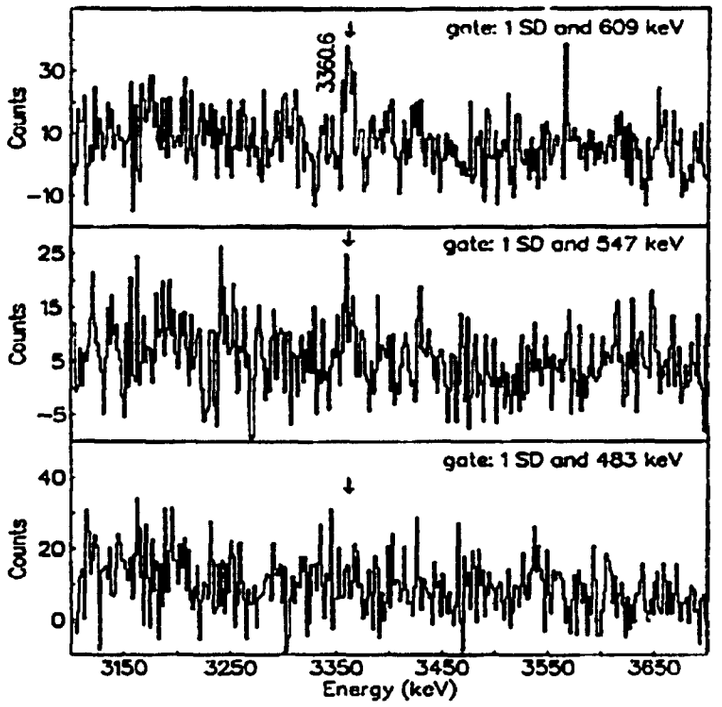

Fig. 3 : Double gated γ-ray spectrum where one gate is set on one of the three lowest SD transitions (a) 483 keV, (b) 547 keV and (c) 609 keV and the second gate is set on one of the few clean, higher lying transitions in the band.

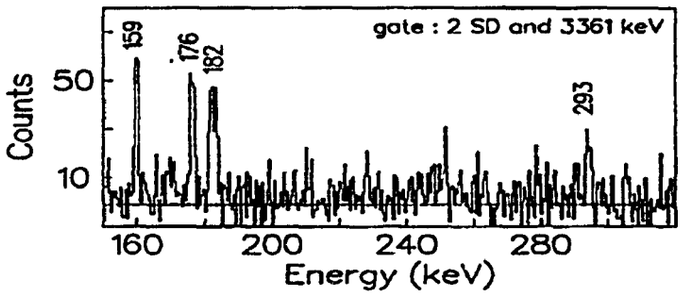

Fig. 4 : The low energy part of a triple gated spectrum which has two gates on the cleanest transitions between the SD states and a gate on the 3360.6 keV high energy line. A portion of the total projection is subtracted as background and the spectrum is corrected for the relative detector efficiencies.

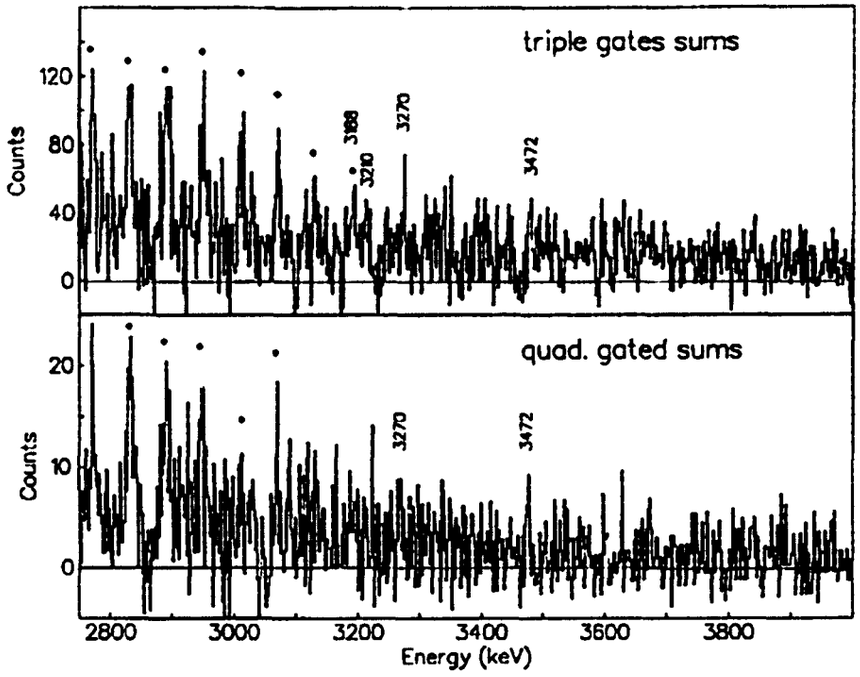

Fig. 5 : The energy sum of two γ-ray transitions which are in coincidence with the SD band members It is obtained by adding 15 clean gates and is background subtracted. The sums of two transitions which are in the SD band are shown by (•)'s.

The single-step link has an energy which agrees very well with the sum energies identified as two-step links in the previous work [7], where energies between 3187-3925 keV were reported. It also feeds into the same region of the ND level scheme as the two-step links. Furthermore, four out of six sum peaks reported earlier, namely the 3188, 3210, 3270 and 3472 keV transitions, are observed in this experiment at a 2-4 σ level, see fig. 5. Their energies agree with the earlier results within the error limits of 4-5 keV.

References:

1) E. Vigezzi et al., *Phys. Lett.* *B*249 (1990) 163.
2) T. L. Khoo et al., *Phys. Rev. Lett.* 76 (1996) 1583.
3) A. Lopez-Martens et al., *Phys. Lett.* *B* 380 (1996) 18.
4) M.J. Brinkman et al., *Phys. Rev.* *C*53 (1996) R1461.
5) A. Ataç et al., *Z. Phys.*, in press.
6) S. Lunardi et al., *Phys. Rev.* *C*52 (1995) R1 and M. Deleplanque et al., *Phys. Rev.* *C*52 (1995) R2302.
7) A. Ataç et al., *Phys. Rev. Lett.* 70 (1993) 1069.
8) P.J. Nolan et al., *Annu. Rev. Nucl. Part. Sci.* 45 (1994) 561.
9) M. Piiparinen et al., *Nucl. Phys.* *A*605 (1996) 191.
10) S. Leoni et al., *Phys. Rev. Lett.* 76 (1996) 3281.

The Quasi-Continuum of Gamma Rays Following the Decay of Superdeformed Bands in the Hg Region

T. Lauritsen[a], A. Lopez-Martens[b], T.L. Khoo[a], R.V.F. Janssens[a], M.P. Carpenter[a], G. Hackman[a], D. Ackermann[a], I. Ahmad[a], H. Amro[a,c], D.J. Blumenthal[a], S.M. Fischer[a], F. Hannachi[b], A. Korichi[b], E.F. Moore[c] and D.T. Nisius[a].

[a]*Argonne National Laboratory, Argonne, Illinois 60439, USA.* [b]*Centre de Spectrométrie Nucléaire et de Spectrométrie de masse, IN2P3-CNRS, bat 104-108, F-91405 Orsay, France and Institut de Physique Nucléaire, F-91406, Orsay Cedex, France.* [c]*North Carolina state University, Raleigh, North Carolina 27695, USA*

The quasi-continuum part of the spectrum associated with the decay-out of the yrast superdeformed band in ^{194}Hg has been extracted. It has for the first time been possible to compare the spin and excitation energy determined from the analysis of the quasi-continuum γ rays to the exact result obtained from the one-step linking transitions.

INTRODUCTION

About 175 superdeformed (SD) bands have by now been found in the A=80,150 and 190 mass regions; yet only a few of these have been firmly linked to the normal deformed (ND) states they decay into. Thus, fundamental quantities such as *spin, parity* and *excitation energy* have not been experimentally determined for the vast majority of the SD bands. In order to address issues of great recent interest such as: [i] the presence of identical SD bands, [ii] the magnitude of shell corrections at large deformation, [iii] the mechanisms responsible for the sudden decay-out of the SD bands, [iv] the description of pairing and level densities in the SD well, some or all of those quantities must be determined for as many SD bands as possible.

Recently, one-step decays out of the yrast SD bands in ^{194}Hg and ^{194}Pb have been reported [1,2]. One-step decays allow for an unambiguous determination of the spin, parity and excitation energy of the states in a SD band. However, the intensity of these special decay branches is only a fraction of that of the SD band itself, and most of the decay proceeds through a quasi-continuum (QC) of γ rays. Moreover, the strength of one-step decays varies considerably from nucleus to nucleus and may be subject to Porter-Thomas fluctuations. Therefore, it may not always be possible to observe one or two-step decays – even when data of very good statistics are available. In such cases, the analysis of the QC provides an alternative way to determine the spin and energy of the SD bands, provided that the analysis methods are proven to be reliable.

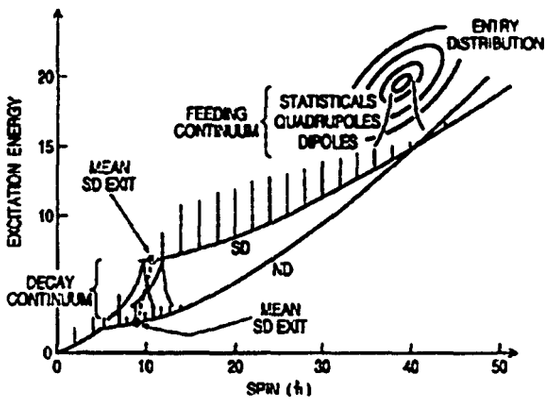

FIG. 1. Schematic diagram of the feeding and decay of SD bands. Gamma emission starts from the entry distribution. After emission of statistical, quadrupole and M1/E2 dipole QC γ rays, the deexcitation cascades are trapped either in the ND or SD wells, where discrete gamma rays are emitted. If a γ cascade is trapped in the SD well, QC γ rays are also emitted when the SD band decays into the ND states.

A schematic diagram of the feeding and decay of a SD band in figure 1 shows that there are two components to the QC: [i] one associated with the feeding of the SD states and [ii] the other originating from the decay towards the yrast states [3]. A simple way to assess where the decay QC γ rays are located is to compare coincidence spectra gated on ND and SD transitions. Only the spectra gated on SD γ rays should have the 'extra' QC component from the decay-out to ND states at or near the yrast line. Such a comparison for ^{194}Hg is given in figure 2 (with the discrete peaks left in the spectrum). It is clearly seen in the figure that extra strength is present in the SD gated spectrum above 1 MeV - exactly where the γ rays from a statistical decay of the levels at the bottom of the SD band are expected [4]. The spectrum has close similarities with that reported earlier for ^{192}Hg [3]. In particular, as in the latter nucleus, the excess strength above 1 MeV is ascribed to the decay out of the SD band.

Differences below 1 MeV are also seen in figure 2, but those have to do with the different paths the nucleus takes in the feeding of the ND and SD bands.

In the feeding of the yrast SD band, about six γ rays of stretched E2 character are emitted while the nucleus decays through excited, damped SD bands [5]. A pronounced 'E2-bump' is therefore seen in the SD gated spectrum (and it should result in ridges in coincidence matrices). On the other hand, the cascades feeding the ND bands involve less collective states and, as a result, the E2-bump associated with this decay mode is much smaller.

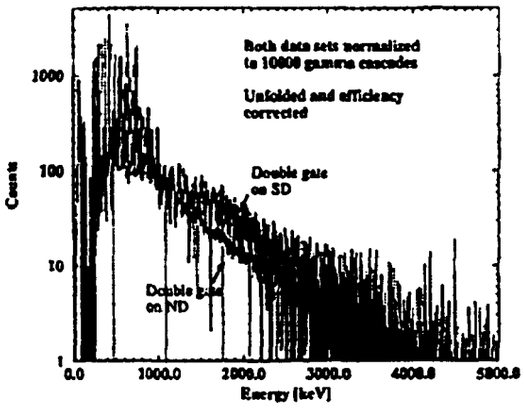

FIG. 2. Comparison of ND and SD gated coincidence spectra in ^{194}Hg. The spectrum gated on the the SD band shows additional strength above 1 MeV from the QC γ rays associated with the decay of the SD band to ND states.

By extracting the QC γ rays in coincidence with the SD band, it is possible to deduce both the spin and energy of the SD band at the point of decay. When the QC intensity is normalized to the number of γ cascades, the area of the spectrum determines the average multiplicity, i.e., the number of γ rays involved in the decay. Similarly, the mean energy of the decay-out QC determines the average energy removed by these γ rays. Thus, by simple multiplication of these two quantities, the mean energy removed by the QC is established. It is likewise possible to determine the average amount of spin removed by the γ rays.

From the intensities, spins and energies of the ND transitions in coincidence with the SD band, the average spin and energy corresponding to the entry into the ND states can be derived (see figure 1). By vectorially adding the spin and energy removed by the QC to the mean ND entry-point, the *mean SD exit-point* can be found. From this information the spins and energies of the SD band levels can be deduced, once the branching ratios between in-band and out-of-band decay are taken into account for the lower SD states.

THE EXPERIMENT

The SD band in ^{194}Hg was populated using the reaction ^{150}Nd(^{48}Ca,4n). The beam, delivered by the 88" cyclotron at LBNL, had an energy of 202 MeV. A total of 1.9×10^9 quadruple or higher fold coincidence events was collected with GAMMASPHERE, which at the time comprised 85 detectors. The target consisted of a 1.2 mg/cm^2 ^{150}Nd layer evaporated on a thick Au backing, which ensured that all γ rays associated with the decay-out of the SD band would not be subject to any Doppler shift.

THE EXTRACTION OF THE QC

In order to extract the QC γ rays from the total spectrum, the data must be processed carefully in a number of steps. Double coincidence gates were placed on SD transitions in order to obtain SD spectra almost free of contaminant coincidences, yet with sufficient statistics for an angle sort. Only 9 of 36 possible double gate combinations were deemed clean enough for use in this analysis. (Triple gating would have provided even cleaner spectra; but the statistics in the angle sort would have been marginal.) Correct background subtraction of the double-gated spectra is vital. The FUL method [6] developed at ANL was used to subtract background-background and peak-background contributions. The data was also sorted according to the prescription in [7] in order to avoid 'spikes' in the gated spectra. In addition, any lines left in the spectra as a result of contaminant coincidences (despite careful selection of gates) were identified, characterized and subtracted.

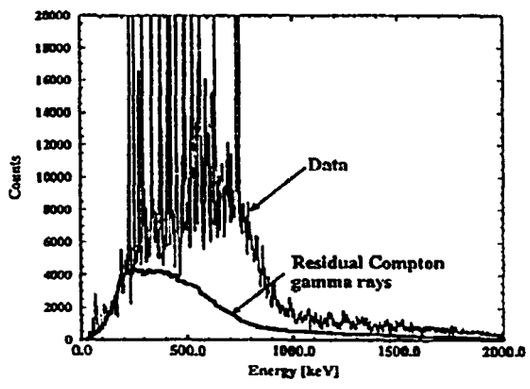

FIG. 3. Residual Compton events in a typical spectrum. The figure shows a gated spectrum before unfolding and the lower solid curve shows the residual Compton events subtracted by the procedure described in [7], using a measured response function for GAMMASPHERE.

The angle sorted spectra were corrected for the response of the GAMMASPHERE array in successive steps described below. First the contributions due to true coincidence summing was removed following a prescription by Radford [8]. The γ rays generated from neutron interactions in the Ge detectors (mostly in the forward direction) were subtracted next. This contribution is small (2-3%) and has very little impact in the energy region of the decay-out γ rays. A more significant correction is the removal of the Compton events in the spectra . Even with efficient BGO shields, about 1/2 of all Compton events is not suppressed and to extract the true QC, it is necessary to subtract these unwanted γ rays.

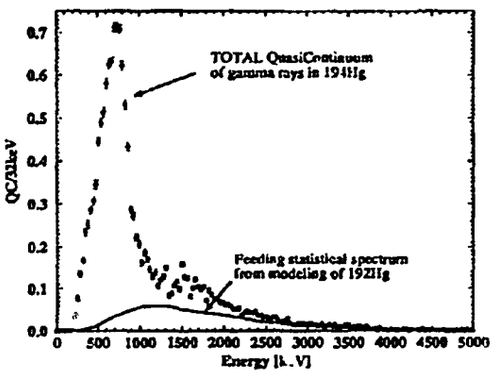

FIG. 4. The total QC after discrete peaks have been removed and the spectra contracted to 32 keV/ch. Also shown is the calculated statistical spectrum from ^{192}Hg.

By measuring the spectra from single-line and two-line coincidence sources placed at the target position, the response function of GAMMASPHERE was carefully measured. Using the unfolding procedure described in [8], which interpolates between the response-measurement at discrete energies, the residual Compton γ rays for the entire spectrum were deduced and subtracted. Figure 3 shows a typical spectrum before the unfolding, together with the residual events left in the spectrum despite Compton suppression (lower curve). It is clearly seen that the procedure by Radford works well, even in the low energy region where it is most difficult to unfold.

Next, the spectra were corrected for detector efficiency, the discrete γ rays were removed and the spectra were contracted to 32keV/ch. The remaining QC γ rays consist of the three feeding QC components, i.e., [i]statistical, [ii]quadrupole and [iii]dipole transitions from the last step in the feeding [3]. The fourth QC component is the sought-after decay-out spectrum which will be extracted by subtracting the feeding statistical and quadrupole components.

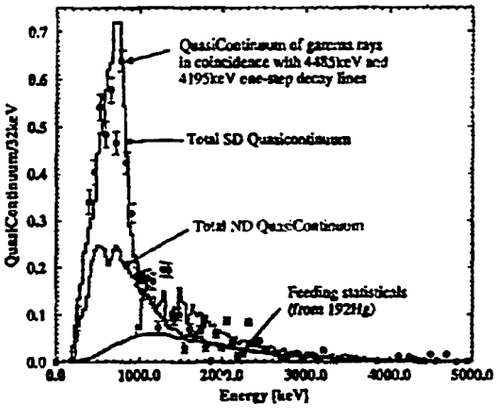

FIG. 5. The QC γ rays obtained from double gates placed on the one-step decay-out lines and SD lines in ^{194}Hg (data with error bars). Also shown are the total SD and ND QC spectra and the calculated statistical spectrum from ^{192}Hg.

Finally, the QC spectra are normalized so that the area of the $2^+ \longrightarrow 0^+$ ground-state transition in the spectrum is unity, after corrections for internal conversion, angular distribution and changes to the intensity due to isomers have been taken into account. After this normalization, it follows that any area is equal to multiplicity, since the spectrum represents an average γ cascade. Figure 4 shows the total QC spectrum corrected for angular distribution effects ('A0' spectrum).

THE STATISTICAL FEEDING COMPONENT

In reference [5], the statistical spectrum feeding the SD band in ^{192}Hg was calculated using as input the experimentally measured entry states distribution. This statistical spectrum is also expected to be applicable in the case of ^{194}Hg. Because the one-step decay lines have been observed in this nucleus [1], it is possible to confirm experimentally this hypothesis by extracting the QC in coincidence with the one-step decay-out lines. This spectrum should *not* contain the decay QC and thus, at higher energies, it should follow the calculated statistical spectrum rather than the total QC.

The sum of coincidence spectra, with double coincidence gates placed on the one-step decay-out γ rays and the SD lines, has been corrected for the response of GAMMASPHERE. It is presented in figure 5 overlaid with the total QC spectrum and the calculated statistical spectrum. Despite low statistics, the agreement between this spectrum and that obtained with double gates on SD lines is very good over the 'E2-bump' region, although there appears

to be some contaminant lines just above 1 MeV. At higher energies, the data are seen to follow the statistical spectrum, thus justifying our hypothesis. It should be noticed that the QC spectrum gated on ND transitions also follows the calculated statistical spectrum at higher energies, again suggesting that the calculated statistical spectrum from ^{192}Hg can be used in ^{194}Hg. The calculated statistical spectrum is subtracted from the total QC spectrum shown in figure 4, thus eliminating one of the four QC components.

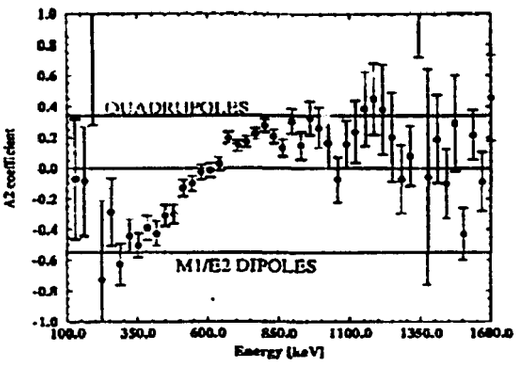

FIG. 6. Angular distribution coefficients, channel by channel, for the QC after the statistical γ rays have been subtracted.

THE QUADRUPOLE FEEDING COMPONENT

After the statistical spectrum has been subtracted, the A2 angular distribution coefficient of the remainder of the spectrum can be found channel by channel: the result is shown in figure 6. If the coefficient is close to the calculated E2 limit of $\approx +0.34$, the QC content of the channel is assumed to be of pure E2 character. Conversely, if the coefficient is close to the large negative value of the M1/E2 dipole transitions, ≈ -0.55 , the channel content is taken to be of pure M1/E2 dipole character. (In the analysis, it is assumed that there is no remaining E1 strength in the spectrum up to $\approx$1MeV following the subtraction of the statistical spectrum). For A2 coefficients with values between those extremes, the counts in the channels are split proportionally between the two contributions. In this way, the E2 QC-component was extracted. The QC quadrupole γ rays are emitted early in the γ cascade, while the nucleus is is still in flight, with a velocity close to the maximum recoil velocity. Hence, the A2 angular distribution analysis is performed on spectra transformed into the center of mass system, and the E2 QC component is subtracted from the spectra of each detector ring after corrections for Doppler shift, angular distribution and relativistic aberration.

SPIN AND ENERGY OF THE SD BAND

After both the statistical and quadrupole components from the feeding have been subtracted, the remaining spectrum still consists of the M1/E2 feeding γ rays and the sought after QC decay-out γ rays. There are clear indications of two components in fig. 7. The low energy component has large negative A2 coefficients (indicating M1/E2 nature) and the upper component resembles the 'extra' strength shown earlier in the SD-ND gate comparison in figures 2. Thus, the upper component ($\approx$1MeV and higher) is assigned to the decay out process as it was in reference [3] for the case of ^{192}Hg.

The mean energy of this decay-out component is 1.8(1) MeV and its area, equal to multiplicity, is 2.3(2). Therefore, it immediately follows that this QC of γ rays removes 4.1(4) MeV of energy. From Monte Carlo simulations [5] of a statistical decay at the proper spin and energy it is found that, on the average, 0.5(2)$\hbar$ of spin is removed by these γ rays. Thus, 1.1(4)$\hbar$ of spin is removed by the decay γ rays in this QC component.

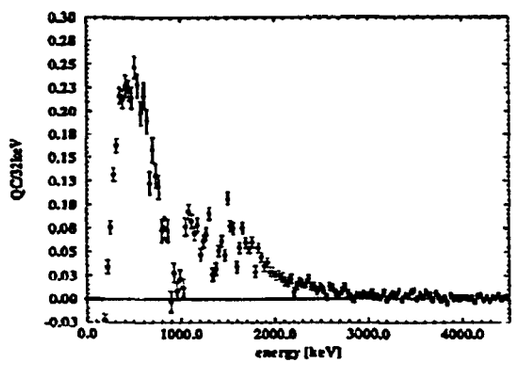

FIG. 7. The QC γ rays in ^{194}Hg after both the feeding statisticals and quadrupoles have been subtracted. The spectrum shows the dipole component of the feeding at low energies and the decay-out QC component at higher energies.

Some SD decay paths will feed into states located above the yrast line, which are either not populated or populated weakly when ND bands are feed. The γ rays from the decay of these states can be found by close inspection of all the discrete γ rays that were removed in the early stages of the analysis; but have not been assigned in the ND level scheme. (By placing coincidence gates on those candidate transi-

tions, it was checked that the lines are not the result of contaminant coincidences). In [3] it was estimated that, on the average, half (multiplicity 0.5(2)) of the γ cascades deexciting the SD band goes through such states and gives rise to discrete lines in a region up to 1 MeV. These γ rays need to be taken into account when the spin and energy of the SD band are calculated. In total, these γ rays remove $0.8(3)\hbar$ and 0.3(1) MeV which must be vectorially added to the 'regular' QC spin and energy vector in order to find the mean SD exit-point (see figure 1).

From the intensities, spin and energies of the known ND lines in coincidence with the SD band, it is found that the entry point of the SD band into the known ND states is located at a spin of $9.3(5)\hbar$ and an energy of 2.4(1) MeV. The errors quoted here are due [i] to difficulties in assigning intensities to some low energy lines which are not observed well with GAMMASPHERE, and [ii] to the presence of two low spin isomers in the yrast level structure, which complicate the determination of γ-ray intensities for transitions involved in their deexcitation.

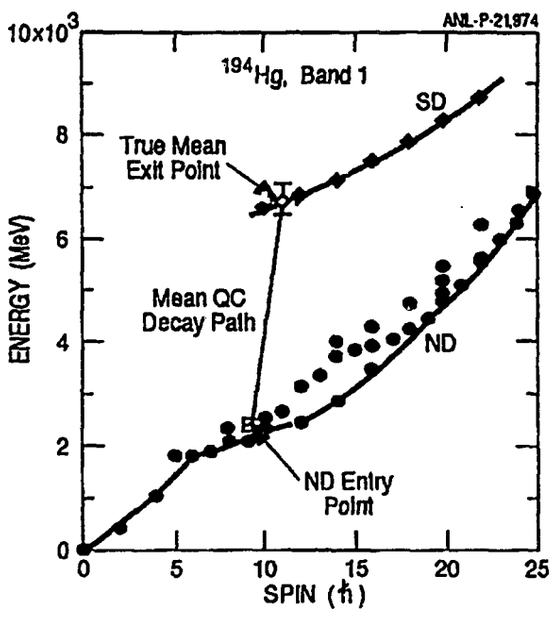

FIG. 8. The mean SD exit-point found by adding the spin and energy removed by known ND lines, new unassigned ND lines and the decay-out QC γ rays.

By adding all the contributions; i.e., the known ND lines, the new weak ND lines just discussed and the decay-out QC γ rays, the *mean SD exit-point* is determined. The result is displayed in figure 8. In the figure, a vector characterizing the mean QC decay path obtained as described above links the entry point into the ND levels and the SD exit point. It is this SD exit-point located at $11.1(7)\hbar$ and 6.8(3) MeV that can be compared directly to the result from the one-step decays [1]. According to the analysis in [1], 48% of the decay of the SD band occurs from the 6.88 MeV 12^+ state and 52% from the 6.63 MeV 10^+ state, establishing the true mean SD exit-point as: ($11.0\hbar$, 6.8 MeV).

The main conclusion of the present analysis is as follows: *the mean exit-point measured from the QC is in remarkably good agreement with the exact result established from the one-step decay γ rays.* Another way to present this result is to calculate the spin and energy the QC method would assign to the '10^+' state: i.e.,

$$I = 10.1(7)\hbar \quad [\text{true: } 10\hbar]$$
$$E = 6.7(3) \text{ MeV}[\text{true: } 6.6 \text{ MeV}]$$

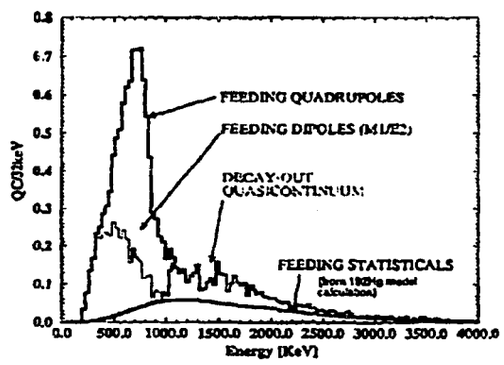

FIG. 9. All the QC components in the feeding and decay of the yrast SD band in ^{194}Hg.

THE DECAY MECHANISM

As the nucleus removes spin and energy by emitting stretched E2 γ rays along the SD yrast line, the SD states become hotter and hotter with respect to the ND yrast line (see figure 1). Thus, the ratio of ND to SD level densities increases as the nucleus decays in the SD well. Moreover, the in-band transition rates diminish because of the rapidly decreasing transition energies. In addition, there is also evidence that the barrier height is reduced at lower spin. A SD band decays to the ND states when the states in the SD band acquire a sufficient component of the wave-function of the hot ND states located on the other side of the barrier separating the two wells [3,5,9]. Because of the exponential dependence of the mixing as a function of spin, the decay happens suddenly, over a few SD states.

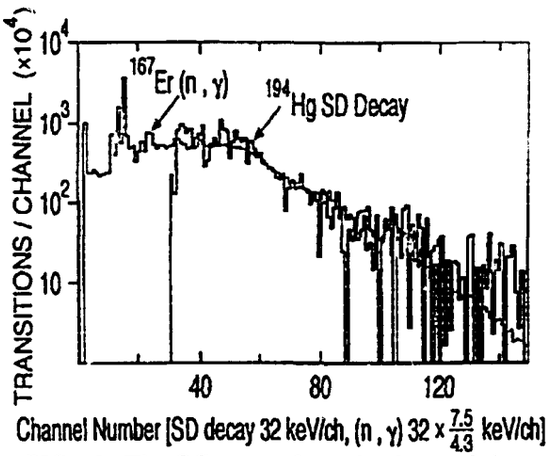

FIG. 10. The QC γ rays from the decay of the yrast SD band in ^{194}Hg overlaid with the gain adjusted QC γ rays following neutron capture in ^{167}Er.

It follows from the above picture of the decay of a SD band that the spectrum of the γ rays emitted in the decay process is governed by the levels in the ND well. The end-point of the QC spectrum is determined by the excitation energy of the SD states. Thus, a decay from a fission isomer or from a state populated in neutron capture is expected to be characterized by a decay spectrum of the same form as the one seen in this work. This follows since all these processes are governed by statistical emission of γ rays from 'sharp' states, i.e. states with a well defined energy.

The QC γ rays following neutron capture in ^{167}Er have been measured using Tessa-3 at Brookhaven [10]. The spectrum after unfolding, efficiency correction and removal of the discrete peaks below 600 keV is presented in figure 10, where it is overlaid with the SD decay-out QC discussed in this paper. Since the sharp states populated by neutron capture are located at higher energy than the SD levels (7.7 MeV vs. 4.3 MeV), the neutron capture spectrum was gain-adjusted so that its end-point matched that of the SD decay spectrum. The similarity (in shape and magnitude) of the two spectra is striking and suggests that, in both cases the decay is governed by the same mechanism, statistical decay from hot 'compound' states.

CONCLUSIONS

It has been shown that the *spin* and *excitation energy* of the yrast SD band in ^{194}Hg which are extracted from the analysis of the QC γ rays from the decay-out process are in excellent agreement with the exact result obtained from one-step decay transitions. Thus, spins and excitation energies can be determined with this method in cases where Porter-Thomas fluctuations or other conditions prevent the observation of direct one-step or two-step decays from SD bands.

component	$\overline{m}$	$\overline{\varepsilon}$
Statisticals	3.2	1.68 MeV
Quadrupoles	6.0(1)	0.73(1) MeV
M1/E2 dipoles	3.37(6)	0.54(1) MeV
Decay-out QC	2.28(6)	1.77(6) MeV
new ND lines	0.5(2)	0.6(2) MeV

TABLE I. The mean multiplicities and mean energies of the QC components in ^{194}Hg. Only statistical errors are given. Also listed are the current results of the cataloging of the new ND states (where the error bars are dominated by systematics).

Figure 9 shows all the components of the QC: [i]the statistical, [ii]quadrupole and [iii]dipole γ rays associated with the feeding and [iv]the QC γ rays from the decay-out of the SD band. Table I shows the mean multiplicities and mean energies of all these components.

Work is still in progress to improve on the errors associated with various contributions by [i]gathering more statistics, [ii]removing contaminant coincidences in the spectra and [iii] doing a more thorough cataloging of the new, unplaced ND lines. The latter process has already yielded more two-step decays which have been added to the decay level scheme in reference [1].

This work was supported in part by the U.S. Dept. of Energy, under Contract No. W-31-109-ENG-38.

[1] T.L. Khoo *et al.*, Phys. Rev. Lett. 76(1996)1583 and G. Hackman, this conference
[2] A. Lopez-Martens *et al.*, Phys. Lett. B380(1996)18, Hannachi *et al.*, this conference
[3] R.G. Henry *et al.*, Phys. Rev. Lett. 73(1994)777
[4] T. Døssing *et al.*, Phys. Rev. Lett. 75(1995)1276
[5] T. Lauritsen *et al.*, Phys. Rev. Lett. 69(1992)2479
[6] B. Crowell *et al.*, Nucl. Instr. & Methods A235(1995)575
[7] C.W. Beausang *et al.*, Nucl. Instr. & Methods A364(1995)560
[8] D.C Radford *et al.*, Nucl. Instr. & Methods A258(1987)111
[9] E. Vigezzi *et al.*, Nucl. Phys. A520(1990)179c and E. Vigezzi *et al.*, Phys. Lett. B249(1990)163
[10] F. Soramel *et al.* to be published

First Measurement of the Degree of Fragmentation of the Decay Out Cascade from the Superdeformed Yrast Band in ^{192}Hg

A Lopez-Martens[1], F Hannachi[1], C Schück[1], R Collatz[1], E Gueorguieva[1], Ch Vieu[1] T Dossing[2], S Leoni[2], B Herskind[2] I Ahmad[3], D Blumenthal[3], M Carpenter[3], D Gassmann[3], R V F Janssens [3], T L Khoo[3], T Lauritsen[3], D Nisius[3] A Korichi[4], C Bourgeois[4] A Astier[5], L Ducroux[5], Y Le Coz[5], M Meyer[5], N Redon[5] J F Sharpey-Schafer[6,*], A N Wilson[6] W Korten[7] A Bracco[8] R Lucas[9]

[1]C.S.N.S.M, IN2P3-CNRS, bat 104-108, Orsay Campus, France
[2]Niels Bohr Institute, 4000 Roskilde, Denmark
[3]Argonne National Laboratory, Argonne, IL 60439, US
[4]I.P.N, bat 104, Orsay Campus, France
[5]I.P.N, Université Lyon-1, Villeurbanne, France
[6]Oliver Lodge Laboratory, University of Liverpool, PO Box 147, L69 3BX UK
[7]Institut fur Strahlen und Kernphysik, Universitat Bonn, Germany
[8]University of Milano, Institute of Physics, I-20133 Milano, Italy
[9]DAPNIA SPHN, CEA Saclay, 91191 Gif sur Yvette, France
*present address: National Accelerator Center, PO Box 72, Faure, ZA-7131 South Africa

Abstract

The decay spectrum of the yrast superdeformed band in ^{192}Hg comprises a quasicontinuum with discrete lines ranging from 1 to 3.2 MeV . The intensity fluctuations of this quasicontinuum give information on the degree of fragmentation of the decay cascades and on the effect of pairing correlations on the level density ρ(U) in the normal deformed well ($0 < U < U_{SD}$).

As was explained in the previous talk by Torben Lauritsen, if we compare superdeformed (SD) and normal-deformed (ND) gated spectra in Hg and Pb isotopes, the SD-gated spectrum lies above the ND-gated spectrum for a broad range of transition energies when both spectra are normalised to the same number of γ cascades. This excess intensity has been indentified in previous work [1] to be the spectrum of γ rays connecting the SD to ND states. It is a quasicontinuum with intermediate-width structures. From a quasicontinuum analysis, the excitation energy of the decaying SD state in ^{192}Hg was found to be U=4.3±0.9 MeV above the yrast line [1]. If we zoom in on the decay spectrum, we see that it also contains sharp lines which account for only a few percent of the total decay flux. In ^{192}Hg, for example, 51 resolved lines have been identified [2]. However, no single-step decays could be observed. So far, these have been reported only in 2 nuclei of the mass 190 region: ^{194}Hg and ^{194}Pb [3,4,5].

A quasicontinuum as well as primary and secondary lines are also observed in the γ spectrum following thermal neutron capture. This is further evidence for the stochastic coupling of the localised SD state with highly excited ND states across the potential barrier [6]. So, effectively, it is the statistical decay from the hot ND states which is observed.

What spectrum does one expect in such a decay ?

T. Dossing et al have calculated the spectra corresponding to the statistical decay

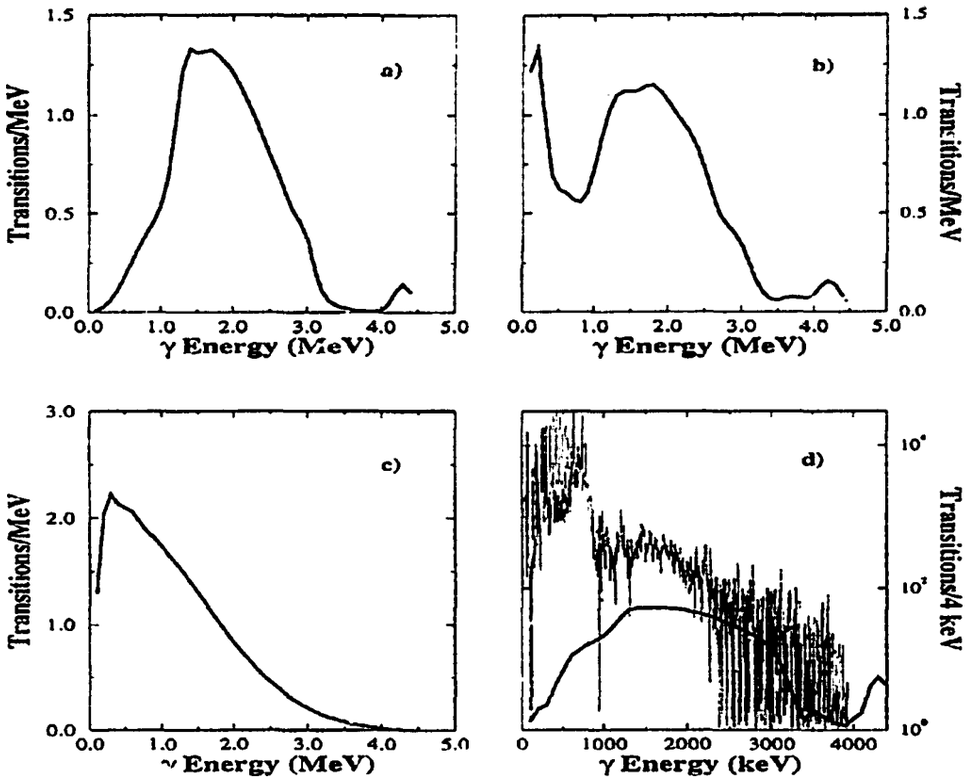

Figure 1: Statistical decay spectra from an initial state at U=4.3 MeV calculated with (a) the paired even-even level density, (b) the paired odd-even level density and (c) the unpaired even-even level density. (d) Efficiency-corrected experimental decay spectrum and calculated decay spectrum from (a)

from a ND state at 4.3 MeV in three different cases [7]. The level densities are obtained by counting quasiparticle energies starting from equidistant single-particle levels, with pairing treated using the BCS method, followed by particle-number projection and diagonalisation. The decay spectra for an even-even and odd-even paired nucleus and for an even-even nucleus without pairing are shown in fig 1a-c. In the unpaired case, the monotonic increase of the level density with excitation energy gives rise to a smooth decay spectrum. In the even-even paired case, there is a depleted yield below 1.2 MeV and between 3.2 and 4 MeV. Both these features are due to the pair gap below the energy for 2 quasiparticle excitations. The compression of the spectrum, together with the last step transitions across the pair gap, give rise to a broad bump centered around 1.6 MeV. For the odd-even case, the filling of the pair gap gives an appreciable yield at low energy. Above 1 MeV transition energy, the best experimental approximation of the spectrum of γ rays feeding the SD band is the ND-gated spectrum stripped of all strong high-energy lines. The difference between the SD-gated spectrum and this smoothed ND-gated spectrum is then the decay spectrum. In fig 1d, the efficiency-corrected decay spectrum is shown together

with the calculated spectrum obtained with the even-even paired level density. The qualitative agreement is very good since the calculations reproduce the general shape of the decay spectrum. The model also predicts up to 5% yield at high energy which corresponds to the expected intensity for single-step decays. The fact that this yield varies so much from one nucleus to the other may be due to the chaoticity of the excited decaying ND state, in which case, we would expect the fluctuations in the strengths of the primary γ rays to follow a Porter-Thomas distribution [8].
What can we learn from the decay spectrum ?
If it contains strong sharp lines, we can directly deduce the excitation energy, spin and parity of the SD state. If these lines are too weak, we can carry out a quasicontinuum analysis [9] to extract the average excitation energy and spin of the SD state. With the Fluctuation Analysis Method (FAM), we can extract the effective number of transitions sampled by the nucleus in the decay; in other words, we can measure *the degree of fragmentation of the decay.* As it turns out, this method goes even further and can be used as a new probe of the ND level density up to high excitation energy.
How does it work ?
The aim of the FAM [10,11,12] is to determine the effective number of transitions sampled by the nucleus without knowing the details of the transition energies or transitions strengths involved. This number can be directly extracted from the first (mean) and second (variance) moments (μ_1 and μ_2) of the intensity distribution of the decay spectrum. The method relies on the fact that, below the excitation energy of the SD state at the point of decay, the level density in the 1st well, although large, is finite. If the number of recorded events (N_{evt}) is larger than the number of available transitions (N_t), this will lead to an enhancement of the intensity fluctuations in the decay spectrum above those generated by pure counting statistics. Correction factors have to be added to account for finite detector resolution (p), probable Porter-Thomas fluctuations (2), background subtraction and the separation of true coincidences into 2 components, such as into the SD decay spectrum and the underlying continuous statistical feeding spectrum in the 1 to 3 MeV region of the SD-gated spectrum. One then obtains the following equation for the effective number of transitions:

$$N_t = 2 \times p \times f^2 \times \frac{N_{evt}(A) \times \mu_1(A)}{\mu_2(A) - \mu_1(C) - g^2\mu_1(B)} \tag{1}$$

Spectrum A = C - gB, where C is the raw spectrum of all the events in coincidence with the SD band and B the appropriate background spectrum scaled by a factor g. Spectrum A needs to be corrected for the detector response [13]. f is the fraction of events belonging to the decay in spectrum A. Fig 2a shows the effective number of sampled transitions as a function of transition energy obtained for the SD decay and feeding cascades in ^{192}Hg studied with the Eurogam 2 array [14]. Above 2 MeV, fewer transitions are sampled by the nucleus in its decay from the SD band. This can be explained by the fact that these transitions are primary γ rays starting off from a few initial states and taking the nucleus down to regions of low level density. Thus, for the decay cascade, the number of transitions is expected to decrease at high transition energy in proportion to the final state level density $\rho(U_{final})$. On the other hand, the feeding cascade starts from a multitude of initial states populated by the neutron decay; in this case, the number of transitions reflects the product of the final and initial state level densities $\rho(U_{initial})\rho(U_{final})$. The low-energy transitions of the

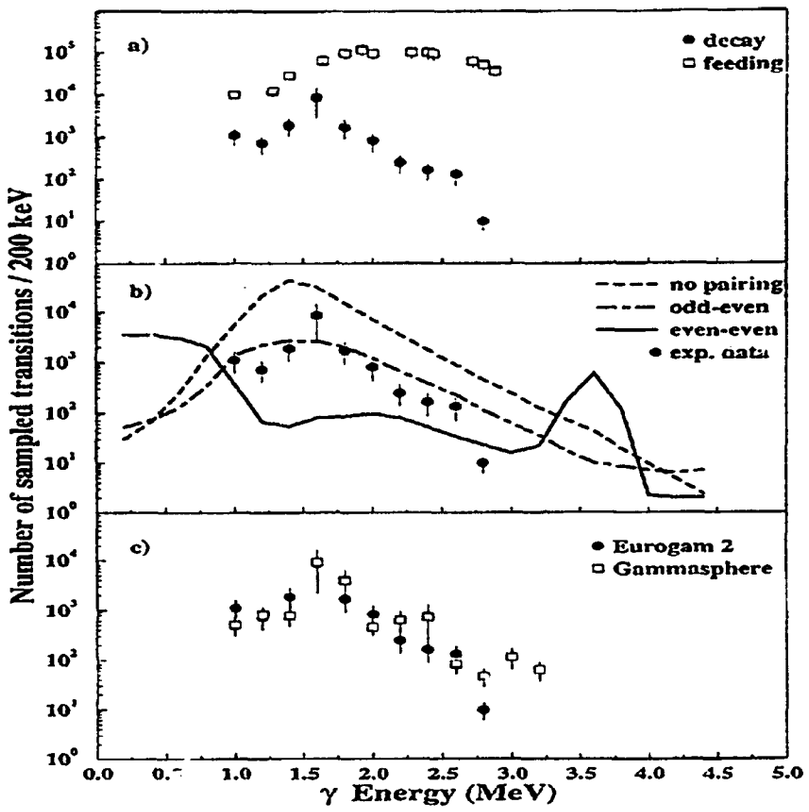

Figure 2: (a) Experimental effective number of transition sampled in the decay and feeding cascades in ^{192}Hg. (b) Calculated and experimental effective number of transitions sampled in the decay cascade. (c) Comparison between the experimental effective number of transitions in the decay cascade obtained with Eurogam 2 and Gammasphere data

decay cascade tend to come from the last decay steps. They connect states in a region of low level density. This explains the initial increase in the number of transitions as a function of transition energy. A total of ~9000 transitions are sampled in the decay out of the SD band in ^{192}Hg. By examining figure 2a above 2 MeV where the first decay steps dominate the fluctuations, one can see that ~1000 transitions are available in the initial stage of the decay [2]. This tells us that the decay is indeed highly fragmented, as expected in a statistical decay. In figure 2b, the experimental effective number of transitions is compared to calculations based on the schematic model described earlier on. The comparison between the experimental data and the calculations is satisfactory and is a stringent test for calculations of the decay and of $\rho(U)$ up to high excitation energy. The fact that the experimental values are in better agreement with the odd-even calculated values may be due to factors that have not been included in the model: first of all, angular momentum which causes the pairing correlations in the even-even nucleus to weaken and hence lowers the ground state

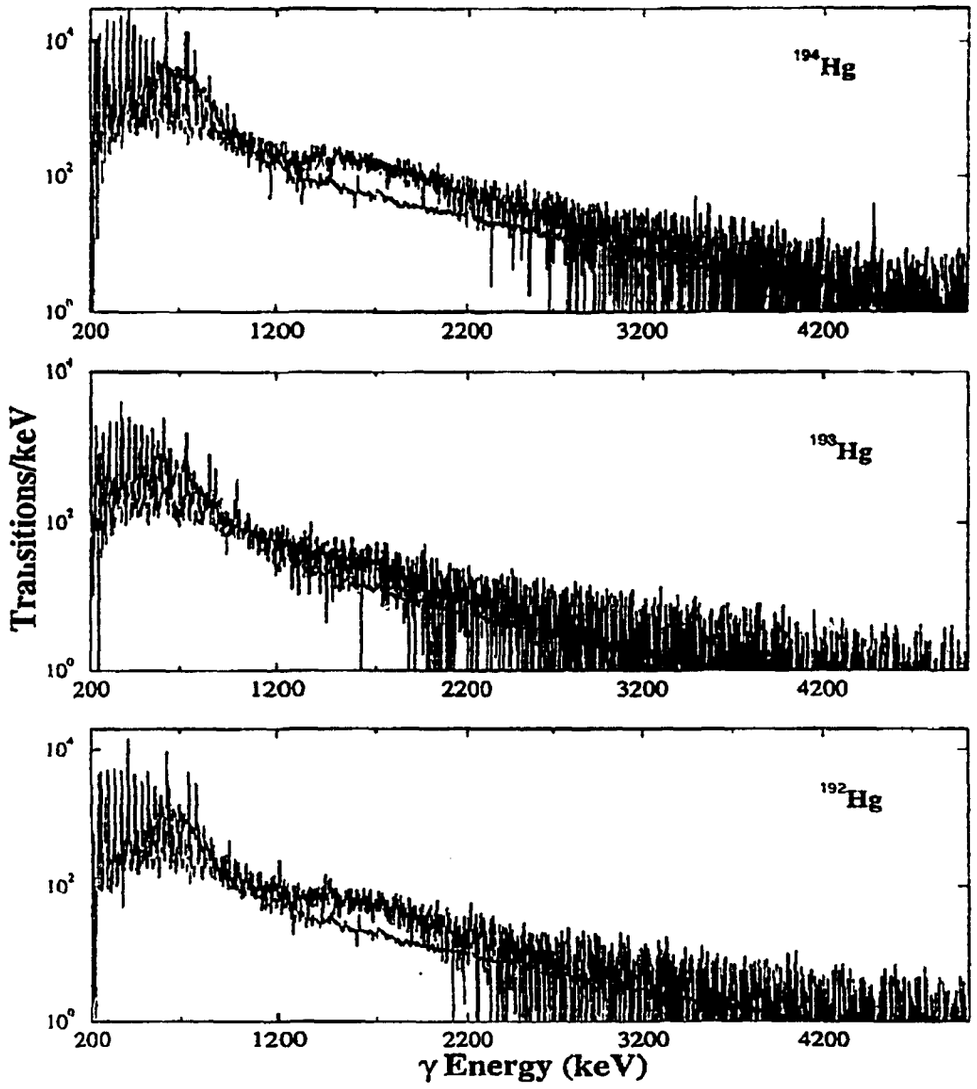

Figure 3: SD and ND-gated spectra obtained in ^{192,193,194}Hg

pairing gap, secondly, symmetries in the nuclear potential and shell effects which may slightly displace both calculated curves. It is essential to carry out a similar analysis on other nuclei and especially an odd-even nucleus of the same mass region. In fig 3 are shown the SD and ND-gated spectra for 3 Hg isotopes studied at Gammasphere [15]. We can immediately see that both even-even nuclei present a more pronounced bump than the odd-even nucleus. A careful inspection of the ^{193}Hg spectra reveals an excess intensity at low energy, as predicted by T. Dossing's calculations. A preliminary Fluctuation Analysis on the ^{192}Hg decay spectrum gives practically an identical distribution of effective number of transitions as the Eurogam ^{192}Hg data. The comparison is shown in fig 2c. The analysis of the ^{193}Hg and ^{194}Hg decay spectra is still in progress.

In conclusion, we have shown that the decay from the SD band in ^{192}Hg starts off from

a few initial states and is highly fragmented. We have measured of the order of 1000 different first step transitions. The decay has been shown to be of statistical nature but it remains to be proven that Porter-Thomas fluctuations govern the distribution of the SD intensity among the different decay paths. This can be done by measuring the intensity distribution of the discrete transitions lying above 2 MeV which stem directly from the hot ND states. This analysis could then provide a direct measure of the onset of chaos in excited nuclear states. By studying the various components of the decay spectrum, we are able to extract the fundamental spectroscopic quantities for the SD band, such as excitation energy, spin and parity. These quantities can help us check the assignments of yrast and excited SD bands and measure the mixing of the SD and ND states. We can also study the statistical feeding via the single-step decays. Finally, we have direct access to the ND level density and the quenching of pairing with excitation energy and spin via the Fluctuation Analysis Method. The decay spectrum is thus a very good laboratory for the study of fundamental properties of SD and ND nuclei and the study of the SD-to-ND shape transition.

[1] R. G. Henry *et al.*, Phys. Rev. Lett **73**, 777 (1994)
[2] A. Lopez-Martens *et al.*, Phys. Rev. Lett **26**, 1707 (1996)
[3] T. L. Khoo *et al.*, Phys. Rev. Lett. **76**, 1583 (1996)
[4] A. Lopez-Martens *et al.*, Phys. Lett. **B380**, 18 (1996)
[5] K. Hauschild *et al.*, proceedings of this conference
[6] E. Vigezzi *et al.*, Phys. Rev. Lett. **B249**, 163 (1990)
[7] T. Dossing *et al.*, Phys. Rev. Lett. **75**, 1276 (1995)
[8] C. E. Porter and R. G. Thomas, Phys. Rev. **104**, 483 (1956)
[9] T. Lauritsen *et al.*, proceedings of this conference
[10] B. Herskind and S. Leoni, Nucl. Phys. **A520**, (1990) 539c-554c
[11] S. Leoni, thesis work
[12] T. Dossing *et al.*, Phys. Rep. **268**, 1 (1996)
[13] D. C. Radford *et al.*, Nucl. Instrum. Methods Phys. Res., Sect. A **258**, 111 (1987)
[14] P. J. Nolan *et al.*, Nucl. Phys. **A520**, (1990) 657c
[15] I. Y. Lee *et al.*, Nucl. Phys. **A520**, (1990) 641c

Superdeformation

F. S. Stephens
Nuclear Science Division, Lawrence Berkeley National Laboratory, Berkeley, CA 94720, USA

Recent progress in the study of superdeformed nuclei is reviewed. Topics covered include: the onset of superdeformation in the mass 130-150 region; collective octupole bands; identical bands; and ΔI=2 staggering. Some comments about the futureof studies on superdeformed nuclei are included.

1. Introduction

This talk will consist of three parts: an introduction to the current situation regarding superdeformed bands; some recent highlights; and a quick look at the future. Due mainly to the large gamma-ray detectors coming into use, there is a lot going on in this area and I will not try include it all here. Rather, after a few general observations I will select several highlights and try to discuss those in some depth. Finally I will give my thoughts as to the future of studying superdeformed nuclei.

My definition of superdeformation is rather broad and generally includes nuclei where the long axis is 1.5-2 times longer than the short axis. Typically this is a second minimum in the potential energy surface; the first having smaller (perhaps "normal") deformation. With this definition there are now five regions of superdeformation known in the heavier elements, having masses centered around 80, 130, 150, 190 and 240, the last of these being the fission isomers discovered more than 30 years ago. Altogether there are around 200 bands presently known in these five regions. The newest region is that around mass 80, where already some 20 bands are known in 10 nuclei. These bands show all the familiar properties seen in the heavier regions: assigned configurations, band crossings, identical bands, etc. It is an exciting area and Cyrus Baktash is going to talk about it tomorrow morning, so I will not discuss it further here.

There are some special properties in the mass 130-150 region that are interesting and perhaps unique. The other three superdeformed regions mentioned above are well isolated from each other and transitions into or out of these regions involve changes in the occupation of several orbitals which do not occur easily. In fact, this morning we heard that in the mass 190 region the decay out of the superdeformed bands is a statistical process that occurs through a small mixing of normal states into the superdeformed ones. Only in the mass 130-150 regions can we observe the onset of superdeformation orbit by orbit.

In the mass 130 region it is the N=6 neutrons that trigger the onset of superdeformation, and this transition can be observed to occur in individual bands in ^{134}Nd. Fig. 1, taken from a contribution by Petrache et al., shows several band energies in ^{134}Nd (minus a rotational contribution). The normal deformation bands in this figure are sharply rising; whereas, the superdeformed bands are horizontal or slightly down sloping. Both bands 2 and 3 start out as normal bands and then undergo rearrangements, presumably involving the filling of two N=6 neutrons, that induce the superdeformation. Another way to view this change is as a crossing of the normal and superdeformed bands with a reasonably large interaction so that the lower energy pieces of the two bands looks like a single band with a deformation change. In either picture the differences between the bands cannot be large - probably only the change of this pair of neutrons.

As we move up in N and Z, the deformation increases in superdeformed bands, but not always smoothly. First the N=6 protons are filled and then, above N=80, the N=7 neutrons fill. In both cases there is evidence that the key changes can occur within individual bands. Later today Zhu will talk about lifetimes in ^{144}Gd, where a backbend at frequency about 0.45 MeV is

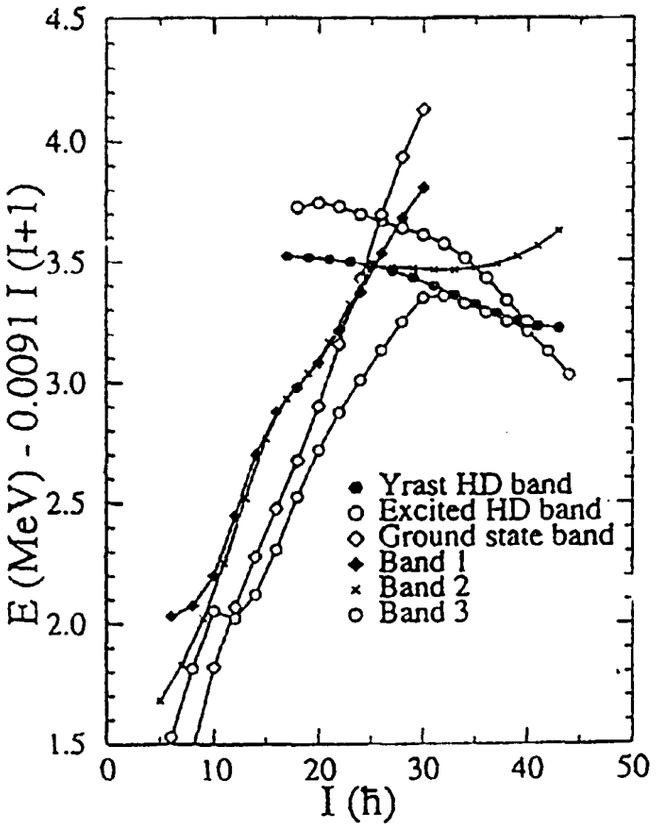

Fig. 1 Rotational bands in ^{134}Nd from the contribution of Petrache et al. Bands 2 and 3 appear to change character form normal deformed to highly (super-) deformed.

shown to be associated with a change in deformation from $\varepsilon = 0.45$ to 0.51. Again a large shift in deformation occurs with apparently a small configuration change that is associated with a pair of N=6 protons. Similarly, in ^{148}Gd de France et al., [1] have proposed that a backbend in one of the bands may be due to the occupation of the first N=7 neutrons. There is additional work in this region on Pm and Sm nuclei in abstracts to this Conference by Pfohl et al., and Jin et al.

This is a fascinating region where we can follow the evolution of deformation step by step from the normal deformed mass 130 region to the strongly superdeformed nuclei of the N=150 region. One can observe the effect of filling each of the key sets of intruder orbitals. This region offers an opportunity to learn about the microscopic origins of deformation effects.

2. Some Highlights

There are a lot of recent superdeformation highlights, one of which on links we heard about this morning and another on the mass 80 region we will hear about tomorrow. I will discuss three others: evidence for octupole effects; the news about identical bands; and the situation on $\Delta I=2$ staggering. One other point I would like to mention here is the progress in identifying configurations in superdeformed bands. Mottelson [2] emphasized here in Argonne eight years ago how important this is for understanding superdeformation. Not only does this place these nuclei in the TRS calculations (or vice versa), but it also gives the microscopic background for all the new and unusual effects we may hope to see. Fortunately there has been real progress in this area, and most bands in most nuclei have been assigned configurations.

Octupole Bands. Earlier this morning Dirk Schwalm presented some evidence for excited collective bands in the superdeformed fission isomers, and such bands have been predicted in other regions. Collective octupole excitations should be especially important in superdeformed

nuclei due to the proximity of orbitals with both parities, as was also pointed out by Mottelson [2] here in Argonne eight years ago. He emphasized particularly the Y_{31} "banana" shapes.

The first evidence for an octupole band in superdeformed nuclei came from Crowell et al.,[3] for a band in ^{190}Hg that decayed to the lowest superdeformed band rather than to normally deformed states. The connecting transitions were shown to be stretched dipole, rather than quadrupole and, if E1, were about 10^{-3} Wu, which is typical for collective octupole states in normal nuclei. Recently Nakatsukasa [4] has calculated the octupole effects in ^{190,192,194}Hg and he will discuss these calculations tomorrow morning. He has found impressive agreement with these ^{190}Hg experimental results. In addition he predicts band crossings in ^{192}Hg and there is evidence to support this, although the situation is not yet clear.

Nakatsukasa also predicts a small octupole-type signature splitting (odd spins lower) in ^{194}Hg which inverts at higher frequencies due to non-collective quasi-particle admixtures. This is a very characteristic signature inversion for which we have found experimental evidence. Fig. 2 shows the situation. The plot is the signature splitting (α=0 Routhian minus α=1 Routhian) *vs.* the rotational frequency, so that positive values indicate octupole-type splitting. There are two calculated lines: the upper for a constant pairing strength as a function of frequency; and the lower for pairing that decreases at the higher frequencies. The data points are connected by a line and fall rather convincingly between the two pairing limits of the calculations. The initial octupole-type splitting and the later downturn (toward signature inversion) in both data and calculations are clear. The sensitivity to the pairing is surprising and it seems likely that a good fit to the data could be achieved by an intermediate value for the pairing. We take this agreement to be rather strong support for octupole effects in these excited bands of ^{194}Hg.

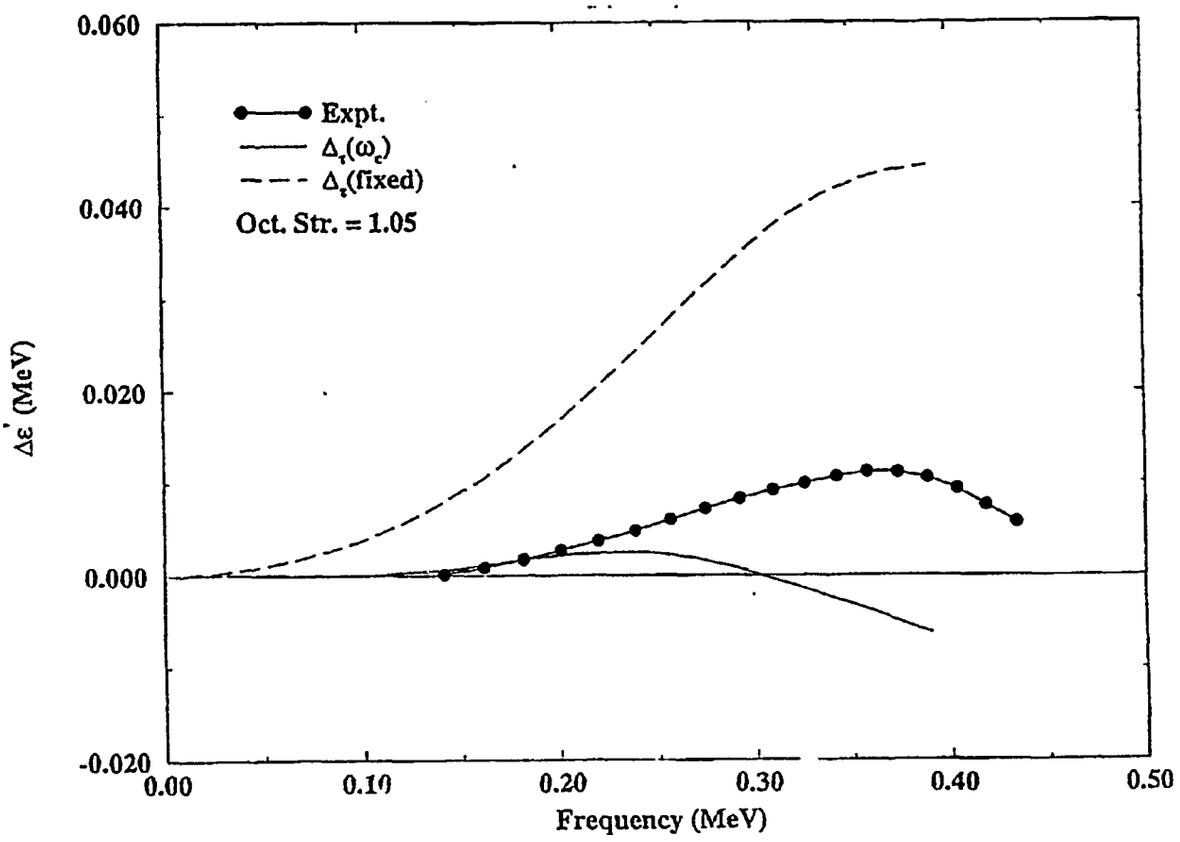

Fig. 2 Signature splitting in ^{194}Hg compared with calculations of Nakatsukasa.

In summary, there are two pieces of evidence for octupole effects in these superdeformed Hg nuclei: the connecting transitions in ^{190}Hg and the signature splitting in ^{194}Hg. Work is underway to see if ^{192}Hg fits this pattern and it looks promising at present. Tomorrow, Azaiez will also report some new evidence for octupole bands in ^{196}Pb. This has become a "hot" topic now as we try to establish the types and strength of the octupole effects in superdeformed nuclei.

Identical Bands. The identical bands are a rather long-standing puzzle in nuclear structure physics and significant progress has been made recently. There are two aspects of these bands that are necessary in our definition of "identical". First, the moments of inertia, $dI/d\omega$, have to be equal (and some people already call such bands "identical") and second, there must be a relationship between the gamma-ray transition energies in the two bands. Either these energies must be equal or they must fall at the one-quarter, half, or three-quarter point of the interval between transition energies in the other band. These points arise because they are the allowed points on a single I *vs.* ω line due to the quantization of spin (where the interval between transitions in each band is $2\hbar$). Thus, <u>if confined to this single line</u>, a band in an even-mass nucleus (having integer spin) would always fall at the zero or half points of the interval (assuming an even-even reference nucleus); whereas one in an odd-mass nucleus would fall at the quarter or three-quarter point. Since we generally do not know the spins in superdeformed bands, the above "identical" relationship only implies that the bands lie on parallel lines that are the same (as assumed above) or are shifted in spin by integer or half-integer values. Half-integer shifts invert the even- and odd-mass relationships given above. These shifts in spin at a given frequency are called "alignments" and identical bands, in our definition, imply quantized alignments (in integer or half-integer values).

The first important question about identical bands is: do they occur more often than expected if alignments are random. The answer from an analysis of superdeformed bands in the mass-190 region [5] seems to be that they do. The next important question is; what are the alignments, and to answer this question one must know the spins. This is an area where important progress has recently been made with the discovery of linking transitions. The spins of superdeformed bands in the mass-190 region were first proposed from model-dependent analyses of the rotational energies [6]. These indicated that a number of bands identical to ^{192}Hg had alignments very close to one. The recent discovery [7] of links between two superdeformed bands in ^{194}Hg and the known states near the ground state have been extended by Hackman this morning, establishing the partial level scheme shown in Fig. 3 which determines the spins of this superdeformed band as indicated. These agree with those from the rotational-energy analyses and show that this band, which is identical to the yrast SD band in ^{192}Hg, has a relative alignment of one. This is not so easy to understand, because either "no change" or "several small compensating changes" would result in an alignment close to zero. It may involve some new physics, as has been discussed [8].

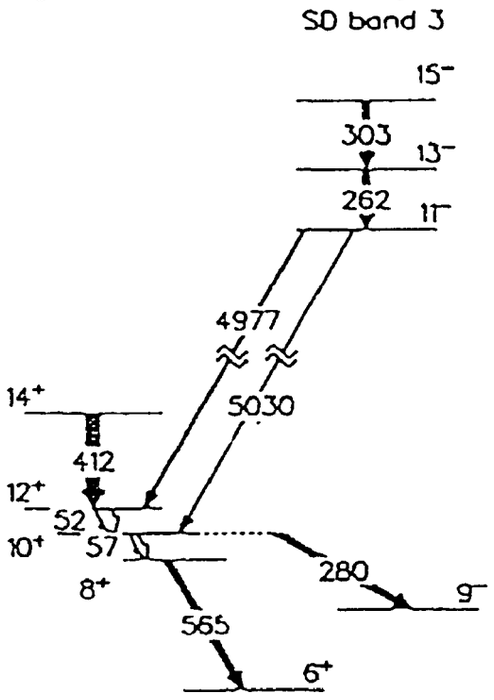

Fig. 3 Level scheme of ^{194}Hg.

Another important advance coming with the large arrays is the ability to make precise relative lifetime measurements. When comparing recoiling nuclei of the same atomic number, made in the same reaction and

Table 1: Precise Quadrupole Moments of Identical Bands.

Ref.	Nucleus (band #)	Relative Q_t (exp)	β/β_{ref}	Deformation
*	^{192}Hg	16.6(10)		
ref[9]	^{194}Hg (3)	16.7(10)	1.00(9)	Same
*	^{192}Hg	17.2(13)		
ref[10]	^{193}Hg (1-5)	13.8-14.7(8)	0.83(8)	Different
	^{152}Dy	17.5(7)		
ref[11]	^{151}Dy (4)	17.5(10)	1.00(7)	Same
**	^{152}Dy	17.5(2)		
	^{149}Gd (4)	17.5(6)	1.05(4)	Different?
ref[12]	^{148}Gd (5)	17.8(13)	1.07(7)	Different?
	^{132}Ce	7.4(3)		
ref[13]	^{131}Ce (4)	8.5(4)	1.15(7)	Different
	^{131}Ce	7.4(4)		
ref[13]	^{132}Ce (2)	7.3(3)	0.99(7)	Same

recoiling in the same backing material, the large uncertainties associated with stopping times cancel out and the relative precision can be 5% or better. These lifetimes give the transition quadrupole moments and, assuming axial symmetry, the deformations. Another interesting question about two identical bands is whether they have the same deformations, and we can begin to answer that question. In Table 1 are collected all the precise data on relative lifetimes that are currently available. It is pretty clear that for three pairs of identical bands the deformations are the same within the accuracy of the measurements. In two cases the deformations are very likely different, and in the sixth case, the two gadolinium bands are similar to each other, but probably different than the identical band in ^{152}Dy. Note that some of these data are still preliminary (*) and for one set (**) the nuclei have different atomic numbers and were made in different reactions. Nevertheless, it seems likely that identical bands do not always have the same deformation.

The conclusion seems to be that identical bands do not necessarily have all properties the same or very similar. This rules out the simplest picture of such bands, namely that essentially nothing changes. In the case of the deformations, the effects of the observed changes on the transition energies must be compensated by other effects, but whether these compensations are accidental or systematic (implying something new) is not clear. The situation for alignments is different. The alignment shifts to a completely different (though integer) value and is not likely the result of compensations of several small effects. Either it is a complete accident or due to some new physics. More data on other cases should tell us which. The identical bands are still a puzzle; however, we are now making progress toward a solution.

ΔI=2 Staggering. One of the exciting recent events in high-spin physics was the announcement by Flibotte et al., [14] of a regular staggering pattern in the transition energies of one of the superdeformed bands in ^{149}Gd. States differing by four units of angular momentum were found to have small similar shifts in energy of about 60 eV compared to a smooth rotational sequence. Since that time several apparently similar cases were reported in the literature. One

proposed explanation of a long regular staggering of this type was based on a deformed shape with a component having C_4 symmetry. However, some of the observed patterns were not so long or regular and might be explained more simply by a crossing of two bands. Since the former explanation involves entirely new and unexpected physics and the latter would be quite puzzling without evidence for the crossing band, it is important to check the data and that has been underway very recently.

Some of the data that gave evidence for long regular staggering sequences came from three superdeformed bands of ^{194}Hg, which were studied by Cederwall et al [15]. This experiment has been repeated and Krucken will talk about the results tomorrow morning. He concludes that there is no clear evidence in ^{194}Hg for long regular staggering patterns, although there are very likely short irregularities in some bands. New measurements have also been made on the other cases of staggering reported. These confirmed the original ^{149}Gd long regular stagger [16], but the other two similar cases were not reproduced. The remaining cases did not involve long sequences and thus look more like band crossings. So up until last week there was only one case of long regular staggering remaining -- the original one.

Today Stephane Flibotte gave me some preliminary results on a new superdeformed band in ^{148}Eu coming from a Gammasphere experiment run only last week. This nucleus was chosen because it has one proton less than ^{149}Gd and, if the proton hole is in the [301]1/2 orbital, a band identical to the one with the staggering in ^{149}Gd should result. Whether this band also has the staggering is an intriguing question. The result is shown in Fig. 4. There appears to be a rather long staggering sequence with, however, a phase opposite to that in ^{149}Gd. These experiments

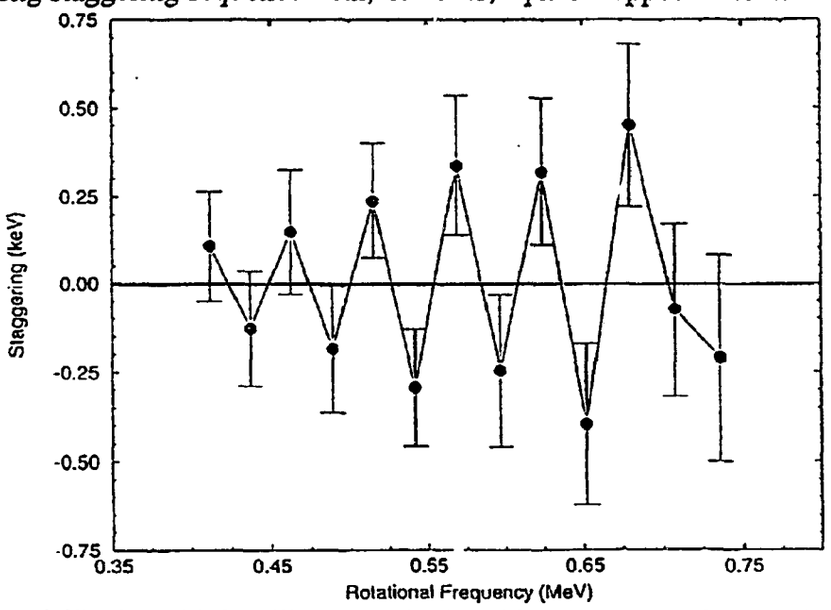

Fig. 4 Staggering plot for ^{148}Eu from Flibotte et al.

are difficult and it is still very early, but this is a spectacular, albeit puzzling, result.

The cause of such long regular staggering sequences, as well as that of the shorter sequences, is not clear. One problem is that a C_4 symmetry in the nuclear shape may not always generate long regular sequences, so that even for the shorter sequences one could not rule out C_4 effects. This is a fascinating problem and, with the large arrays, it is progressing rapidly.

3. The Future

There are many exciting things going on right now concerning superdeformed nuclei and a lot of open questions. We now have a good idea of configurations for most bands, providing a framework to look for new and unexpected phenomena. The study of linking transitions is just

beginning. Our study of excited collective bands in these nuclei is developing rapidly. I discussed octupole excitations and Peter Twin will tell us about some other types of collective excitations later in this session. We have also taken a big step forward in understanding identical bands and probably have the tools now to solve this long standing puzzle. The mystery of $\Delta I=2$ staggering is deepening, however even if this phenomenon is just band crossing it is interesting. Why do we not see the crossing bands?

There are other still more open questions regarding superdeformed bands. We can study shape evolution, step by step, in the mass 130-150 regions, perhaps helping us understand the decay mechanisms and if or where non-statistical effects show up in these decays. Understanding nuclear pairing is a challenge and the superdeformed nuclei can provide different insights. If there are higher multipoles in the pairing they are likely to show up in superdeformed nuclei due to the different mixture of orbits at the Fermi surface. Dynamic pairing is a real mystery and the large shell gaps coupled with the regular high spin states provide a very different approach to its study. And finally two continua exist; feeding and decay. The feeding is different than that in the normally deformed nuclei -- due to the lower giant dipole resonance, for example. The decay out is a completely new unresolved spectrum. It promises systematic information on mixing matrix elements, level densities and information on both statistical and (perhaps) non-statistical transition probabilities as a function of excitation energy and spin. These continua are a reservoir of new phenomena.

Superdeformed nuclei provide unique information on all the topics mentioned above. It is currently an exciting area with many directions to explore. The new arrays provide the access into these mysteries. For superdeformed nuclei, resolving power delivers!

Acknowledgments

I am indebted to a number of colleagues for permission to quote data prior to publication and for help and advice in preparing this talk. This work was supported in part by the Director, Office of Energy Research, Office of High Energy and Nuclear Physics, Nuclear Physics Division, of the U. S. Department of Energy under Contract No. DE-AC03-76SF00098.

References

1. G. de France et al., submitted to Phys. Lett. B
2. B. Mottelson, Proceedings of the Conference on High-Spin Nuclear Structure and Novel Nuclear Shapes, Argonne, Illinois, April 1988, ANL-PHY-88-2 (1988) p1.
3. B. Crowell et al., Phys. Rev. **C51** (1995) R1599
4. T. Nakatsukasa et al., Phys. Rev. **C53** (2213) 1996
5. P, Fallon et al., Proceedings of the Conference on Physics from Large Gamma-Ray Detector Arrays, Berkeley, California, LBL pub-35687 (1994) p89.
6. J.A. Becker et al., Nucl. Phys. A520 (1990) 187c.
7. T.L. Khoo et al., Phys. Rev. Lett., 76 (1996) 1583.
8. F.S. Stephens et al., Phys. Rev. Lett. 64 (1990) 2623; Phys. Rev. Lett. 65 (1990) 301.
9. E.F. Moore et al., to be published.
10. B. Busse et al., to be published.
11. D. Nisius et al., to be published.
12. H. Savajols et al., Phys. Rev. Lett. 76 (1996) 4480.
13. R.M. Clark et al., Phys. Rev. Lett. 76 (1996) 3510.
14. S. Flibotte et al., Phys. Rev. Lett. 71 (1993) 4299.
15. B. Cederwall et al., Phys. Rev. Lett. 72 (1994) 3150.
16. P.J. Twin, reported at the Workshop for Gammasphere Physics, Berkeley, California, Dec. 1995, to be published (World Scientific).

Microscopic Description of Nuclear Shapes

J.L. Egido, L.M. Robledo, A. Valor and A. Villafranca
Departamento de Física Teórica C-XI
Universidad Autónoma de Madrid, E–28049 Madrid, Spain

Abstract

The approximate particle number theory for density dependent forces is sketched, the theory is applied to discuss properties of the superdeformed ground state and excited bands of ^{192}Hg. The force used in the calculations is the finite range density dependent Gogny force. The agreement with the available experimental results is very satisfactory.

The most popular approaches to describe high spin phenomena -we restrict ourselves to descriptions within the cranking model- have been the mean-field (Woods-Saxon or Nilsson) plus Strutinsky shell corrections [1] and the self-consistent Hartree-Fock-Bogoliubov (HFB) one.

Within the HFB approaches the most successful calculations have been performed with density dependent hamiltonians. The most popular, because of its simplicity, is the Skyrme force, most of the calculations have been performed by Bonche et al. [2, 3, 4] with the SkM* parametrization. Recently the Gogny force [6, 7, 8] has been also applied to high spin problems at normal deformations [9] and to superdeformed shapes [10, 11]. Relativistic mean field calculations [12] has been also very successful in the description of superdeformed bands.

In these calculations Lagrange multipliers were used to adjust on the average the particle number and the angular momentum, the so-called cranked HFB approximation (CHFB). It turned out [9], however, that in spite of the finite range of the force, the condition of conserving the particle number on the average was not enough and a sharp phase transition was found, contrary to what one would expect for a finite system. The same results were obtained with the Skyrme force either with a pure monopole pairing or with a density dependent pairing force in the particle-particle channel. To remedy this problem one has to introduce further correlations as those present in mean field approaches, i.e. ones has to go beyond the mean field approximation. The ideal treatment of pairing correlations in nuclei is particle number projection before the variation [13].

An exact particle number projection at high spin is rather complicated and up to now it has only been applied to separable forces [16]. On the other hand, the semi-classical recipe of solving the mean field equations with a constraint on the corresponding symmetry operator can be derived as the first order approach of a full quantum-mechanical expansion (the Kamlah expansion) [17] of the projected quantities. The second order in this expansion takes into account the particle number fluctuations and might cure some of the deficiencies

of the first order approximation. However, full calculations up to second order are rather cumbersome and just a simple model calculation has been carried out up to now [18]. Most second order calculations have been done using the Lipkin-Nogami (LN) recipe originally proposed in Refs. [19, 20, 21]. We shall now display the corresponding equations for a density dependent hamiltonian. For a derivation see [26].

The projected energy to second order is given by

$$E_{proj} = \langle \hat{H} \rangle - h_2 \langle (\Delta \hat{N})^2 \rangle + h_1 (N - \langle \hat{N} \rangle) + h_2 (N - \langle \hat{N} \rangle)^2, \tag{1}$$

with $\langle \hat{A} \rangle \equiv \langle \Phi | \hat{A} | \Phi \rangle$. In a full variation after projection method one should vary eq. (1). In the Lipkin-Nogami prescription, however, the coefficient h_2 is held constant during the variation, the resulting equation is much simpler [15], one has to minimize

$$E_{proj} = \langle \hat{H} \rangle - h_2 \langle (\Delta \hat{N})^2 \rangle \tag{2}$$

with the constraint

$$\langle \hat{N} \rangle = N. \tag{3}$$

For density dependent forces the coefficient h_2 takes the form

$$h_2 = \frac{\langle \hat{\mathcal{H}} - \langle \hat{\mathcal{H}} \rangle (\Delta \hat{N})^2 \rangle - \langle \hat{\mathcal{H}} - \langle \hat{\mathcal{H}} \rangle \Delta \hat{N} \rangle \langle (\Delta \hat{N})^3 \rangle / \langle (\Delta \hat{N})^2 \rangle}{\langle (\Delta \hat{N})^4 \rangle - \langle (\Delta \hat{N})^2 \rangle^2 - \langle (\Delta \hat{N})^3 \rangle^2 / \langle (\Delta \hat{N})^2 \rangle} \tag{4}$$

with

$$\hat{\mathcal{H}} = \hat{H} + \frac{\partial \hat{H}}{\partial \rho(r)} \hat{\rho} \tag{5}$$

The last term in this equation is a consequence of the density dependence of the hamiltonian and does not appear in the standard derivation of the Lipkin-Nogami approximation. The presence of this term might be very important for forces with density dependent pairing.

We have applied the LN formalism with the Gogny force to study the superdeformed ground state band and one excited band of the nucleus ^{192}Hg. These bands have been study experimentally in refs. [22, 23] and theoretically in [24] with the Skyrme force and in [25] with the Wood Saxon plus Strutinsky method. In the calculations we are using the standard DS1 parametrization set [8]. In all our results we shall also present the ones obtained with the plain cranked HFB theory (CHFB) [9].

In fig. 1, left hand side, we show the angular momentum dependence of the charge quadrupole moment, Q_0, for the superdeformed ground band of the nucleus ^{192}Hg. The CHFBLN and the CHFB results differ mostly at low spins where the pairing correlations are larger. As a function of the angular momentum we observe first an increase of the quadrupole moment due to a reduction of the pairing correlations and then a decrease of Q_0. This anti-stretching effect is caused by the Coriolis force. In spite of the different values of the CHFB and the CHFBLN approaches, specially at low spins, both predictions coincide with the experimental value (18.6 ± 1.4 eb) [22] within the experimental errors. The nucleus is axially symmetric, i.e. $\gamma = 0$, for all spin values.

In the right hand side of fig. 1 we display the transition energies versus the angular momentum for the superdeformed ground band. The agreement with the experimental data

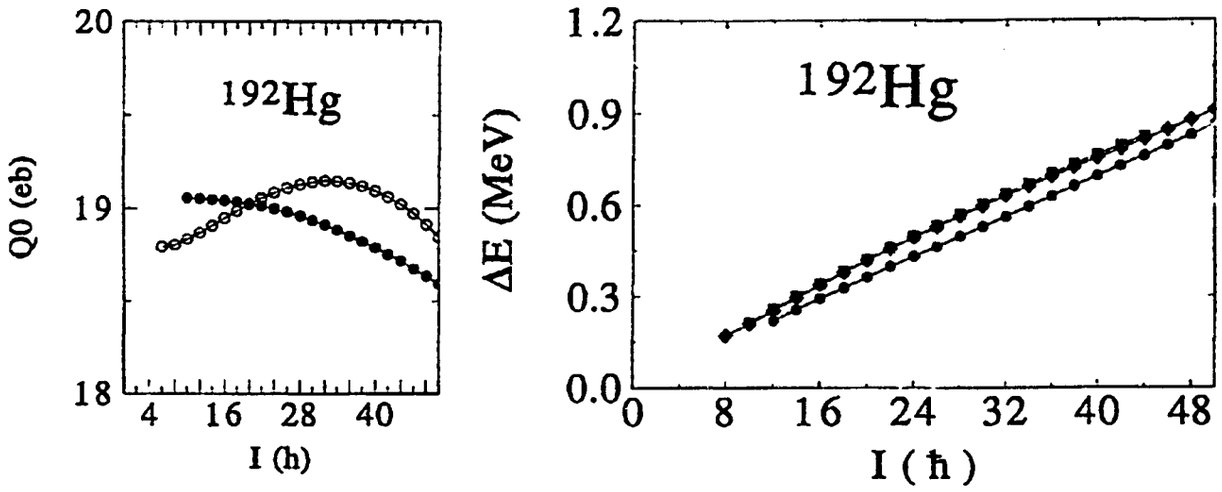

Figure 1: Left hand side, the charge quadrupole moment of the superdeformed ground band for ^{192}Hg, CHFB (full circles), CHFBLN (open circles), versus de angular moment. Right hand side, the transition energies, CHFB (circles), CHFBLN (diamonds), experiment (squares), [22].

is good in the CHFBLN approach, in the CHFB one obtain too lower values. The reason for it is again the smallness of the pairing correlation in the CHFB approach (the transition energy is inverse proportional to the moment of inertia).

In fig. 2, the second moment of inertia $\mathcal{J}^{(2)}$ as a function of the angular frequency is represented. Here, as in the previous picture, the CHFB results are in poor agreement with the experiment. At small spin values the moment of inertia is too large and the neutron alignment sets in too early. The CHFBLN results, however, are in very good agreement with the experimental results, the correlations induced by the approximate particle number projection produce the desired effect, namely, to diminish the moment of inertia at small spin values and to delay the alignment to higher spin values.

We find that the orbitals responsible for the alignment at $\hbar\omega \approx 0.4$ MeV in ^{192}Hg is the $\nu[761]\frac{1}{2}$. The proton alignment take place at higher frequencies ($\hbar\omega \approx 0.45$) and it is due to the $\pi[642]\frac{5}{2}$*orbital*.

Concerning the excited bands of ^{192}Hg, we shall show CHFBLN results concerning the so-called band 3 in the literature [23], a band of negative parity. The theoretical description is based in the blocked CHFBLN theory. We have found two signature partner bands (we call them C_1 and C_2), which transition energies agree very well with the experimental data. Band C_1 is obtained by blocking of the lowest quasineutron states of negative signature in the positive and negative parity channels, band C_2 is obtained by blocking of the lowest positive parity quasineutron with positive signature and the lowest negative parity quasineutron with negative signature. The experimental transition energies agree slightly better with band C_1 than with band C_2. In fig. 3a we display the charge quadrupole moment of this bands, it is rather constant as compared with the ground band and about 1.5 (eb) smaller than this one. As we can see both bands have almost identical deformation. The bands are also axially

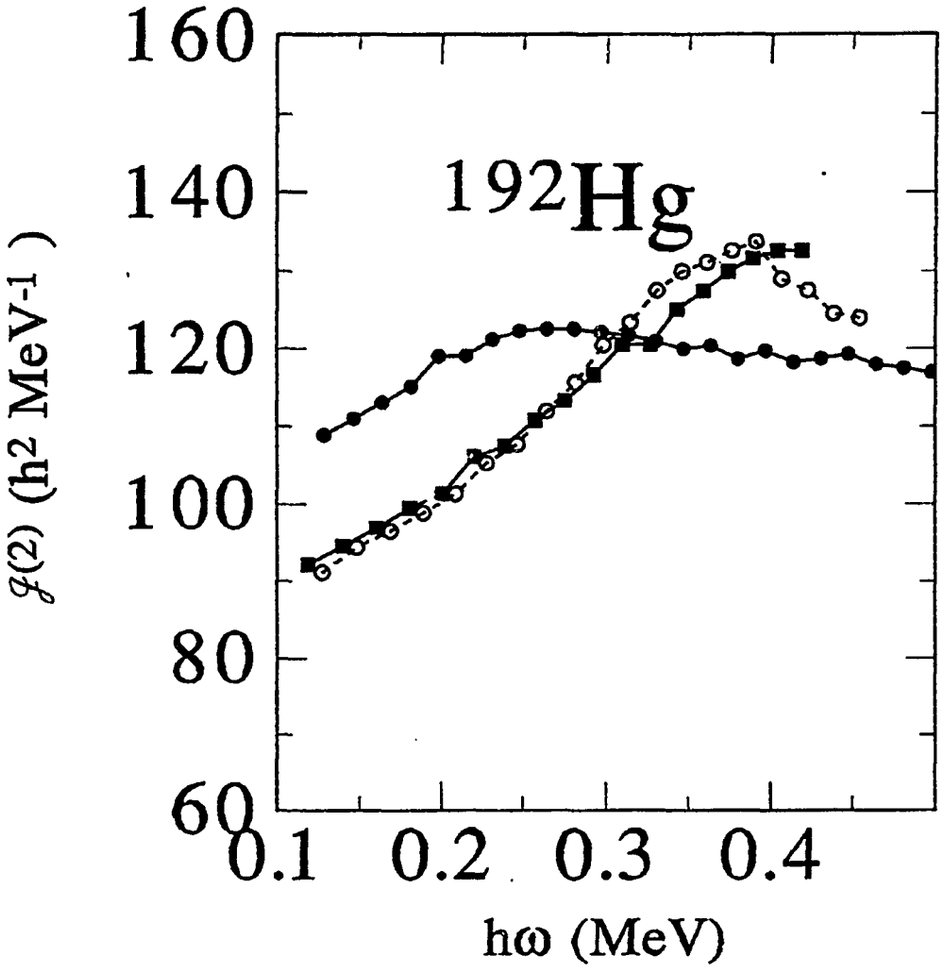

Figure 2: Second moment of inertia for the superdeformed ground band of ^{192}Hg. Squares for the experimental data [22], full circles for the CHFB approach and open ones for the CHFBLN theory.

symmetric ($\gamma = 0$).

In fig. 3b we show the results for the second moment of inertia as well as the experimental data [23]. Experimentally the moment of inertia grows gradually up to $\hbar\omega = 0.3$ MeV, from this point on a sharp increase take place, producing an upbend at $\hbar\omega = 0.33$ MeV. These features are nicely reproduce by bands C_1 and C_2. If we identify band C_1 with the experimentally measured band 3 it is not clear to us why the signature partner band has not been measured.

In conclusion, the ground state band and the superdeformed band 3 of the nucleus ^{192}Hg have been study within the approximate particle number projected theory with the density dependent Gogny force. Global properties as well as sensitive properties as the second moment of inertia are very well reproduced, specially within the CHFBLN approximation. We believe that the Gogny forces with the approximate particle number projected mean field theory provides a good description of nuclear properties under a large variety of situations.

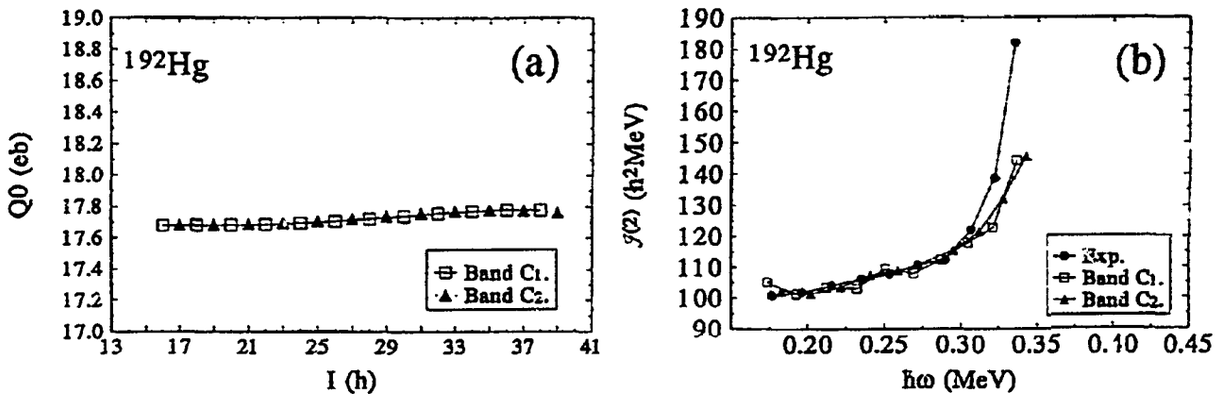

Figure 3: Left hand side, theoretical values of bands C_1 and C_2 for the charge quadrupole moment of band 3 of ^{192}Hg. Right hand side, second moments of inertia for band 3 of ^{192}Hg.

This work was supported in part by DGICyT, Spain under Project PB94–0164.

References

[1] R. Bensgtsson et al. Phys. Lett. **B57**, 301 (1975); C. G. Anderson et al. Nucl. Phys. **A268**, 205 (1976); K. Neergard, H. Toki, M. Ploszajczak and A. Faessler Nucl. Phys. **A287**, 48 (1977).

[2] P. Bonche, P.H. Heenen and H.C. Flocard. Nucl. Phys. **A467**, 115 (1987).

[3] H.C. Flocard. *Nuclear Structure of the Zirconium Region,* J. Eberth, R.A. Meyer and K. Sistemich (Eds.). Research Reports in Physics. Springer-Verlag, p 143 (1988).

[4] J. Terasaki, P.-H. Heenen, P. Bonche, J. Dobaczewski and H. Flocard, Nucl Phys. **A593** (1995)1

[5] B.R. Mottelson and J.G. Valatin. Phys. Rev. Lett. **5**, 511 (1960).

[6] D. Gogny. *Nuclear Selfconsistent fields.* Eds. G. Ripka and M. Porneuf (North Holland 1975).

[7] J. Dechargé and D. Gogny. Phys. Rev. **C21**, 1568 (1980)..

[8] J.F. Berger, M. Girod and D. Gogny. Nucl. Phys. **A428**,23c (1984).

[9] J. L. Egido and L. M. Robledo, Phys. Rev. Lett. **70**, 2876 (1993).

[10] J. L. Egido, L. M. Robledo and R.R. Chasman, Phys. Lett. **B322** (1994) 22-26

[11] M. Girod, J.P. Delaroche, J. F. Berger and J. Libert, Phys. Lett. **B325** (1994) 1-6

[12] J. Konig and P. Ring, Phys. Rev. Lett. **71**, 3079 (1993)

[13] P. Ring and P. Shuck, *The Nuclear Many Body Problem* (1980), Springer–Verlag Edt. Berlin.

[14] P. Bonche, J. Dobaczewski, H. Flocard, P.-H. Heenen and J. Meyer, Nucl. Phys. **A510**, 466 (1990).

[15] A. Valor, J.L. Egido and L.M. Robledo, Phys. Rev. **C53**, 172 (1996).

[16] J.L. Egido and P. Ring, Nucl. Phys. **A388**, 19 (1982).

[17] A. Kamlah, Z. Phys. **216**, 52 (1968).

[18] D. C. Zheng, D.W.L. Sprung and H. Flocard, Phys. Rev. bf C46, 1335 (1992).

[19] H. J. Lipkin, Ann. Phys. (N.Y.) **12**, 425 (1960).

[20] Y. Nogami, Phys. Rev. **B134**, 313 (1964); Y. Nogami and I.J. Zucker, Nucl. Phys. **60**, 203 (1964).

[21] J. F. Goodfellow and Y. Nogami, Can. J. Phys. **44**, 1321 (1966). and W. Nazarewicz, Phys. Rev. **C48**, 1681 (1993). 2317 (1983).

[22] P. Willsau et al., Nucl. Ohys, **A574**(1994) 560

[23] P. Fallon et al, Phys Rev. **C51** (1995) R1609

[24] G. Gall, P. Bonche, J. Dobaczewski, H. Flocard and P.-H. Heenen, Z. Phys. **A348**, 183 (1994).

[25] W. Satula, S. Cwiok and W. Nararewicz, Nucl. Phys. **529**, 289 (1991)

[26] A. Valor, J.L. Egido and L.M. Robledo, to be published.

Around the back-bend in an excited ^{150}Gd Superdeformed Band

P. J. Twin[a], S. Ertürk[a], C. W. Beausang[a], P. Fallon[b],
D. Appelbe[a], S. Asztalos[b], A. Macchiavelli[b], T. Lauritsen[c],
I. Y. Lee[b], F. S. Stephens[b] and M. A. Deleplanque-Stevens[b]

a *Oliver Lodge Laboratory, University of Liverpool, Liverpool, L69 3BX, United Kingdom.*

b *Nuclear Science Division, Lawrence Berkeley National Laboratory, Berkeley, California 94720, USA.*

c *Physics Division, Argonne National Laboratory, Illinois 60439, USA.*

Abstract: The excited superdeformed band (band 5) in ^{150}Gd has a discontinuity (back-bend) in the smooth variation of gamma-ray energy with spin at around 1 MeV. It has been established that the band also has a decay branch that is probably a continuation of band 5 below the back-bend. Gamma-rays have been identified which link band 5 with the yrast superdeformed band in ^{150}Gd.

1. Introduction

There are four strongly excited superdeformed (SD) bands[1]) in ^{150}Gd. The strongest (SD2) at 50% intensity of the yrast SD band is associated with a proton excitation from the low N [301]½ orbital into the high N $[651]^3/_2$. SD band 3 and 4 are signature parties and they exhibit $\mathfrak{J}^{(2)}$ moments of inertia similar to the yrast SD band in ^{149}Gd and thus they are associated with neutron excitations from the high N [770]½ orbital into the $[402]^5/_2$ orbitals. This report concerns SD band 5 which has an intensity of 38% relative to the yrast SD band and an $\mathfrak{J}^{(2)}$ of a large magnitude similar to that of the yrast SD band in ^{152}Dy. In addition the γ-ray energies are within 1 - 2 keV of those in ^{152}Dy at the highest energies. These data have led to the proposal [2]) that ^{150}Gd SD band 5 is associated with a two proton excitation from the [301]½ orbital into the $[651]^3/_2$ orbital. The γ-ray energies slowly diverge from those in ^{152}Dy as the spin of the band decreases until there is a discontinuity or back-bend at a γ-ray energy of just below 1 MeV. This feature is unusual in SD bands in the A = 150 region, the other examples have been interpreted as neutron pairing effects in ^{150}Gd band 1 [3]) and ^{149}Gd band 2 [4,5]); proton pairing alignments [6]) in ^{144}Gd band 1; and an interaction [7]) between the neutron [651]½ and $[642]^5/_2$ orbitals (^{146,147,148}Gd). In the case of Gd SD band 5 it has been suggested [2]) that the back-bend is linked to proton pair excitation.

The excited SD bands in ^{150}Gd have been investigated in an experiment at Gammasphere (with 84 detectors installed) using the ^{130}Te (^{26}Mg, 6n) reaction on 2 tellurium foils of thickness 500μg cm^{-2} on 500μg cm^{-2} gold with a thin layer of aluminium to prevent migration of the tellurium. Over 10^9 events were recorded with unsuppressed fold greater than 5. Analysis has focussed on setting three selection conditions and thus using data with at least four coincidence γ-rays. Details of the decay scheme around the back-bend have been established and links between SD bands 5 and 1 have been identified [8].

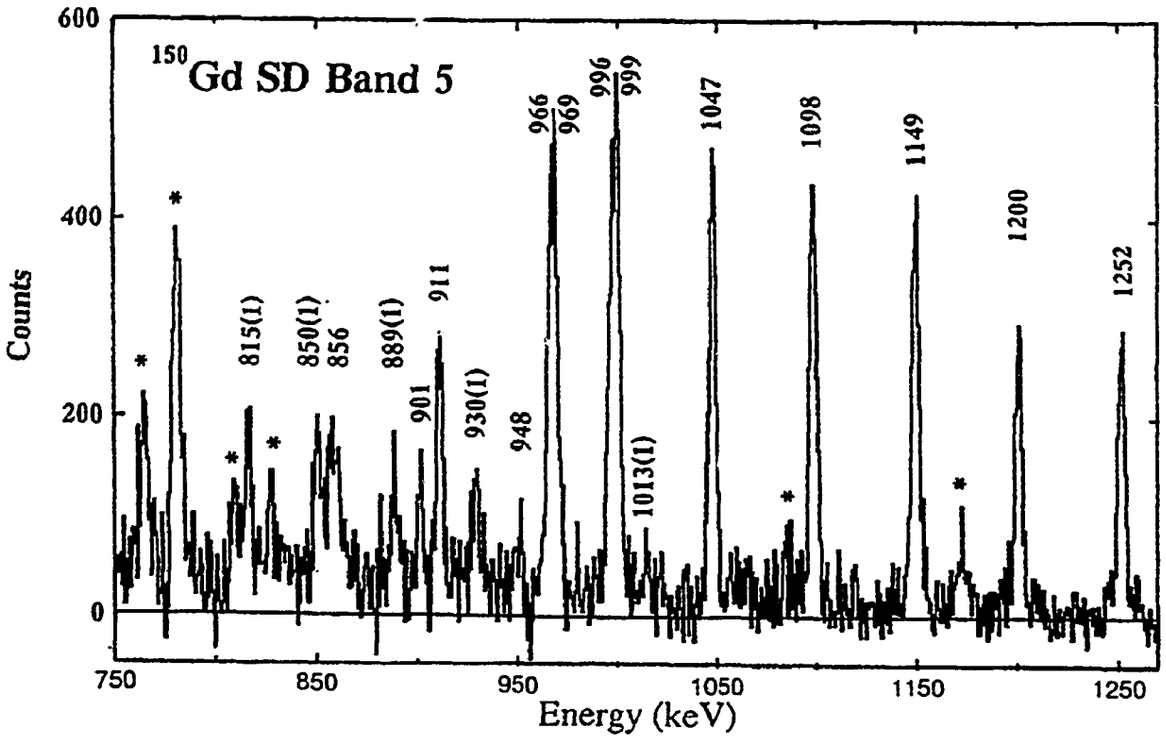

Figure 1. Spectrum of SD band 5 in ^{150}Gd obtained by setting three gates on γ-rays in the band from 1047 keV to 1450 keV. The gamma-rays with energies of 815 keV, 850 keV, 889 keV, 930 keV and 1014 keV are identical to γ-rays in the yrast SD band (band 1) of ^{150}Gd. Gamma-rays marked with an asterisk (*) are associated with the decay out of the band into normally deformed states.

2. The back-bend in ^{150}Gd

The spectrum of ^{150}Gd SD band 5 shown in figure 1 has been obtained by setting 3 gates on γ-rays between 1047 keV and 1450 keV (except 1098 keV as this is very similar to the energy of a γ-ray in the yrast SD band). The major intensity flow is via the doublets at 996, 999 keV and 966, 969 keV followed by the 911 keV transition. There are other γ-rays in the spectrum which are not observed in other SD bands and therefore are probably not associated with the decay out via normally deformed states. These include γ-rays with energies identical

to those at the lower spin end of the yrast band which will be discussed later and those at 856, 901 and 948 keV. The later transition is close to the strong 950 keV decay between normally deformed states but this decay is only very weakly seen in spectra obtained for other superdeformed bands in ^{150}Gd.

A spectrum with two gates on SD band 5 on or above the 1047 keV transition and one gate on the 901 keV transition shows that this γ-ray is in coincidence with the 999 keV member of the higher energy doublet and weakly with the 966 member of the lower - energy doublet. However it is not in coincidence the two other members of those doublets. It is concluded that it is parallel with the 969 keV γ-ray as shown in the decay scheme proposed in figure 2. The 948 keV and 856 keV γ-rays are in coincidence with the 901 keV transition and thus they are placed with the 901 keV as a continuation of SD band 5 below the band crossing. The intensities of the four members of the back-bend doublets have been estimated from a series

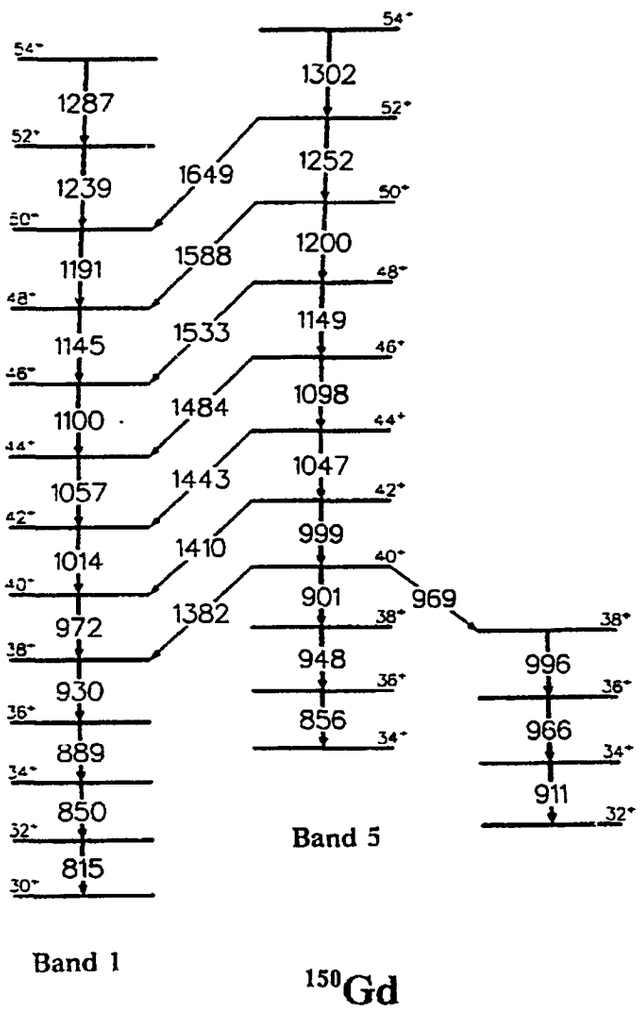

Figure 2. Decay scheme of SD band 5 in ^{150}Gd showing the proposed continuation of the band below the band crossing and the transitions linking SD bands 5 and 1.

of spectra including those with the final condition being a narrow gate on one of the doublet members. These show that the intensities of the 966, 969 and 996 keV transitions are approximately equal and that the difference between these intensities and that of the 999 keV is equal to that of the 901 keV γ-ray. Thus there appears to be no loss of total intensity around the back-bend. The level scheme is consistent with a strong interaction between two levels of spin 38^+ which are separated by 68 keV (fig. 2) whereas their unperturbed separation is 5 - 10 keV. Adjacent levels in the band would have much larger unperturbed separations and thus have much smaller perturbations of a few keV. Thus the level scheme in figure 2 is consistent with an accidental degeneracy of two states which have different SD configurations and thus it may not be a pairing interaction as previously [2]) suggested.

3. Decays between band 5 and band 1

The spectrum (figure 1) of SD band 5 in ^{150}Gd indicates the presence of the lowest four transitions (815, 850, 889 and 930 keV) of the yrast SD band. The next members are the 972 keV transition, which is not fully resolvable from the 966/969 keV doublet, and the 1014 keV transition which is weaker. Higher energy members are not observable in the spectrum. The intensities of the lowest 4 band 1 γ-rays are each approximately 24% of the intensity of band 5. Gamma-rays linking bands 5 and 1 were identified from spectra generated by setting two gates on band 5 and one gate on band 1. In figure 3a the spectrum has two gates from 999 keV to 1450 keV on band 5 and one gate from 850 keV to 930 keV on band 1 whereas in figure 3b the gates on band 5 have been restricted to 1149 to 1450 keV and that on band 1 extended up to 1057 keV. A series of 7 transitions from 1382 keV up to 1649 keV are observed in these spectra. The 1381 keV γ-ray is much stronger in figure 3a which has gates extending down to 999 keV and the higher energy transitions are stronger in figure 3b where the gates on band 1 are extended to the higher energies. These transitions indicate unambiguously that the bands are linked as shown in figure 2. The γ-ray energies are consistent with this interpretation and it is possible that the links extend to even higher spins. The decay between the bands occurs at spins above the back-bend and it appears to stop at the back-bend. This is at variance with the initial suggestion that the inter-band decays were initiated by the back-bend. The linking transitions are currently being further investigated to establish their intensities and to measure angular correlation information which should give definite information on the multipolarity of the transitions. In fig. 2 the transitions are assumed to be of E2 character and the spins of the states to be even. These assignments are based on the identity of the γ-ray energies with those of the yrast SD band in ^{152}Dy. However these spin assignments are two lower than currently assumed [7]) for the yrast SD band in ^{152}Dy. If confirmed by the multipolarity information it shows that the spins of all SD bands with four N = 6 protons should be 2ħ lower relative to Tb and Gd SD bands with two and three N = 6 protons.

The intensity data should enable conclusions about the character of band 5 and that of the linking transitions.

Support for this project is acknowledged from the UK EPSRC and the US DOE Nuclear Physics Division.

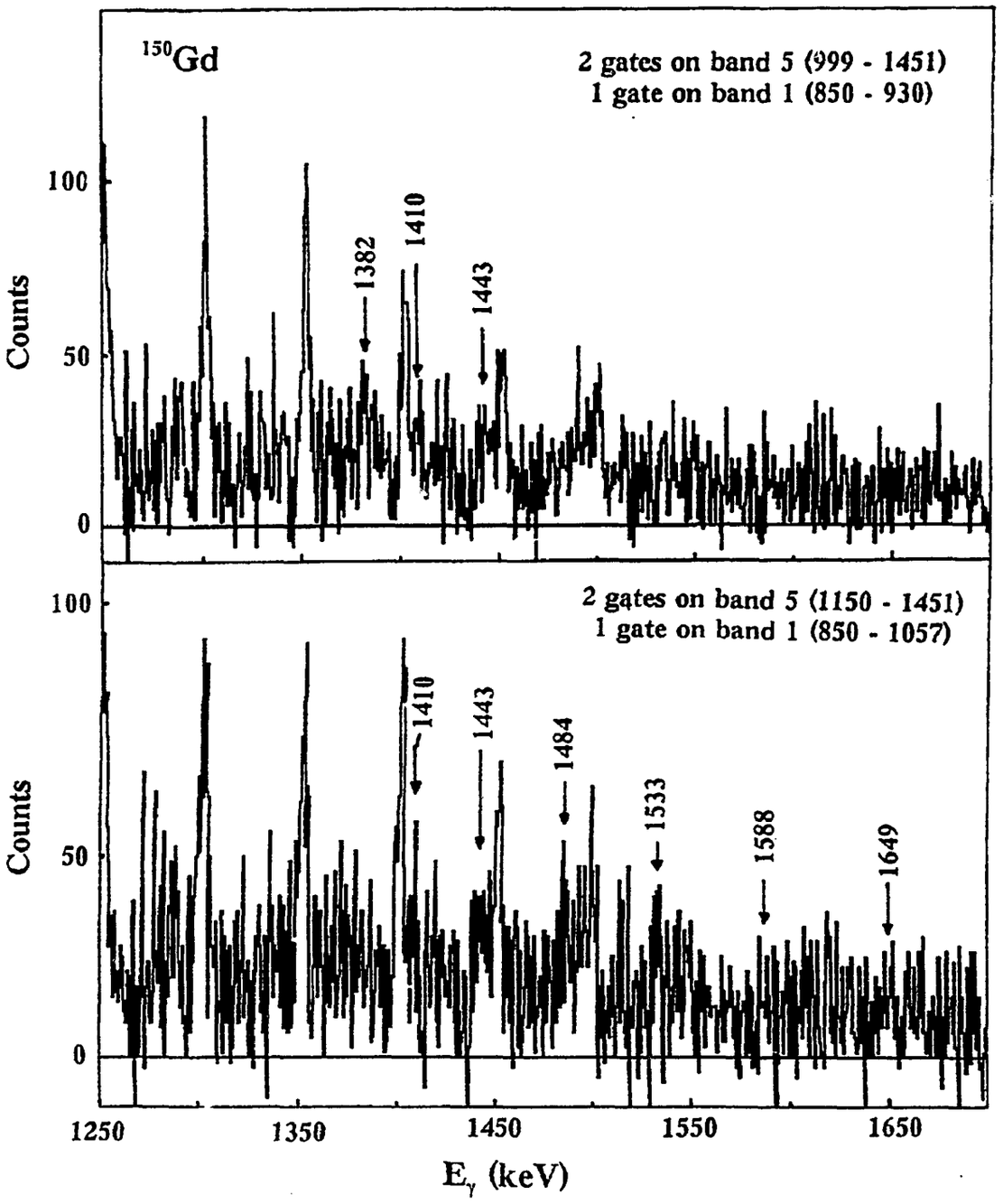

Figure 3. Spectra of SD band 5 in ^{150}Gd showing linking transitions to SD band 1. a) Two gates are set on transitions in band 5 from 999 keV to 1451 keV (except 1098 keV) and one gate on transitions in band 1 from 850 keV to 930 keV. b) Two gates are set on transitions in band 5 from 1150 keV to 1451 keV and one gate on transitions in band 1 from 850 keV to 1057 keV (except 972 keV).

References

1. C. W. Beausang et. al., Phys. Rev. Lett. 71 (1993) 1800.
2. P. Fallon et. al., Phys. Rev. Lett. 73 (1994) 782.
3. P. Fallon et. al., Phys. Lett. B218 (1989) 137.
4. B. Haas et al., Phys. Rev. C42 (1990) R1817.
5. S. Flibotte et. al., Phys. Rev. Lett. 71 (1993) 688.
6. S. Lunardi et. al., Phys. Rev. Lett. 72 (1994) 1427.
7. I. Ragnarsson, Nucl. Phys. A557 (1993) 167c.
8. P. J. Twin et. al., (to be published).

Microscopic study of superdeformation in the A=150 mass region

C. Rigollet[a], P. Bonche[b], H. Flocard[c], P.-H. Heenen[d] and B. Gall[a]

[a] CRN, IN2P3-CNRS, F67037 Strasbourg, France
[b] SPhT, CEN Saclay, F91191 Gif sur Yvette Cedex, France
[c] IPN, IN2P3-CNRS, F91406 Orsay Cedex, France
[d] Service de Physique Nucléaire Théorique,
ULB - CP 229, B1050 Brussels, Belgium

We are presently investigating the properties of superdeformed (SD) nuclear states in the A=150 mass region. For that purpose, we use the cranked HFB method in which pairing correlations are treated dynamically by means of the Lipkin-Nogami prescription [1]. Our goal is to take advantage of the large amount of experimental data to test the predictive power of our microscopic approach and of the effective interaction.

In the present communication, we focus on ^{152}Dy and^{153}Dy for which there are recent experimental data. In particular lifetime measurements have allowed to extract electric quadrupole moments. The new Skyrme effective force SLy4 is used to describe the nucleon-nucleon interaction [2], while for the pairing channel we use a density-dependent zero-range interaction.

The SLy4 interaction is based on a complete study of symmetric and very asymmetric infinite nuclear matters. It improves older Skyrme parametrization with respect to the isospin dependence of nuclear properties. It makes use of more realistic ingredients such as the incompressibility modulus K_∞ which has a too large value in SIII for instance; also, the spin-orbit strength is adjusted on the neutron states of ^{208}Pb.

Pairing correlations are generated by a density-dependent zero-range interaction. Its intensity is chosen to reproduce the experimental dynamical moment of inertia of the yrast band in ^{150}Gd. There is also a 5 MeV energy cut-off in the valence single particle space which limits the active pairing field in the vicinity of the Fermi energy.

As in our previous publications we used extensively the Skm* parametrization of the Skyrme force, we first compare the dynamical moment of inertia of ^{150}Gd and ^{152}Dy calculated both with Skm* and Sly4 to the experimental data. As shown in Fig.1, Sly4 leads to equally good or better results with respect to Skm*. In both cases, the magnitude of the $\mathcal{J}^{(2)}$ moment of inertia is slightly overestimated. Both forces give similar values for the charge quadrupole moments. In ^{152}Dy we obtain 17.5 eb, which agrees with experiment [3]. At the present time, there is no experimental value for ^{150}Gd. For this nucleus, SkM* and SLy4 predict very similar values, 16 eb [1] and 16.2 eb respectively. In what follows, we only present results obtained with Sly4.

In Table 1, we compare calculated charge quadrupole moments with the available experimental data for yrast bands. Indeed lifetime measurements of superdeformed bands in $^{148-149}Gd$ and ^{152}Dy have been recently performed through the Doppler Shift Attenuation Method (DSAM) with the Eurogam array in Strasbourg [3]. Yrast

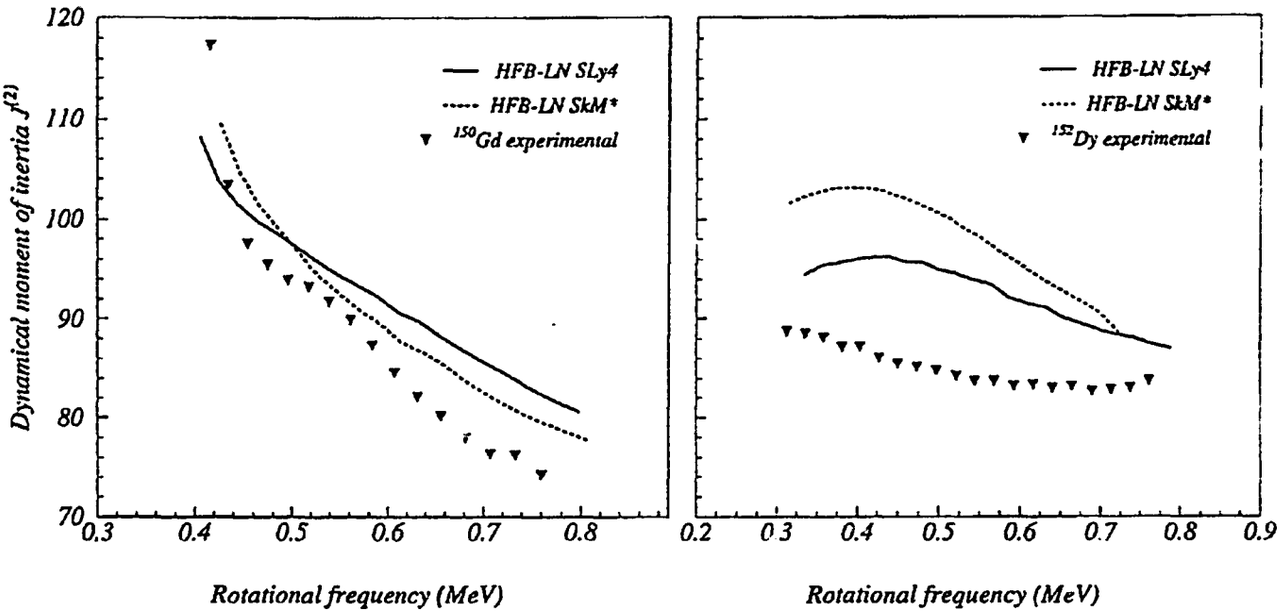

Figure 1: Dynamical moment of inertia calculated with SkM* and SLy4.

bands and some excited bands have been analysed and quadrupole moments were deduced. The different yrast band quadrupole moments are related to the different occupancy of the high-N orbitals [4]. The calculated values agree remarkably well with the data.

Nucleus	Q_0^{exp} (eb)	Q_0^{cal} (eb)
^{152}Dy	17.5	17.5
^{149}Gd	15.0	15.5
^{148}Gd	14.6	15.2

Table 1.

To extract further informations on deformation, lifetime measurements of SD identical bands belonging to nuclei differing by only one neutron, ^{153}Dy and ^{152}Dy, have been performed with the Gammasphere array in Berkeley [5]. The two nuclei were produced in the same fusion-evaporation reaction $^{124}Sn(^{34}Si, 5n-6n)^{153-152}Dy$ at a beam energy of 175 MeV.

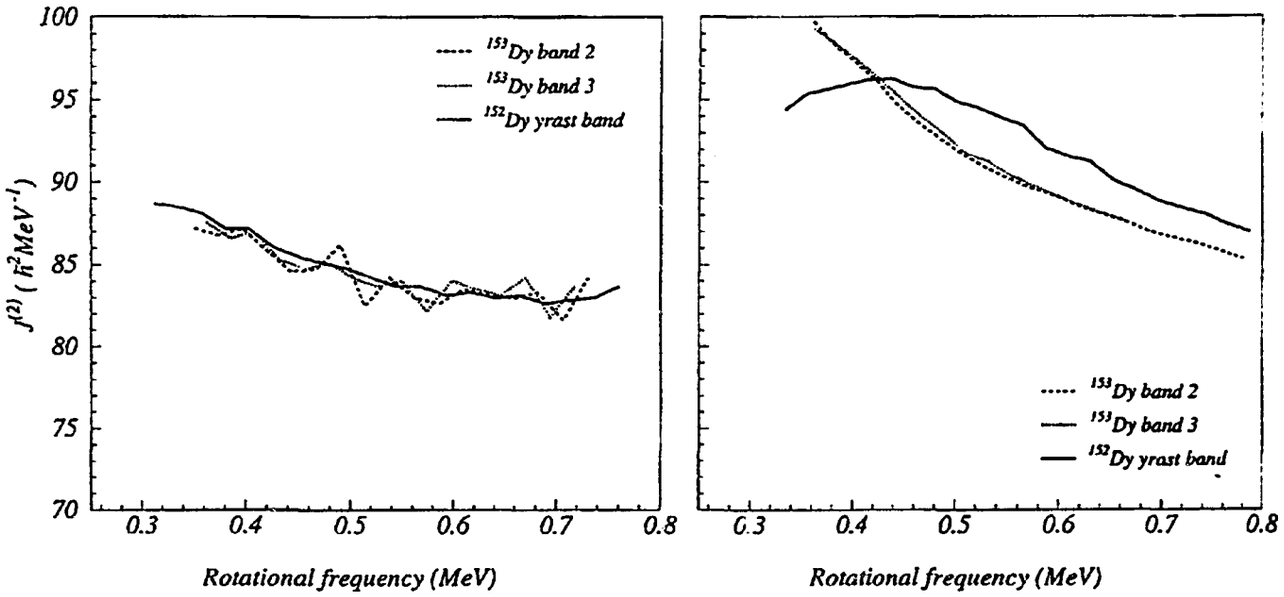

Figure 2: Experimental (left) and calculated (right) dynamical moments of inertia of ^{153}Dy (bands 2 and 3) and ^{152}Dy (yrast).

The first two excited bands in ^{153}Dy (bands 2 and 3) have their moment of inertia identical to that of the yrast band of ^{152}Dy (see Fig.2). Their transition energies are lying at the 1/4 and 3/4 points of those of the ^{152}Dy yrast band. This feature suggests the same occupancy of intruder orbitals for these 3 bands. Therefore, the last unpaired neutron should lie in an orbital with no signature splitting. Looking to Fig. 3, the best candidates are the [402]5/2±, [514]9/2± and [521]3/2± orbitals. As there is no evidence of band interactions in the $\mathcal{J}^{(2)}$ moment of inertia of those two excited bands in ^{153}Dy, the most probable orbitals are the [402]5/2± ones.

On the other hand, the yrast band in ^{153}Dy has no signature partner. Therefore, its last unpaired neutron most probably occupies the intruder orbital [761]3/2$^-$. For this band, the calculation shows that this configuration lies 400 keV lower than the two excited bands. We found for this band a pattern typical of a band crossing around a rotational frequency of 550 keV, which is not found in the data. This feature is probably related to the large number of negative parity orbitals in the vicinity of the Fermi level. Further analysis is required before drawing any definite conclusions.

On the right-hand side of Fig. 2, we show the calculated moment of inertia of the excited bands of ^{153}Dy. They are remarkably equal, however they are significantly smaller than that of ^{152}Dy, in contrast with experiment. This deviation suggests that a careful analysis of other configurations is necessary to confirm the present assignement in ^{153}Dy.

The quadrupole moments of these three bands are displayed in Fig. 4. As the two excited bands of ^{153}Dy are build on degenerate signature partner orbitals, they have the same quadrupole moment. The quadrupole moment of the ^{152}Dy yrast

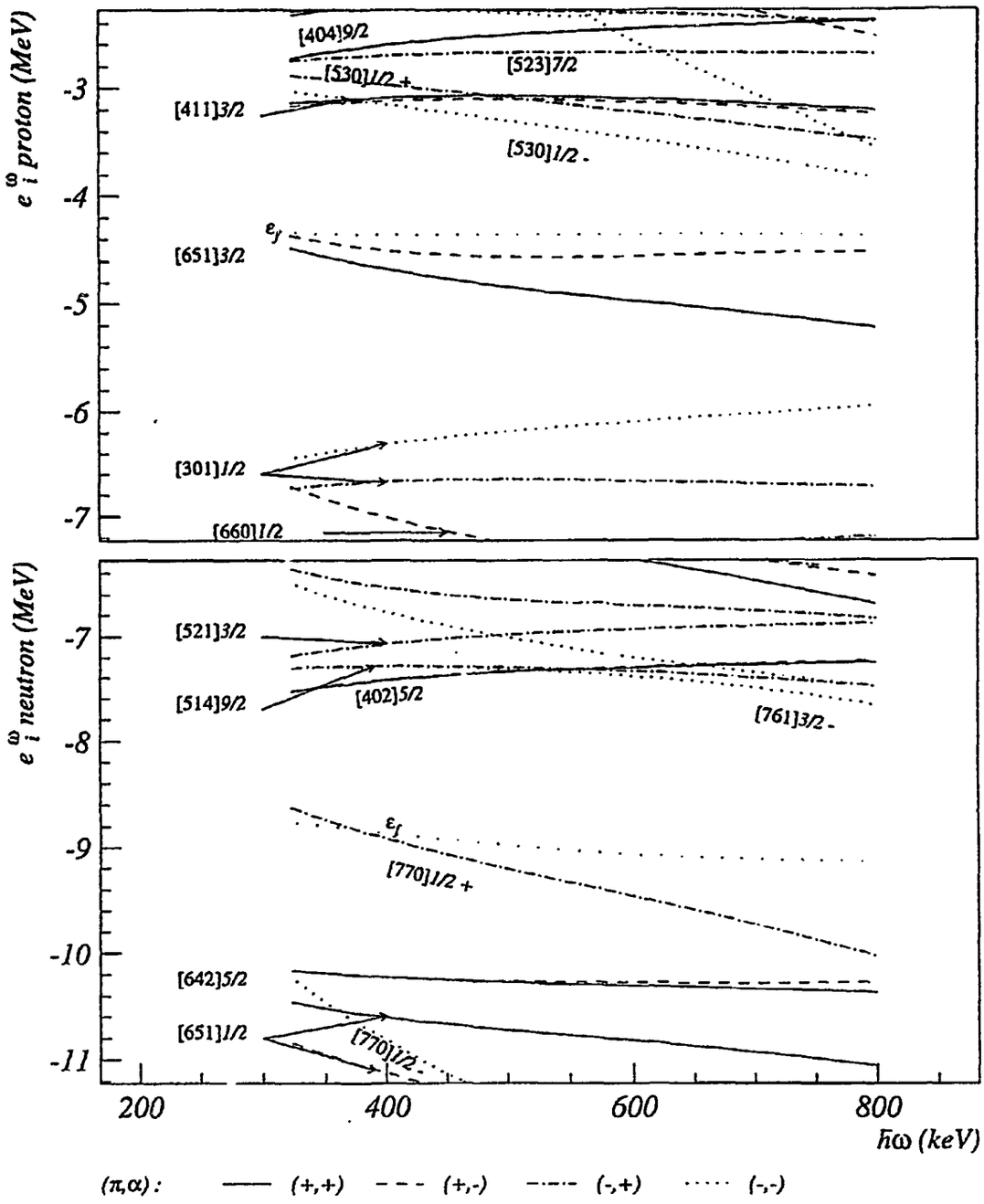

Figure 3: Single particle spectra for ^{152}Dy.

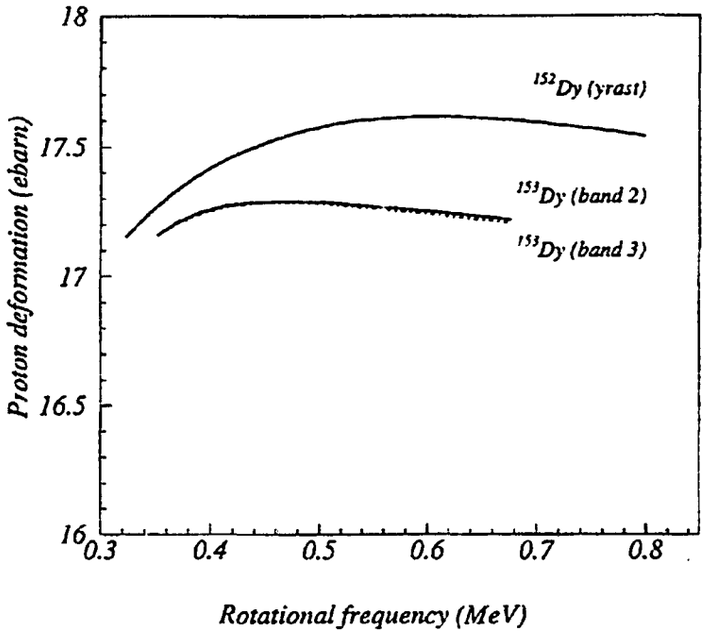

Figure 4: Proton deformations for the identicals bands $^{152}Dy(1)$, $^{153}Dy(2)$, $^{153}Dy(3)$.

band is larger. This can be related to the behavior of the [402]5/2 orbital as a function of deformation.

As the two nuclei were produced in the same reaction, the ratios of quadrupole moments can be extracted unambiguously. The theoretical values agree within the error bars with the experimental numbers, as shown in Table 2.

Nucleus	$R_{th} = \frac{Q_0^{153Dy}}{Q_0^{152Dy}}\%$	$R_{exp} = \frac{Q_0^{153Dy}}{Q_0^{152Dy}}\%$
$^{153}Dy(yrast)$	101.7	99.5 (3.4)
$^{153}Dy(2)$	98.6	96.8 (3.4)
$^{153}Dy(3)$	98.6	98.4 (3.4)

Table 2.

In summary, microscopic calculations based on the SLy4 parametrization of the Skyrme force prove to be very powerful for a detailed analysis of the structure of SD bands in the A=150 mass region.

References

[1] P. Bonche, H. Flocard and P.-H. Heenen, Nucl. Phys. **A598** (1996) 169; B. Gall, P. Bonche, J. Dobaczewski, H. Flocard and P.-H. Heenen, Z. Phys. **A348** (1994) 183; J. Terasaki, P.-H. Heenen, P. Bonche, J. Dobaczewski, and H. Flocard, Nucl. Phys. **A593** (1995) 1

[2] E. Chabanat, P. Bonche, P. Haensel, J. Meyer and R. Schaeffer Phys. Script. **56** (1995) 231

[3] H. Savajols *et al.*, Phys. Rev. Lett. **76**, 4480 (1996)

[4] C. Baktash, B. Haas, W. Nazarewicz, Annu. Rev. Nucl. Sci. 45, 485 (1995)

[5] C. Rigollet, Thesis work in progress.

Lifetime Measurements and Identical SD Bands in the A=190 and A=150 Regions

E. F. Moore[1], D. Nisius[2], R. V. F. Janssens[2], T. L. Khoo[2], T. Lauritsen[2], D. Ackermann[2], I. Ahmad[2], H. Amro[2], D. Blumenthal[2], M. P. Carpenter[2], S. Fischer[2], G. Hackman[2], P. Fallon[3], S. J. Asztalos[3], R. M. Clark[3], M. A. Deleplanque[3], R. M. Diamond[3], R. Krueken[3], I-Y. Lee[3], A. O. Macchiavelli[3], F. S. Stephens[3], F. Hannachi[4], A. Lopez-Martens[4], J. A. Becker[5], L. Bernstein[5], L. P. Farris[5], E. A. Henry[5], A. Korichi[6], P. Chowdhury[7], R. H. Mayer[8], A. V. Afanasjev[9,10], I. Ragnarsson[9]

[1] *North Carolina State University, Raleigh, North Carolina 27695-8202, and Triangle Universities Nuclear Laboratory, Durham, North Carolina 27708-0308*

[2] *Argonne National Laboratory, Argonne, Illinois 60439*

[3] *Lawrence Berkeley National Laboratory, Berkeley, CA 94720*

[4] *Centre de Spectrométrie Nucléaire et de Spectrométrie de Masse, IN2P3-CNRS, bat 104-108, F-91405 Orsay, France*

[5] *Lawrence Livermore National Laboratory, Livermore, CA 94550*

[6] *Institut de Physique Nucléaire, F-91406, Orsay Cedex, France*

[7] *University of Massachussets, Lowell, MA 01854*

[8] *Rutgers University, New Brunswick, NJ 08903*

[9] *Lund Institute of Technology, P. O. Box 118, S-221 00 Lund, Sweden*

[10] *Nuclear Research Center, Latvian Academy of Sciences, LV-2169, Salaspils, Latvia*

(September 3, 1996)

The lifetimes of states in Superdeformed (SD) bands in ^{192,194}Hg, ^{151,152}Dy, and ^{151}Tb have been measured using the Doppler shift attenuation method. Intrinsic quadrupole moments Q_0 have been extracted for SD bands in these nuclei. It was found that the quadrupole moments for the "identical" SD bands in these nuclei are the same. In the A=150 region, changes were found in the Q_0 values as a function of the number of high-N intruder orbitals. Changes are present also for excited SD bands with the same high-N content. Recent calculations account for most of the observations in the A=150 region.

I. INTRODUCTION

Following the discovery of a band of coincident γ rays with nearly constant energy separation in ^{152}Dy [1], the large deformation associated with this band was established [2] with a lifetime measurement. With the discovery of similar bands in this mass region, lifetime measurements confirmed their superdeformed character. Similarly, the large deformation associated with a band in ^{191}Hg [3] was confirmed with lifetime measurements. The limited sensitivity of the early generation of γ-ray detection arrays, however, restricted lifetime measurements to the most strongly populated (yrast) SD bands. With the new generation detector arrays coming online, the possibility of performing detailed lifetime measurements on excited SD bands has become a reality.

One of the most intriguing aspects of superdeformation is the existence of pairs of "identical" SD bands [4]. These bands have γ-ray energies that are equal or exhibit a simple relationship to each other (i.e., energies in one band fall at the mid-point energies in the other). Of interest to the present work are two spectacular examples of identical SD bands in both the A=150 and A=190 regions; band 4 of ^{151}Dy has γ-ray energies that fall almost exactly at the mid-point energies of band 1 of ^{152}Dy, and the γ-ray energies of ^{194}Hg band 3 are identical to those in ^{192}Hg band 1 over nearly the entire energy range [4]. The equality of the γ-ray energies requires that the nuclear moments of inertia to be equal to $\sim 0.2\%$. With the improved resolving power provided by the new arrays, it now becomes possible to perform precise lifetime measurements which may shed light on the properties of the identical bands.

II. MEASUREMENTS IN THE A=190 REGION

A. Experimental conditions

In order to establish the relative deformations associated with SD bands, care must be taken to minimize systematic uncertainties, especially those associated with stopping powers. We have used (^{48}Ca,4n) reactions on ^{148}Nd and ^{150}Nd targets to measure lifetimes in the SD bands of ^{192}Hg and ^{194}Hg, respectively. The beams were supplied by the 88 inch cyclotron at Lawrence Berkeley National Laboratory. In each case, the Nd targets were 1.0 mg/cm^2 thick and the recoiling nuclei were slowed down and brought

to rest in Au backings. For the ^{192}Hg measurement, the beam energy of 205 MeV results in a calculated mid-target $v_0/c = 0.0230$, $l_{max} = 47\hbar$, and $E^* = 19$ MeV. In the case of ^{194}Hg the beam energy of 202 MeV results in $v_0/c = 0.0226$, $l_{max} = 45\hbar$, and $E^* = 21$ MeV. It is important to note that since the same stopping material was used and the velocity profiles and nuclear charges are the same for both ^{192}Hg and ^{194}Hg, the difference in stopping powers is negligible.

The γ rays were measured at Gammasphere during two separate beamtimes. The first experiment was performed at a time when Gammasphere consisted of 55 detectors arranged into 11 angular rings, ranging from 17° to 163° with respect to the beam direction. Approximately 1×10^9 triples and higher fold events were recorded for both ^{192}Hg and ^{194}Hg. The second experiment was performed when 85 detectors were present in Gammasphere and were arranged into 16 angular rings ranging from 32° to 163° with respect to the beam direction. In this beamtime, some 1.8×10^9 quadruple and higher fold events were recorded for ^{194}Hg.

B. Analysis and results

Angle sorted spectra were constructed by combining double gates set on stopped and nearly stopped transitions at the bottom of each of the SD bands. Care was taken to ensure that consistent gating conditions were applied to each of the SD bands studied. As is customary for this type of measurement, fractions of the full Doppler shift $F(\tau)$ were extracted from the spectra using the first order relation

$$F(\tau) = \frac{\overline{E_\gamma} - E_{\gamma 0}}{E_{\gamma 0}\beta_0 \cos\theta},$$

where $\overline{E_\gamma}$ is the centroid of the γ-ray energy distribution as measured in a detector located at angle θ with respect to the beam direction, $E_{\gamma 0}$ is the unshifted γ-ray energy, and β_0 is the mid-target initial recoil velocity.

In order to extract the intrinsic quadrupole moments Q_0 for the various SD bands, computer simulations of the γ-decay of the recoiling nuclei were performed using the code FITTAU. The simulations all used stopping powers obtained from the 1995 version of the code TRIM by Ziegler [5]. The simplest version of the simulation makes the following basic assumptions: (1) the Q_0 values are constant within a given SD band, and the partial decay rate T (in ps^{-1}) of a band member of spin I is described within the rotational model by the expression:

$$T(I \rightarrow I\text{–}2) = 1.22 E_\gamma^5 Q_0^2 <IK20|(I\text{–}2)K>^2$$

where E_γ is the γ-ray energy in MeV, (2) the sidefeeding into each SD state has exactly the same time structure as the main band, (3) any delay in feeding a band was approximated by a one-step delay. This model (referred to as model I) then describes the band in terms of two fit parameters, namely Q_0 and τ_{delay} and a two-dimensional χ^2 minimization was performed.

In addition to the model described above, a more realistic model (model II) of the sidefeeding was also used in the analysis. In this model, the sidefeeding is assumed to consist of rotational bands having the same moment of inertia (γ-ray energies) as the main cascade. All sidefeeding cascades were assumed to have a common quadrupole moment Q_{SF} with additional one-step feeding delays (τ_{delay}) at the top. Furthermore, the number of transitions in the sidefeeding cascades was assumed to be proportional to the length of the main cascade above the state of interest. Three fit parameters were therefore used in this case, Q_0, Q_{SF}, and τ_{delay}, and a three-dimensional χ^2 minimization was performed.

The results of the centroid shift analysis are presented in table I, and examples of fits to ^{192}Hg band 1 are shown in Fig. 1. From these results it is clear that model II gives much better fits to the data. This is an indication that the simple treatment of sidefeeding used in model I is inadequate to describe the complicated feeding patterns of the SD bands. The values of Q_{SF} obtained from model II fits to the data are significantly lower than those in the main band. However, given the incomplete knowledge of the "true" characteristics of the sidefeeding and the assumptions that went into this model (i.e. same $\mathcal{J}^{(2)}$, number of transitions in SF cascades), it would be premature to assign too much significance to the Q_{SF} values. One should note that the in-band Q_0 values increase by $\sim 10\%$ when this model of the sidefeeding is used.

With the exception of ^{194}Hg band 1, the in-band Q_0 values are very similar from band to band. The measured value for band 1 in ^{194}Hg is larger than that reported by Hughes *et al* [6], while the value obtained for band 2 is similar to that measured previously. A detailed lineshape analysis is in progress for all of the SD bands reported here. Preliminary results for the yrast SD bands in ^{192,194}Hg indicate that the difference in average Q_0 values is somewhat smaller, 17.6 ± 1.8 eb versus 18.4 ± 1.1 eb for ^{192}Hg and ^{194}Hg, respectively. The lineshape fits also indicate that the Q_0 values are essentially constant over the range of transition energies measured.

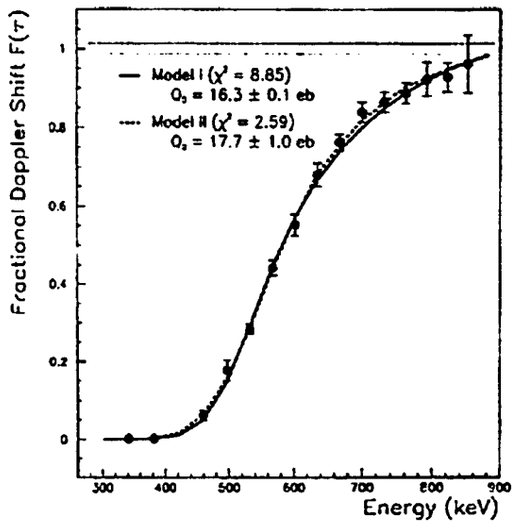

FIG. 1. Fits to the fraction of the full Doppler shift for band 1 in ^{192}Hg using both models described in the text. The dotted horizontal lines represent the spread in recoil velocities due to the slowing down of the beam through the target.

TABLE I. Summary of centroid shift analysis results for SD bands in ^{192,194}Hg. The last column for each model lists the total and reduced best-fit χ^2 values.

Model I Band	Q_0 (eb)	τ_{delay} (fs)	χ^2/χ^2_ν
^{192}Hg (1)	16.2 ± 0.1	1^{+7}_{-1}	8.85/0.68
^{194}Hg (1)	17.3 ± 0.2	34^{+8}_{-12}	8.11/0.62
^{194}Hg (2)	$17.2^{+0.2}_{-0.3}$	24^{+13}_{-19}	4.[illegible] /0.44
^{194}Hg (3)	$16.3^{+0.3}_{-0.1}$	1^{+18}_{-1}	7.13/0.71

Model II Band	Q_0 (eb)	Q_{SF} (eb)	τ_{delay} (fs)	χ^2/χ^2_ν
^{192}Hg (1)	17.7 ± 1.0	10.9 ± 1.0	6 ± 6	2.59/0.22
^{194}Hg (1)	$19.2^{+0.4}_{-0.8}$	$10.0^{+1.2}_{-0.4}$	39 ± 6	4.01/0.33
^{194}Hg (2)	17.6 ± 0.6	11.6 ± 1.2	28^{+3}_{-6}	3.03/0.28
^{194}Hg (3)	17.7 ± 0.8	10.8 ± 0.8	$3.5^{+5.0}_{-3.5}$	2.95/0.33

The most interesting result obtained from this analysis is that the Q_0 values for the identical SD bands, ^{192}Hg (1) - ^{194}Hg (3), are equal to each other. *This result is independent of the sidefeeding assumptions used in the analysis.* While the experimental errors are too large to determine whether the deformation in ^{194}Hg (3) is slightly smaller to compensate for the increase in mass with respect to ^{192}Hg, it is clear that there can be no *large* differences in deformation. As will be shown below, similar results have been obtained from differential DSAM measurements in the A~150 region. For SD bands in ^{151}Dy [7] and ^{149}Gd [8], which are identical to the yrast SD band in ^{152}Dy, the intrinsic quadrupole moments were all found to have the same value.

III. MEASUREMENTS IN THE A=150 REGION

A. Experimental conditions

The differential lifetime measurements in the A=150 region were performed at a time when 56 Compton-suppressed Ge detectors were present in Gammasphere. A 175 MeV ^{34}S beam was provided by the 88 Inch cyclotron at LBNL on a target which consisted of a 1 mg/cm^2 ^{122}Sn layer evaporated on a 20 mg/cm^2 Au backing. In this experiment, ^{151}Dy nuclei were produced via the dominant (^{34}S,5n) fusion-evaporation reaction while the ^{152}Dy and ^{151}Tb nuclei resulted from the weaker (^{34}S,4n) and (^{34}S,p4n) channels, respectively. A total of 1.5×10^9 triple and higher fold coincidence events were recorded.

The fractional Doppler shifts F(τ) were obtained for transitions in four SD bands in ^{151}Dy, as well as for γ rays in the yrast SD bands in ^{152}Dy and ^{151}Tb. The F(τ) values were extracted from the data, as described earlier, under the assumption that F(τ) = 1.0 corresponds to the v/c of nuclei formed at the center of the target. For the present experiment, a calculation of the mid-target recoil velocity gives $\beta_0 = 0.0227$. If one assumes isotropic evaporation of particles in the rest frame of the recoiling compound nuclei, all residues should have the same value for β_0. Furthermore, the velocity profiles for the ^{151,152}Dy nuclei should be the same over the full stopping range, while that for ^{151}Tb may be somewhat different due to electronic stopping power differences resulting from the different Z value. The experimental F(τ) points are presented in Fig. 2. With the exception of ^{152}Dy, all data points approach F(τ) = 1.0 at the highest γ-ray energies.

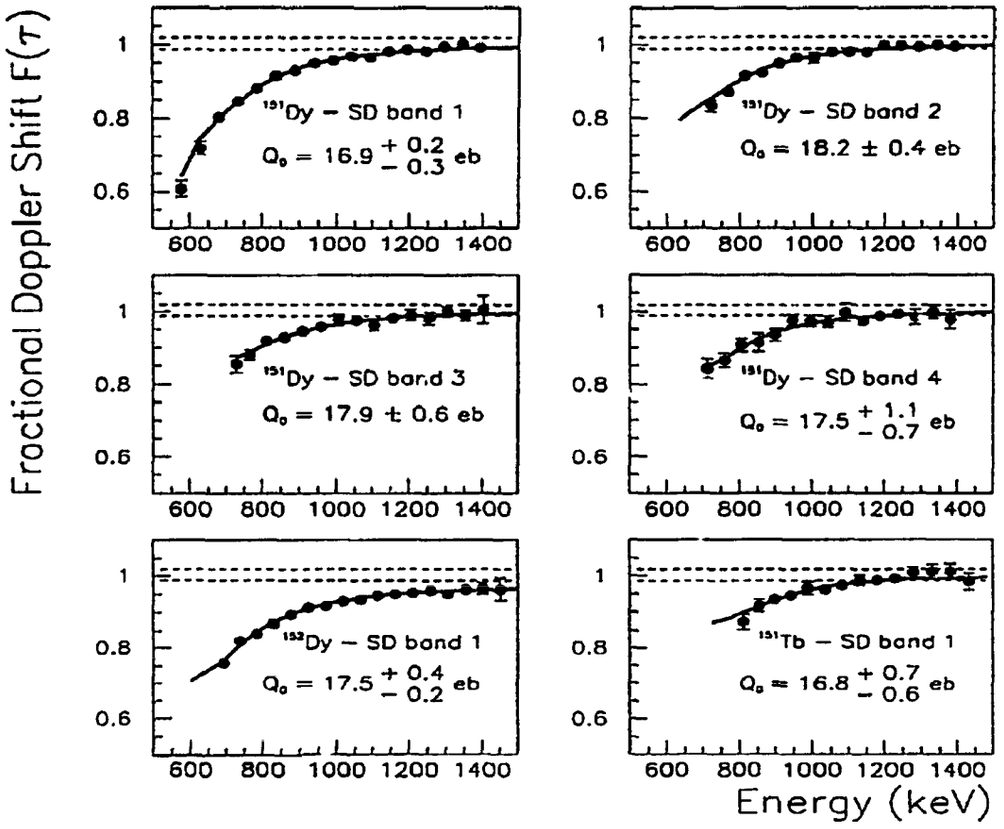

FIG. 2. Fits to the fraction of the full Doppler shift for SD bands in the A=150 region. The dotted horizontal lines represent the spread in recoil velocities due to the slowing down of the beam through the target.

TABLE II. Comparison of the results from this experiment and from the measurement of ref. [8] with recent theoretical calculations described in the text. The quoted errors do not include stopping power uncertainties. Most of the calculated values are taken at a spin value of 40 $\hbar$.

Nucleus	Q_0^{exp} (eb)	Q_0^{MO}	Q_0^{WS}	Q_0^{RMF}	Q_0^{SkP}	Q_0^{SKM*}	Q_0^{DD}
^{152}Dy	17.5 ± 0.2^a $17.5\ ^{+0.4}_{-0.2}$	18.9	18.9	18.9	18.5	18.5	17.6
^{151}Dy	$16.9\ ^{+0.2}_{-0.3}$	18.0	18.0	18.1	17.9	18.0	16.6
^{151}Tb	$16.8\ ^{+0.7}_{-0.6}$	18.1	18.0	18.1	17.5	17.5	17.0
^{149}Gd	15.0 ± 0.2^a	16.5	16.2	16.0	16.1	16.2	15.6
^{148}Gd	14.6 ± 0.3^a	16.0	15.6	15.7	15.5	15.8	15.2

[a]from Savajols *et al.* [8].

B. Analysis and results

The extraction of intrinsic quadrupole moments Q_0 for the various SD bands proceeded in the same manner as described above for the A=190 region. The stopping powers for the various residual nuclei were all calculated using TRIM [5]. The best fit calculated $F(\tau)$ curves are presented in Fig. 2.

In the fit of the $F(\tau)$ values a χ^2 minimization was performed. For the SD bands in ^{151}Dy and ^{151}Tb, the sidefeeding delay was well described in terms of the parameters Q_0 and Q_{SF} only, (i.e., very good agreement with the data was obtained with $T_{SF} = 0$). However, in the case of ^{152}Dy, an additional delay of $T_{SF} \simeq 25$ fs was required to fit the data.

We have examined the possibility that this difference in feeding delay might be an artifact of the analysis. We note that these data points were obtained in exactly the same way as those in ^{151}Dy and ^{151}Tb. Since all the recoils are formed in the same reaction, it is difficult to see how a change in the condition of the target would produce such a difference. We have also investigated the possible difference in the $4n$ and $5n$ production cross sections across the target thickness. The combination of measured excitation functions [9] and statistical model calculations [10] indicate that this difference is too small to explain the observed deviations. The origin of this sidefeeding delay remains an open question which will be the subject of further investigation. It is important to note that the value of Q_0 obtained in the fitting process is most strongly determined by those data point having $F(\tau) < 0.9$, where there is little or no sidefeeding. Finally, we note that the value of Q_0 for ^{152}Dy obtained here is in excellent agreement with that of Savajols *et al.* [8] (see Table 2).

The results of the present analysis show that the quadrupole moment of the "identical" SD band in ^{151}Dy has the same value of the yrast SD band of ^{152}Dy. Furthermore, as shown in Tab. 2, our results combined with those of Savajols *et al.* [8] nicely illustrate the effect of the occupation of specific high-N intruder orbitals on the SD quadrupole moments.

Under the usual assumption that the yrast SD band in ^{152}Dy corresponds to a closed core configuration containing four N=6 protons and two N=7 neutrons ($\pi 6^4 \nu 7^2$), the yrast SD bands can be described as single neutron-hole ($\pi 6^4 \nu 7^1$) and single proton-hole ($\pi 6^3 \nu 7^2$) configurations, respectively. These high-N intruder orbitals are strongly deformation driving and can be expected to have a large influence on the SD Q_0 values, as is seen in the data: the Q_0 value in ^{152}Dy is larger than for the yrast SD bands in ^{151}Dy and ^{151}Tb. The data also suggest that the influence of proton and neutron intruder orbitals on the Q_0 values is similar.

The polarization effects resulting from the occupancy of specific intruder orbitals have recently been calculated in a variety of theoretical approaches, a number of which are compared in Table 2. The results of Nilsson-Strutinsky cranking of the modified oscillator potential with the parameters of ref. [11] are presented as Q_0^{MO} in Table 2, the results for the Gd isotopes and ^{152}Dy were published previously [8]. Results of cranked Strutinsky calculations with a Woods-Saxon potential [12] are given as Q_0^{WS}. The symbol Q_0^{RMF} refers to calculations using the cranked relativistic mean field approach [13]. Finally, the symbols Q_0^{SkP}, Q_0^{SKM*}, and Q_0^{DL} refer to the Hartree-Fock calculations with SkP and SKM* interactions of Satula *et al.* [14], and with density-dependent zero-range pairing interaction of Bonche *et al.* [15]. Clearly, all of these calculations reproduce the relative changes in Q_0 very well. It should be mentioned that the $\sim 10\%$ discrepancies between the experimental values and some of the calculations is not considered serious since they are well within the absolute uncertainties due to stopping powers and the r_0 parameter, for example.

The present measurements also probe the possible dependence of the Q_0 values on the specific configurations occupied in the ^{151}Dy SD well. The excited SD bands in ^{151}Dy are interpreted as excitations in which the the hole (with respect to ^{152}Dy) can occupy some of the natural parity orbitals in the vicinity of the Fermi surface. In contrast with the yrast SD band in ^{151}Dy, the intruder content of these excited bands is then the same as in ^{152}Dy band 1

TABLE III. Calculated Q_0 values for three orbitals which may be involved in the configurations of the excited SD bands in ^{151}Dy. Most of the calculated values are taken at a spin value of 40 $\hbar$. The intruder configuration for band 1 is given for comparison.

Configuration	Q_0^{MO}	Q_0^{RMF}	Q_0^{SkP}	Q_0^{SKM*}
$\nu 7^1$	18.0	18.1	17.9	18.0
[651]1/2	18.3	-	18.1	-
[642]5/2	18.4	18.7	18.3	18.3
[411]1/2	19.0	-	18.7	18.7

($\pi 6^4 \nu 7^2$) and single-particle Routhians indicate that the neutron holes will most likely be created in the [651]1/2, [642]5/2, or [411]1/2 orbitals [12,16]. From Fig. 1 it is clear that bands 2-4 in ^{151}Dy are characterized by Q_0 values which are larger than that of band 1, as would be expected for bands having an additional $\nu 7$ intruder occupied. More surprising is the observation that the Q_0 values for band 2 and, perhaps for band 3, may even be larger than that for ^{152}Dy SD band 1. In order to investigate this point the Nilsson-Strutinsky calculations described above were extended to some of the proposed orbitals. The results of the calculations are given in Table 3, together with values obtained from other approaches where available.

The "identical" band (band 4) of ^{151}Dy was assigned [17] to the [411]1/2 orbital as the transition energies in this band lie half-way between those of band 1 in ^{152}Dy as predicted by Nazarewicz *et al.* [18]. Using the strong coupling picture, these authors showed that, within the pseudospin coupling scheme, the [411]1/2 orbital is associated with a decoupling parameter a having the exact value $a = -1$ (required to obtain transition energies at the half-way point). As shown in Table 3, the Q_0 value calculated for the [411]1/2 configuration is almost exactly equal to the value calculated for ^{152}Dy band 1 (as are the measured values), whereas the values calculated for the [642]5/2 and [651]1/2 orbitals are closer to that of ^{151}Dy band 1. The data seem to favor the scenario proposed by Ragnarsson [16], which assigns both bands 2 and 4 to the [411]1/2 orbital, although the measured Q_0 value for band 2 appears somewhat larger than expected from the calculations. Finally, the calculations of ref. [16] assign band 3 to the [642]5/2 configuration. However, the fact that the measured Q_0 value for this band is closer to that of ^{152}Dy band 1 than that of ^{151}Dy band 1 stands in contrast to the calculations. Further theoretical investigations may be required to account for these bands properly.

IV. SUMMARY

Lifetime measurements for identical SD bands in ^{151,152}Dy and ^{192,194}Hg have demonstrated that another observable, the intrinsic quadrupole moment, associated with these bands is the same. The results in the A=190 region have also shown that the Q_0 values obtained from centroid shift analyses are very sensitive to the treatment of sidefeeding. It is encouraging to note that these types of measurements are no longer limited by the statistical accuracy of the measurement but rather by the fundamental assumptions made in the analysis of the data.

The measurements in the A=150 region combined with those of Savajols *et al.* [8] dramatically illustrate the strong influence that the occupation of specific high-N intruder orbitals have on the Q_0 values. In addition, the present investigation indicates that in certain cases, the occupation of other, non-intruder orbitals can also affect the Q_0 values. It should be pointed out that while a clear picture appears to emerge for the A=150 region, the situation remains less clear for SD nuclei of the A~190 region. It is hoped that the results of detailed lifetime measurements in the A=190 region will stimulate detailed calculations of these quantities, similar to those now available for SD nuclei in the A=150 region.

This work was supported in part by the Department of Energy, Nuclear Physics Division under contract nos. DE-FG05-88ER40441, W-31-109-ENG-38, DE-AC03-76SF00098, and W-7405-ENG-48.

[1] P. J. Twin *et al.*, Phys. Rev. Lett. **57**, 811 (1986).
[2] M. A. Bentley *et al.*, Phys. Rev. Lett. **59**, 2141 (1987)
[3] E. F. Moore *et al.*, Phys. Rev. Lett. **63**, 360 (1989).
[4] C. Baktash, B. Haas and W. Nazarewicz, Annu. Rev. Nucl. Part. Sci. **45** (1995) 485.
[5] J.F. Ziegler, J.P. Biersack, and U. Littmark, The Stopping and Range of Ions in Solids (Pergamon, New York,1985), J.F. Ziegler, private communication (1995).
[6] J. R. Hughes *et al.*, Phys. Rev. Lett. **72**, 824 (1994).
[7] D. Nisius *et al.*, to be published.
[8] H. Savajols *et al.*, Phys. Rev. Lett. **76** (1996) 4480.
[9] G. Smith *et al.*, Phys. Rev. Lett. **68** (1992) 158.
[10] F. Puhlhofer, Nucl. Phys. **A280** (1977) 267, and D. Hofmann, private communication.
[11] B. Haas *et al.*, Nucl. Phys. **A561** (1993) 251.
[12] W. Nazarewicz, R. Wyss and A. Johnson, Nucl. Phys. in press.
[13] A. V. Afanasjev, J. J. König and P. Ring, Nucl. Phys. in press.
[14] W. Satula, J. Dobaczewski, J. Dudek and W. Nazarewicz, private communication and to be published.
[15] P. Bonche, H. Flocard and P. -H. Heenen, Nucl. Phys. **A598** (1996) 169.
[16] I. Ragnarsson, Acta Polonica **B27** (1996) 33.
[17] D. Nisius *et al.*, Phys. Lett. **B346** (1995) 15.
[18] W. Nazarewicz et al., Phys. Rev. Lett **64** (1990) 1654.

RDDS lifetime measurements of low–lying superdeformed states in ^{194}Hg

R. Kühn[a], A. Dewald[a], R. Krücken[a*] C. Meier[a], R. Peusquens[a], H. Tiesler[a], O. Vogel[a], S. Kasemann[a], P. von Brentano[a], D. Bazzacco[b], C. Rossi-Alvarez[b], G. De Angelis[c] and J. de Boer[d]

[a] *Institut für Kernphysik, Universität Köln, Köln, Germany*

[*] *Present address: LBNL, Berkeley, USA*

[b] *Dipartimento di Fisica, Universita and INFN Sezione Padova, Italy*

[c] *INFN, Laboratori Nationali di Legnaro, Italy*

[d] *Sektion Physik, Universität München, Garching, Germany*

(August 30, 1996)

Abstract: The lifetimes of three low–lying states in the superdeformed (SD) yrast band of ^{194}Hg were measured by the recoil-distance Doppler-shift method. The deduced transition quadrupole moments, Q_t, equal those extracted from a DSAM measurement for the high-lying states of the band corroborate the assumption that the decay out of SD bands does not strongly affect the structure of the corresponding states. By a simple mixing-model the decay can be described assuming a very small admixture of normal-deformed (ND) states to the decaying SD states. The deduced ND mixing amplitudes for the yrast SD bands in ^{192,194}Hg and ^{194}Pb are presented along with average transition quadrupole moments for the lower parts of the excited SD bands.

I. INTRODUCTION

The study of the decay mechanism leading to the abrupt depopulation of superdeformed (SD) bands in the $A\approx190$ mass region at low spins is one of the most exciting topics in present nuclear-structure physics. Recently, discrete γ–transitions connecting SD bands with the normaldeformed (ND) part of the level scheme were observed first in ^{194}Hg [1] and later in ^{194}Pb [2]. It was therefore possible to extract the spins, likely parities and particularly the exact excitation energies of the SD states which thus become favorite candidates for further detailed investigations.

In this work, we report on a RDDS measurement of the lifetimes of low–lying states in the SD bands in ^{194}Hg. We succeeded to determine the lifetimes of the 12^+, 14^+ and 16^+ states of the SD yrast band. Using branching ratios for the decay out of the SD band from a experiment [3] with high statistics, transition quadrupole moments, Q_t were deduced directly from the measured lifetimes. The comparison of these Q_t–values with those extracted from a DSAM measurement [4] for the transitions in the upper part of the band shows that the deformation remains constant down to the bottom of the band and is not appreciably disturbed by the decay out of the band. In addition average transition quadrupole moments for the lower parts of SD bands 2 and 3 were determined.

II. EXPERIMENT AND ANALYSIS

Superdeformed states of ^{194}Hg were populated by the reaction ^{150}Nd(^{48}Ca,4n)^{194}Hg using a beam energy of 209 MeV. The beam was supplied by the XTU tandem accelerator at the Laboratori Nazionali di Legnaro, Italy. The sputter sample used in the ion source contained hydrated ^{48}Ca and was supplied by the Cologne group. The plunger target consisted of

TABLE I. Lifetimes, reduced transition probabilities and transition quadrupole moments for low-lying states in SD-band 1 in ^{194}Hg

E_i [keV]	I_i^π [$\hbar$]	E_γ [keV]	I_f^π [$\hbar$]	τ [ps]	B(E2) [10^3W.u.]	Q_t [eb]
6883.1	12^+	254.6	10^+	2.73 (±0.96)	2.1 ($^{+1.3}_{-0.6}$)	20.3 ($^{+5.3}_{-3.1}$)
7179.7	14^+	296.6	12^+	3.26 (±0.57)	1.5 ($^{+0.4}_{-0.3}$)	16.8 ($^{+1.7}_{-1.3}$)
7517.3	16^+	337.6	14^+	1.47 (±0.42)	1.8 ($^{+0.8}_{-0.4}$)	18.3 ($^{+3.4}_{-2.2}$)

a 1 mg/cm^2 ^{150}Nd layer evaporated onto a 1.6 mg/cm^2 thick tantalum foil. The recoiling nuclei with a mean velocity of 2.13 (1) % c were stopped in a 11.6 mg/cm^2 gold foil. Target and stopper were mounted in the Cologne plunger apparatus [6] surrounded by the 40 large-volume Compton-suppressed Ge detectors of the GASP array [7] in its configuration II. In this configuration the 80 element BGO ball is replaced by a compact lead collimator which makes it possible to move the detectors closer to the center of the array. This leads to an increase in efficiency by approximately a factor of two. In total 795 · 10^6 unfolded triple events were recorded at seven target-to-stopper distances ranging from 10 to 83 μm.

The lifetimes of three low-lying states within SD band 1 were determined using the differential decay-curve method (DDCM) [8,9]. The 40 Ge detectors of the GASP array can be grouped into 7 rings whereby the detectors belonging to one ring have approximately the same azimuth angle. For each distance and each detector ring double-gated spectra with gates set on the shifted components of higher-lying SD transitions were produced. Then, the spectra taken at azimuth angles 145°, 120° and 60° were modified in such a way that the Doppler-shifted peaks came to the same position as those in the spectra taken at 35° while the position of the stop peaks remained unchanged. In this way, it was possible to sum up the complete statistics for each distance in one single spectrum which was then used to determine the shifted and unshifted intensities of the transitions of interest for each distance. Examples of the spectra are given in fig. 1.

The resulting lifetimes as well as the corresponding transition probabilities and transition quadrupole moments of the 12^+, 14^+ and 16^+ state are given in table I. In our calculations we adopted the spin assumptions from ref. [1] and relative intensities from ref. [3]. The transition quadrupole moments almost equal those extracted from DSAM data [4] and thus confirm that the dominant SD configuration of the band remains constant down to the region of its decay. This holds also for ^{192}Hg and ^{194}Pb where the lifetimes of low-lying SD states were measured. In fig. 2, the transition quadrupole moments of yrast SD bands for the three nuclei are presented.

Due to insufficient statistics only average transition quadrupole moments could be determined for the lower parts of the excited SD bands 2 and 3 applying the following approach.

For each band we created background-subtracted, double-gated spectra with gates set on the shifted components of the corresponding higher-lying SD transitions. Again, we modified the spectra in such way that all shifted peaks came to the same position as those in the spectra taken under 35°. We then summed up all (modified) spectra to obtain one spectrum for each band containing the complete statistics. Within these spectra, we determined the areas of the Doppler shifted and unshifted peaks of four low-lying transitions for each excited band. Assuming a constant transition quadrupole moment for the lower part of each

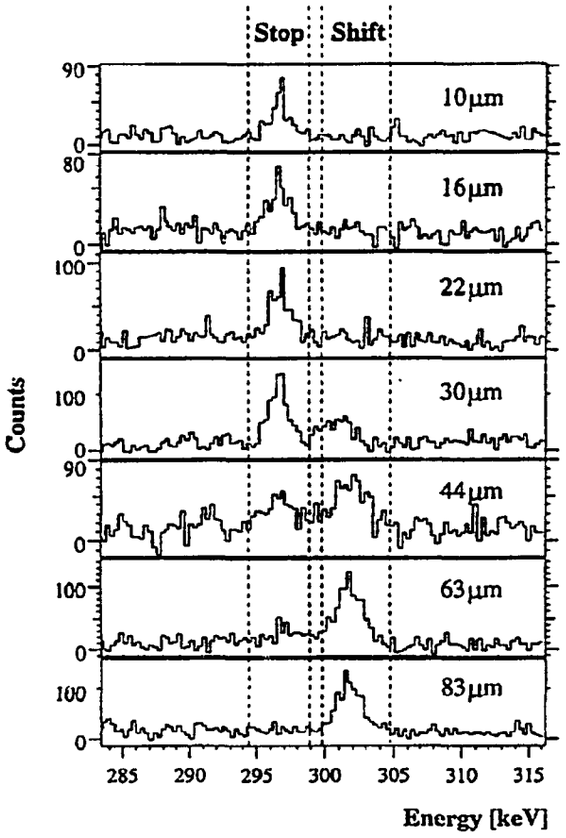

FIG. 1. Doppler shifted and unshifted peaks of the 296 keV transitions of SD band 1 in ^{194}Hg. The spectra result from summed-up, double gated spectra taken at four different azimuth angles. The Doppler-shifted energies are corrected to correspond to an azimuth angle of 35° .

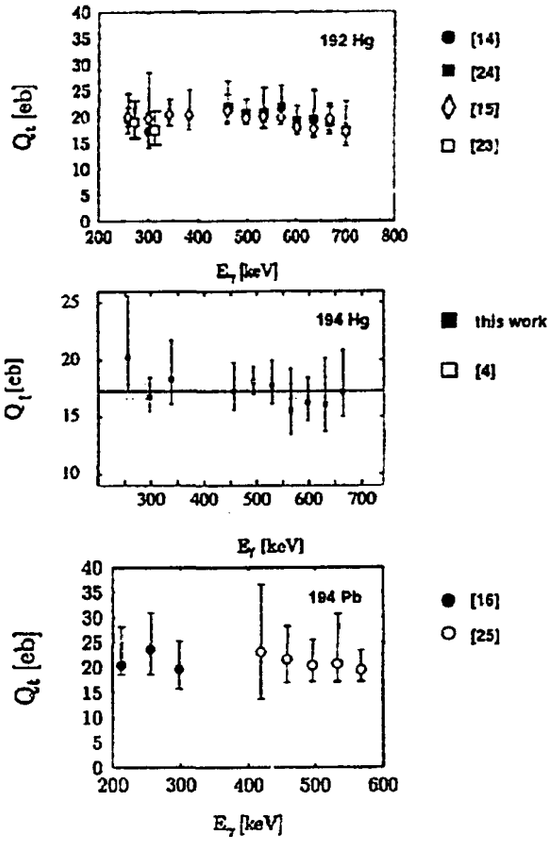

FIG. 2. Q_t–values of the yrast SD bands for ^{192,194}Hg and ^{194}Pb

band we calculated shifted and unshifted components of the transitions of interest for the corresponding target-to-stopper distances. These values – normalized to the total number of corresponding reaction events – were summed over all distances. Finally, the experimental values were fitted applying a least-χ^2 algorithm to determine the transition quadrupole moments of SD bands 2 and 3.

This procedure yielded average $\overline{Q}_t$-values of 16.5(31) eb and 15.1(36) eb for SD band 2 and 3, respectively. A systematic error of 15% is our estimate of the uncertainties arising from this rather complicated procedure.

III. DISCUSSION

In order to describe the decay out of SD bands we followed the approach proposed by Krücken et al. [10], based on a simple level-mixing model, originally proposed by Vigezzi, Broglia and Døssing [11]. This model has previously been used to describe the situation in ^{152}Dy, ^{192}Hg and ^{194}Pb [12–16].

We calculated the partial decay probabilities for an intraband transition λ_{intra} and for the

decay out of the band λ_{out} which add up to the total transition probability $\lambda = 1/\tau$, using the relationship:

$$\lambda_{out}(I^\pi) = \frac{1}{\tau} \cdot (1 - N_{intra}(I^\pi)), \tag{1}$$

where $N_{intra}(I^\pi)$ is the branching of the intra-band transition depopulating the (I^π) state. For the 12^+ state we calculated a value of $N_{intra}(12^+) = 0.58\,(3)$ using intensities from ref. [3] and deduced a partial decay probability of $\lambda_{out}\,(12^+) = 0.15\,(5)\,ps^{-1}$ for the decay out. The wavefunction of the real state Ψ is assumed to consist of a SD part $|s\rangle$ and a ND part $|n\rangle$, $\Psi = a_s|s\rangle + a_n|n\rangle$ with $a_n^2 + a_s^2 = 1$. Postulating that electromagnetic (EM) transitions between pure SD and ND states are negligible and that the squared ND amplitude a_n^2 is small, the probability for the decay out of the band at spin I is given by

$$\lambda_{out}(I^\pi) = a_n^2(I^\pi) \cdot \lambda_n \tag{2}$$

where λ_n is the EM transition probability in the ND well. In order to determine λ_n only statistical $E1$ transitions were considered for the decay between the ND states. Other types of transitions, magnetic ones and those with higher multipolarities were considered to be small and have been neglected. The $E1$ decay probability was calculated as in refs. [16,10] applying a statistical model.

$$\lambda_n^{E1} = \xi_{E1} \int_0^{U-E_{Yrast}} \frac{\rho(U - E_\gamma)}{\rho(U)} f_{GDR}(E_\gamma)\, E_\gamma^3\, dE_\gamma \tag{3}$$

The Fermi-gas approximation was used to describe the level-density at the various excitation energies with a pairing gap of $2\Delta_{12^\pi} = 1.3\,\mathrm{MeV}$ and a level-density parameter of a $22.4\,\mathrm{MeV}^{-1}$ [17]. ξ_{E1} is the $E1$ strength fitted to neutron-resonance data from ref. [18], U is the excitation energy of the decaying SD state taking the pairing gap into consideration and E_{Yrast} is the energy of the corresponding yrast state. We used parameters for the description of the giant dipole resonance (GDR) extracted from photoneutron cross-section measurements on natural mercury from ref. [19] and from references therein.

This gives $\lambda_n = \lambda_n^{E1} = 27.5\,ps^{-1}$ and considering equation (2) a ND squared mixing amplitude $a_n\,(12^+) = 0.5\%, (2)$ for the SD 12^+ state.

In table II, we give the results of our calculations, in particular the calculated E1 transition probabilities λ_n^{E1} and the deduced squared ND mixing amplitudes a_n^2. As the intensities of the decay out for ^{194}Pb [20] and ^{192}Hg [21] are similar to the ones observed in ^{194}Hg, we additionally calculated the corresponding values for these nuclei. For ^{194}Hg and ^{194}Pb, we used the exact excitation energies from refs. [1,2], whereas for ^{192}Hg we assumed an excitation energy of 4.3 MeV above yrast (similar to the value in ^{194}Hg). Note that no lifetimes have yet been measured for the 8^+ state in ^{194}Pb and for the 10^+ states in ^{192}Hg and ^{194}Hg. Therefore, in order to estimate the ND contributions to those states we extracted the corresponding lifetimes assuming constancy of the quadrupole moment in each band. As previously shown for ^{194}Pb and ^{192}Hg in ref. [10] the behavior of the ND mixing amplitudes with decreasing spin for the three nuclei is rather striking: while a_n^2 remains almost constant for ^{194}Pb, it increases for both mercury isotopes by about an order of magnitude. This can be understood in the framework of a simple two-level mixing-model assuming that the pure SD state $|s_I\rangle$ interacts only with its nearest neighbor ND state $|n_I\rangle$. Let x_I be the energy difference and

TABLE II. Calculated E1 transition probabilities λ_n^{E1} and deduced squared ND mixing amplitudes a_n^2 for low-lying SD states in ^{192,194}Hg and ^{194}Pb which decay to ND states. The calculation of the partial decay probabilities λ_{out} involve the lifetime data and intensities from refs. [16,20] (10^+, ^{194}Pb), the weighted average of the lifetime values given in refs. [14,15,22] (12^+, ^{192}Hg) and this work (12^+, ^{194}Hg) as well as the intensities from ref. [21,3]. In order to deduce λ_{out} values for the 8^+ state in ^{194}Pb and 10^+ states in ^{192,194}Hg a constant quadrupole moment was assumed for the bands calculated from the weighted average of the values given in the above references and in refs. [23], [4], [24].

Nucl.	I	λ_{out}	λ_n^{E1}	a_n^2
	[$\hbar$]	[ps^{-1}]	[ps^{-1}]	[%]
^{192}Hg	12	0.026(15)	15.7	0.17(9)
^{192}Hg	10	0.85	15.7	5.4
^{194}Hg	12	0.147(52)	27.5	0.53(19)
^{194}Hg	10	1.2	27.9	4.39
^{194}Pb	10	0.012(8)	2.4	0.48(32)
^{194}Pb	8	0.014	2.5	0.56

$v_I^2 = |\langle n_I|V|s_I\rangle|^2$ the squared matrix element for the interaction V between SD and ND state. The ratio of the amplitudes of the real SD state $|\Psi_I\rangle = a_s(I^\pi)\,|s_I\rangle + a_n(I^\pi)\,|n_I\rangle$ is given by

$$\frac{a_s^2}{a_n^2} = \frac{4v^2}{\left(\sqrt{x^2+4v^2}-x\right)^2}$$

and for $a_n^2 \ll 1$

$$\frac{a_s^2}{a_n^2} \approx \frac{x^2}{4v^2}$$

For small ND amplitudes a_n^2 and constant interaction strength v^2 one finds $a_n^2 \propto 1/x^2$. The different behavior of a_n^2 in the three nuclei is therefore a strong indication that the ND mixing amplitude depends strongly on the arbitrary distance to the nearest-neighbor state in the ND well. This means that the decay pattern of the SD bands in the A≈190 mass region shows clear signs of random behavior.

The members of the Cologne group are very grateful to the INFN for its outstanding hospitality and the permission to use the GASP spectrometer and the Legnaro XTU. This work has been partly funded by the German Federal Minister for Education and Research (BMBF) under Contract No. 06OK602 I, by the Deutsche Forschungsgemeinschaft (DFG) under Contract No. Bo1108/1 and by the Istituto Nazionale di Fisica Nucleare (INFN).

[1] T.L. Khoo et al., Phys. Rev. Lett. 76, 1583 (1996).
[2] A. Lopez-Martens et al., Phys. Lett. B380, 18 (1996).

[3] R. Krücken, submitted to Phys. Rev. C. (1996).
[4] J.R. Hughes et al., Phys. Rev. Lett. **72**, 824 (1994).
[5] M.A. Riley et al., Nucl. Phys. **A512**, 178 (1990).
[6] A. Dewald et al., Nucl. Phys. **A545**, 822 (1992)
[7] D. Bazzacco, in *Proceedings of the International Conference on Nuclear Structure at High Angular Momentum, Ottawa, 1992* (AECL Research, Chalk River, Ontario, 1992), Vol. 2.
[8] Dewald, S. Harissopulos and P. von Brentano, Z. Phys. A **334**, 163 (1989)

[9] G. Böhm et al., Nucl. Instr. Meth. *A329, 248 (1993)*
[10] R. Krücken, A. Dewald, P. von Brentano, D. Bazzacco, and C. Rossi-Alvarez, accepted by Phys. Rev. C., in press,(1996).
[11] E. Vigezzi, R.A. Broglia, and T. Døssing, Phys. Lett. **B249**, 163 (1990).
[12] Y.R. Shimizu, E. Vigezzi, T. Døssing, and R.A. Broglia, Nucl. Phys. **A557**, 09c (1993)
[13] T.L. Khoo et al., Nucl. Phys. **A557**, 83c (1993).
[14] A. Dewald et al., J. Phys. G. **19** (1993).
[15] P. Willsau et al. Nucl. Phys. **A574**, 569 (1994).
[16] R. Krücken et al., Phys. Rev. Lett. **73**, 3359 (1994).
[17] A. Mengoni and Y. Nakajima, J. Nucl. Sci. Technol. **31**, 151 (1994).
[18] S.F. Mughabghab, *Neutron Cross Sections*, (Academic Press Inc., Orlando, FL, 1984), Vol. 1b.
[19] S.S. Dietrich and B.L. Berman, At. Dat. Nucl. Dat. Tab. **38**, 199 (1988).
[20] M.J. Brinkman et al., Proceedings of the Conference on Physics from Large Gamma-Ray Detector Arrays; Berkeley (1994).
[21] P. Fallon et al., Phys. Rev. C. **51**, R1609 (1995).
[22] I.Y. Lee, C. Baktash, D.M. Cullen, J.D. Garrett, N.R. Johnson, F.K. McGowan, D.F. Winchell, and C.H. Yu, Phys. Rev. C. **50**, 2602 (1994).
[23] E.F. Moore et al., Phys. Rev. Lett. **64**, 3127 (1990).
[24] P. Willsau et al., Z. Phys. **A344**, 351 (1993).
D. Blumenthal, M.P. Carpenter, B. Crowell, D. Gassmann, R.G. Henry, R.V.F. Janssens, and D. Nisius, Phys. Rev. Lett. **75**, 1276 (1995).

Change of deformation at the backbending in the yrast superdeformed band of ^{144}Gd

C. A. Ur[1], G. P. Bolzonella[1], L. H. Zhu[2], D. Bazzacco[1] S. Lunardi[1], N. H. Medina[1], C. M. Petrache[1], M. N. Rao[1], C. Rossi Alvarez[1], G. de Angelis[2], D. De Acuna[2], D. R. Napoli[2], W. Gast[3], R. M. Lieder[3], T. Rzaca-Urban[3], S. Utzelmann[3], R. Wyss[4]

[1] *Dipartimento di Fisica dell'Università and INFN, Sezione di Padova, Padova, Italy*
[2] *INFN, Laboratori Nazionali di Legnaro, Legnaro, Italy*
[3] *Institut für Kernphysik, KFA Jülich, Jülich , Germany*
[4] *Royal Institute of Technology, Physics Department Frescati, Stockholm, Sweden*

Abstract

A mean lifetime measurement using the Doppler shift attenuation method has been performed at GASP in order to extract the quadrupole moment of the yrast SD band of ^{144}Gd. The extracted intrinsic quadrupole moments, being Q_0=13.7 eb above the backbending and Q_0=11.8 eb below the backbending, are consistent with a change of deformation from β_2=0.51 (at $\beta_4 \approx$0.050) to β_2=0.45 (at $\beta_4 \approx$0.035). The experimental results are in nice agreement with the theoretical predictions, which revealed that the second well in ^{144}Gd arises essentially from the very favoured shell structure at N=80 and Z=64. The occupation at higher frequency of the aligned N=6 proton orbitals drives the nucleus to a slightly more deformed shape.

1 Introduction

It is known [1] from cranked-Strutinsky calculations using Woods-Saxon potential that some large shell gaps at very elongated shape exist for neutron numbers N=80, 86 and/or proton numbers Z=62, 64, 66. For example, the nuclei ^{144}Gd and ^{152}Dy are predicted to be doubly magic at superdeformed shape. Following these predictions several SD bands have been observed experimentally. One of the questions arised in the study of SD nuclei is on the competition between the shell structure and the occupation of the large deformation-driving high-N intruder orbitals in stabilizing SD nuclear shapes. Recent experimental results in the A=130 mass region [2] show the major importance of the shell-gaps with respect to the intruder orbitals occupation.

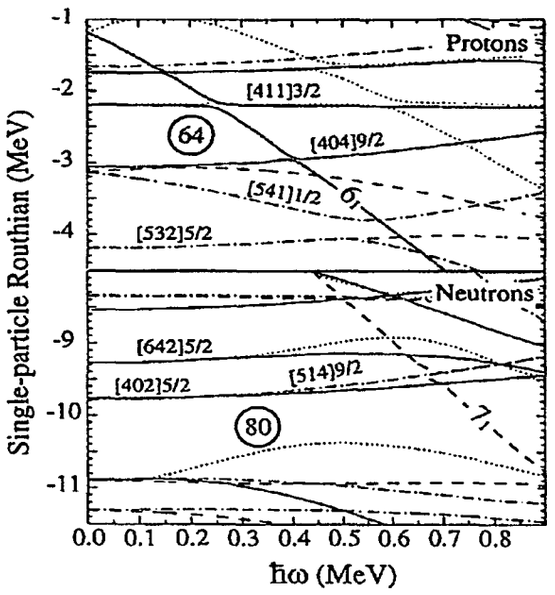

Figure 1: Single particle routhians calculated at β_2=0.45 (β_4=0.035) for ^{144}Gd.

We have now the opportunity to investigate this competition within the SD nucleus ^{144}Gd. In fact, theoretical calculations tell us that superdeformation in ^{144}Gd is originally stabilized by the N=80 neutron shell gap at $\beta_2 \approx 0.45$ without occupying the high-N intruder orbitals. This is shown clearly in Fig. 1 by the single particle routhians calculated at β_2=0.45 (β_4=0.035). At low frequency, none of the high-N intruder orbitals which characterize the SD bands in the A=150 mass region are occupied. Only when cranking, the N=6 proton intruder orbital decreases in energy and becomes occupied at high frequency. The same calculations predict that at a rotational frequency $\hbar\omega \approx 0.45$ MeV the proton configuration is changing from $\pi 6^0$ to $\pi 6^2$ with a change of deformation from $\beta_2 \approx 0.47$ to ≈ 0.51 [3]. This would imply a change of deformation less than 10% when two particles are promoted on high-N intruder orbitals.

2 Superdeformed bands in ^{144}Gd

Very recently, five SD bands have been identified in ^{144}Gd [3, 4] using ^{100}Mo(^{48}Ti,4n) reaction. The coincidence γ-ray spectra of the five SD bands, obtained by setting double gates on clean transitions in each band, are shown in Fig.2. The yrast SD band [3] is one of the few cases which exhibits a backbending, confirming the theoretical prediction [1] of the crossing between $\pi 6^0$ and $\pi 6^2$ configurations due to the alignment of two $i_{13/2}$ protons. The other four excited SD bands [4] are interpreted as proton particle-hole excitation across the Z=64 gap revealing the high stability of the N=80 shell closure at SD shapes. The relative intensity of the yrast SD band with respect to the total population of ^{144}Gd is reported [4] as a function of the beam energy in ^{100}Mo(^{48}Ti,4n) reaction in Fig.3. The data show the well-known saturation pattern (see Fig. 3) in the population of the SD bands. The intensity of the yrast SD band in ^{144}Gd, being 1.2% of the total population, is comparable to that of the other yrast SD bands in the A = 150 mass region. The results

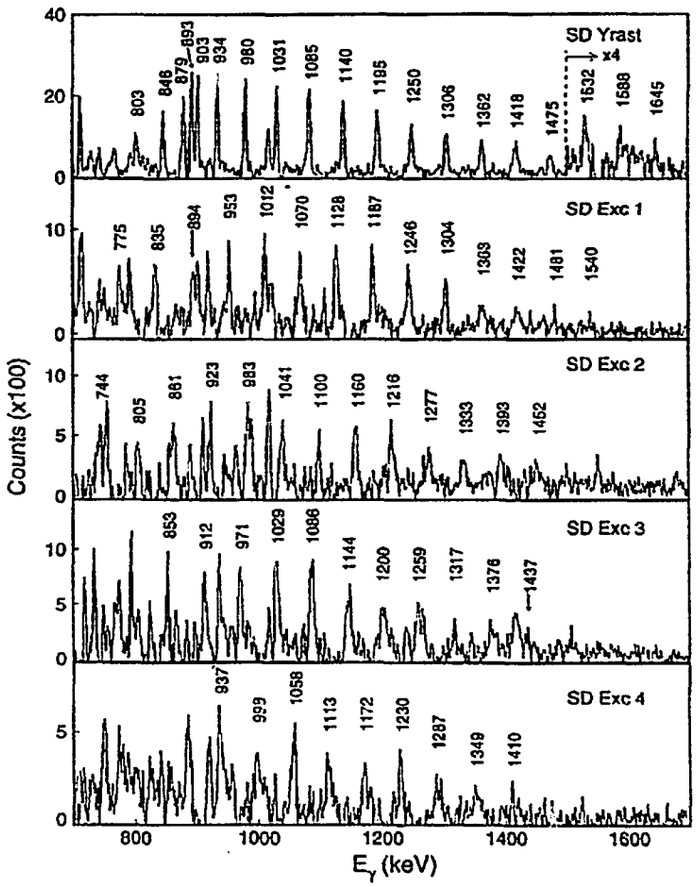

Figure 2: Doubly-gated coincidence spectra of five SD bands of ^{144}Gd identified in ^{48}Ti + ^{100}Mo reaction at 215 MeV. The members of the SD bands are labeled with their energies in keV. Their relative intensities with respect to the total population of ^{144}Gd are also shown.

therefore exclude a possible configuration-dependence in the population of the SD bands around N=80.

On the other hand, the population of superdeformed (SD) bands has been observed to depend, in few cases, on the mass symmetry of the reaction entrance channel [5, 6]. In order to clarify this issue qualitatively, the completely symmetric reaction ^{74}Ge + ^{74}Ge has been recently used where the 318 MeV ^{74}Ge beam was provided by the superconducting Linac post-accelerator ALPI in Legnaro. The intensity of the yrast SD band results to be 1.6% of the total population of ^{144}Gd channel (open circle in Fig.3) to be compared with the 1.2% obtained with the ^{48}Ti beam. For comparison, the x-axis is scaled with the corresponding excitation energy of the compound nucleus. A clear enhancement of the SD band population is observed in the case of the ^{74}Ge + ^{74}Ge reaction, which demonstrates the important role played by the reaction entrance channel. In fact, the failure of earlier attempts [7, 8] to populate SD bands in ^{144}Gd through ^{28}Si induced reactions indicated possibly the importance of entrance channel effects in the population of the SD bands in ^{144}Gd. Other explanations can be given based on the dynamics of the formation of the equilibrated compound system and/or on the interplay between the fusion-evaporation and fusion-fission channels in the decay of the compound nucleus [9].

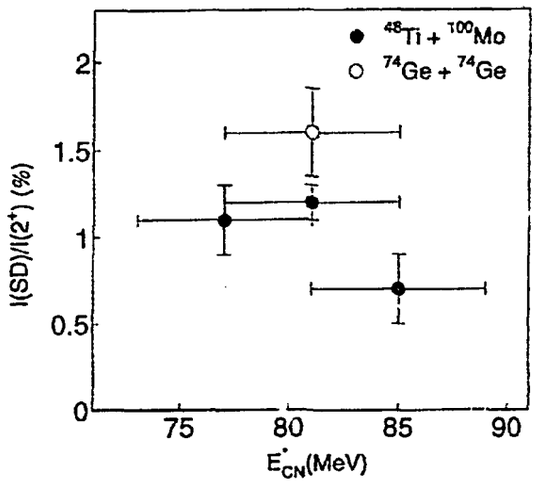

Figure 3: Relative intensities with respect to the total population of ^{144}Gd as a function of the excitation energy of compound nucleus. The errors of the intensity are statistics while the ones of the excitation energy correspond to the energy spread due to the thickness of the target.

3 DSAM experiment and details

In order to measure the deformation of the nucleus in the SD states a Doppler Shift Attenuation Method (DSAM) experiment has been performed. High spin states in ^{144}Gd were populated via the ^{100}Mo(^{48}Ti,4n) reaction at a beam energy of 214 MeV. The beam was delivered by the XTU Tandem accelerator at the National Laboratories of Legnaro. The target consisted of a 1 mg/cm^2 ^{100}Mo foil evaporated on a 10 mg/cm^2 gold backing which completely stops the recoiling nuclei. Gamma-rays were detected by the GASP array which consisted of 10 large volume Compton escape-suppressed HPGe detectors and 80 BGO detectors forming the inner ball. Events were collected only when at least 3 Ge detectors and 5 BGO detectors have been fired. A total of 2.13 $\times$ 10^9 events which after unfolding resulted in 3.94 $\times$ 10^9 triple events were collected on tape. The Ge detectors in the GASP array are placed symmetrically with respect to the beam direction in seven rings, as follows: 6 at 35°, 6 at 60°, 4 at 72°, 8 at 90°, 4 at 108°, 6 at 120° and 6 at 145°. In the offline

analysis the high spin states of ^{144}Gd were enhanced by proper gates on the energy sum and the multiplicity from the BGO inner ball. In order to simplify the analysis, the data were reduced by considering only the energy region from 750 keV to 1625 keV where the SD band transitions are located. We enhanced the transitions in the SD band by double gating on in-band transitions and incrementing directly spectra corresponding to the seven rings of detectors in coincidence with all the detectors. In Fig.4 the spectra obtained for the most forward and backward rings of detectors, after background subtraction, are shown.

The experimental fractional Doppler shift, F(τ), was calculated according to the following relation:

$$F(\tau) = \frac{\Delta E_\gamma}{2 \cdot \beta \cdot \overline{E}_\gamma \cdot \cos\theta_{forward}} \tag{1}$$

where ΔE_γ is the energy difference between the centroids of the shifted γ-rays corresponding to the forward and backward angles ($\theta_{forward}$ and $\pi - \theta_{forward}$, respectively), $\overline{E}_\gamma$ is their mean value and $\beta = v_0/c$ where v_0 is the mean initial recoil velocity. The experimental F(τ) curve is represented in Fig. 5, where the errors are only from the statistics of the spectra of the rings at forward and backward direction and the points corresponding to the 1084 keV and 1134 keV transition are taken only from the forward ring in order to avoid the strong contaminants in the backward ring.

The slowing down process of the recoils and, accordingly, the velocity profile has been simulated with the Monte Carlo procedure developed on the basis of the code of Bacelar *et al.* [10] using a number of 5000 histories and up to 1600 time steps of $\approx$ 1.0 fs. The electronic stopping power was calculated according to the formalism of Braune [12]. The calculation of the theoretical F(τ) value depends on the mean time of the decay of the state (often called "apparent lifetime"), which is defined by the mean lifetime of the state and the entire decay history above the state, including the unknown sidefeeding. The program we used is a modified version with respect to the one reported in [13] and is dealing with a rotational cascade, having a constant intrinsic quadrupole moment Q_0, where each state has a sidefeeding provided by a rotational sideband with the same dynamical moment of inertia $\Im^{(2)}$ as the SD

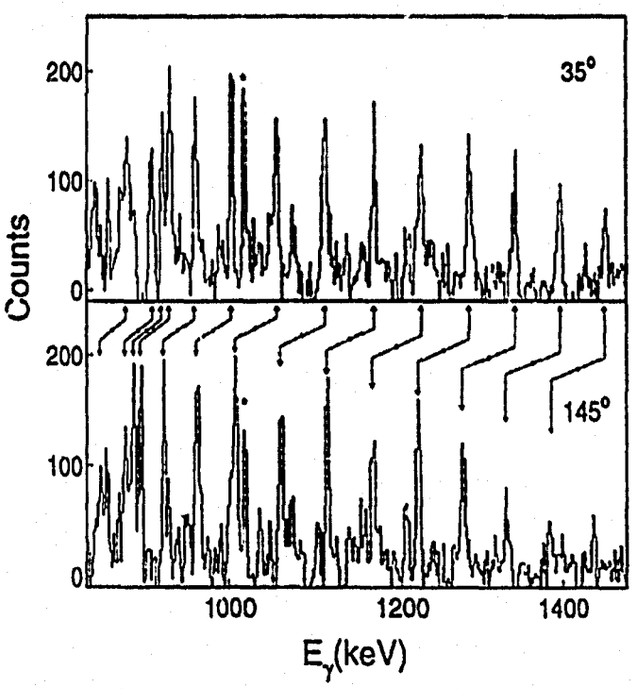

Figure 4: Coincidence spectra corresponding to the ring of detectors at 35° and 145° related to the beam direction respectively, double gated on the members of the yrast SD band in ^{144}Gd. The shifts of the γ-rays are positioned with the arrows. The lines marked with asterisk indicate the unshifted γ-ray of ND states.

band and an intrinsic quadrupole moment $(Q_0)_{SF}$.

The calculations were performed under the assumption that $(Q_0)_{SF}$ has the same value for all the sidebands, as it was suggested in previous works [11, 13] for this mass region. The values for Q_0 are extracted by minimizing the χ^2 of the calculated curve fit to the experimental points. The best fit of the experimental data above the backbending (see Fig.5) was obtained for Q_0=13.7±1.2 eb. Below the backbending there is no sidefeeding but we have to consider the decay out of the states. For this part the data indicate a value of Q_0=11.8 eb. Since the number of points below the backbending is low it was not possible to make a fit of the data and, consequently, it was difficult to evaluate the error for this value. We estimated the limits of Q_0 to be ≈±1.5 eb as suggested by the error bars for the F(τ) experimental points. We have to notice at this point that the results are subjected to 10-15% of errors due to the uncertainties on the stopping power. However, this does not affect the relative deformation below and above the backbending. The corresponding axial deformation was calculated using the exact expansion of liquid drop model expression for Q_0 in terms of the β_2 and β_4 and under the assumption that β_4=0.5β_2-0.19 for 0.45 < β_2 < 0.60 [1]. We obtained that the deformation of the nucleus is changing from β_2=0.45±0.05 to β_2=0.51±0.04, which agrees with what is expected theoretically when two protons occupy N=6 intruder orbitals [3].

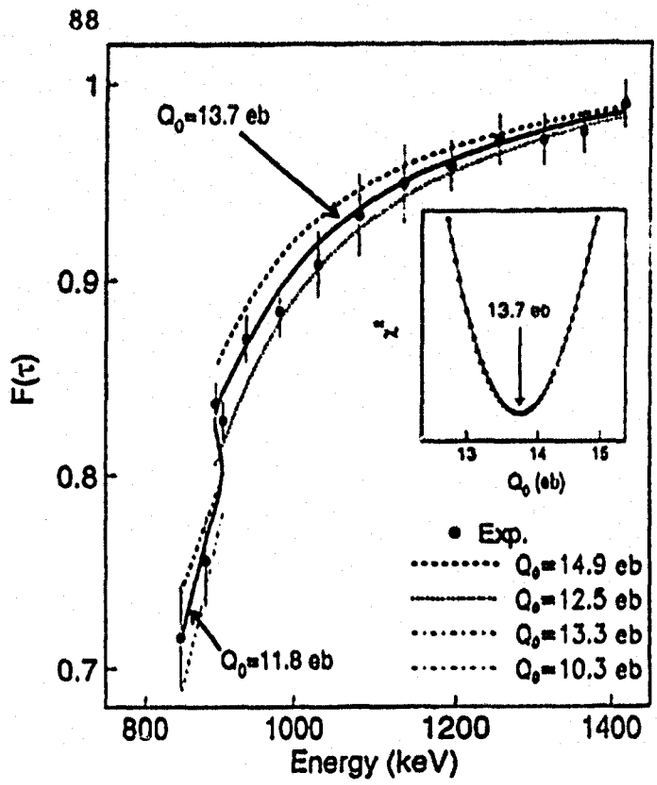

Figure 5: Experimental fractional Doppler shift extracted from the spectra corresponding to the most forward and backward rings of detectors. The solid line indicated with the Q_0 values gives the best description of the data under the assumption that the sidefeeding has the same time structure as the in-band feeding. The inset shows the χ^2 minimization for the part above the crossing.

4 Conclusions

We have measured the deformation along the yrast SD band of ^{144}Gd by means of the DSAM technique and obtained for the quadrupole deformation β_2=0.45 and β_2=0.51 below and above the backbending, respectively. This results is nicely confirming the theoretical prediction that the change of configuration from $\pi 6^0$ to $\pi 6^2$ induces a change of deformation of about 10%. The major contribution to the deformation in the second minimum of ^{144}Gd is due therefore to the very favoured shell structure at N=80 and Z=64, without involving the